Appendix A.8:

Parnwell St and Bassett St – CPT 27709

Table 1: Site Description for Parnwell St & Bassett St (CC LIQ 2 – CPT 27709).

Attribute	Yes/No			Description/Date	Symbol in Figure 1
	10-m Buffer	20-m Buffer	50-m Buffer		
Near a body of surface water or other free face features?	No	No	No	The center of the site is 430 meters away from the Avon River. The direction of the free face is roughly W-E, while its height is ~1.5 m.	NA
Lateral spreading observed during the CES?	No	No	No	Absence of ground cracks indicates no lateral spreading, as observed by the mapping team.[1]	NA
Nearby buildings or structures?	Yes	Yes	Yes	Building coverage of the 10-m, 20-m, and 50-m buffers is 35%, 36%, and 26%, respectively.	White Fill + Brown Outline
Sloping land?	No	No	No	Flat land, residential area.	NA
Step changes in the ground surface?	No	No	No	NA	NA
Retaining walls?	No	No	No	NA	NA
Vegetation?	Yes	Yes	Yes	Trees and bushes cover 7% of the 10-m buffer, 13% of the 20-m buffer and 32% of the 50-m buffer. They are in the N half of the 10-m buffer and throughout all quadrants of the 20-m and 50-m buffers.	White Fill + Green Outline
Manmade changes to the site between the LiDAR surveys?	No	Yes	Yes	A building outside of the 10-m and 20-m buffers but within the 50-m buffer was removed between June 2012 and October 2012. Another building outside of the 10-m buffer but within 20-m and 50-m buffers was demolished in July 2015 and rebuilt sometime between September 2015 and November 2015.	Building Removal after June 2012: Orange Crossline
Other important factors?	No	No	Yes	Moderate-motor-vehicle-volume, two-way roadway occupies 11% of the 50-m buffer and stretches throughout the NE and SE quadrants. Beach umbrella is in the NW quadrant of the 20-m and 50-m buffer.	Road: Gray Fill + Red Outline; Beach Umbrella: White Fill +Yellow Outline

Note: Buffer is the area within a circle of a specified radius with CPT investigations done at its center (172.687992°, -43.496341°).

[1] Canterbury Geotechnical Database. (2012). "Observed Ground Crack Locations", Map Layer CGD0400 - 23 July 2012, retrieved July 09, 2018 from https://canterburygeotechnicaldatabase.projectorbit.com/

Figure 1: Site plan with areas where LiDAR survey data is considered.

Note 1: Four patches (outlined in red) in the free field were selected for settlement assessment as areas free of vegetation, structures, and manmade changes. Other factors that played a role in their selection were ejecta distribution and close proximity to a CPT. In addition, since significant amounts of ejecta were observed on roads in the CES, the entire road and the driveway were considered for settlement assessment. Roads as hard, relatively flat surfaces provide many ground-classified points.

Table 2: LiDAR flight error adjustments, global adjustments for the difference between average LiDAR point elevations and benchmark survey elevations, and vertical tectonic movement adjustments.

	Adjustments (mm)		
Earthquake Event(s)	LiDAR Flight Error	Global Offset[2]	Tectonic Vertical Movement
Sep-10	-100	-3	0
Feb-11	0	16	-43
Jun-11	0	38	-42
Dec-11	0	-65	0
CES	-100	-14	-85
Any LiDAR survey affected by ejecta?*			Yes

Notes: The negative sign indicates the subtraction from the ground surface subsidence, while the positive sign indicates the addition to the ground surface subsidence; * Ejecta likely remained within Patch A during the Mar 2011 and/or May 2011 LiDAR survey (as seen in the satellite image from 8 Mar 2011) hence ~50 mm is added to the ground surface subsidence for the Feb-11 EQ and subtracted from the ground surface subsidence for the Jun-11 EQ for Patch A.

Table 3a: LiDAR Measurement Error for Patch A.

Surveys	Buffer	Area Averaged Difference Indicating Repeat Measurement Error (mm)	$σ^*_{\text{individual LiDAR points}}$ (mm)	%Reduction in σ due to Area Averaging of LiDAR Points
Post Feb 2011: Mar 2011 and May 2011	10-m	51	59	[86,86]
	20-m	51		
	50-m	51		
Post Dec 2011: Feb 2012 and Oct 2015	10-m	2	70	[3,3]
	20-m	2		
	50-m	2		

*Standard deviation.

[2] Russell, J., & van Ballegooy, S. (2015). *Canterbury Earthquake Sequence: Increased liquefaction vulnerability assessment methodology*. New Zealand: Tonkin & Taylor Ltd.

Table 3b: LiDAR Measurement Error for Patch B.

Surveys	Buffer	Area Averaged Difference Indicating Repeat Measurement Error (mm)	σ*$_{individual}$ LiDAR points (mm)	%Reduction in σ due to Area Averaging of LiDAR Points
Post Feb 2011: Mar 2011 and May 2011	10-m	NA	59	[97,97]
	20-m	57		
	50-m	57		
Post Dec 2011: Feb 2012 and Oct 2015	10-m	NA	70	[109,109]
	20-m	76		
	50-m	76		

*Standard deviation.

Table 3c: LiDAR Measurement Error for Patch C.

Surveys	Buffer	Area Averaged Difference Indicating Repeat Measurement Error (mm)	σ*$_{individual}$ LiDAR points (mm)	%Reduction in σ due to Area Averaging of LiDAR Points
Post Feb 2011: Mar 2011 and May 2011	10-m	NA	59	[107,107]
	20-m	NA		
	50-m	63		
Post Dec 2011: Feb 2012 and Oct 2015	10-m	NA	70	[20,20]
	20-m	NA		
	50-m	14		

*Standard deviation.

Table 3d: LiDAR Measurement Error for Driveway.

Surveys	Buffer	Area Averaged Difference Indicating Repeat Measurement Error (mm)	$\sigma^*_{\text{individual LiDAR points}}$ (mm)	%Reduction in σ due to Area Averaging of LiDAR Points
Post Feb 2011: Mar 2011 and May 2011	10-m	1	59	[2,2]
	20-m	1		
	50-m	6		
Post Dec 2011: Feb 2012 and Oct 2015	10-m	11	70	[11, 16]
	20-m	8		
	50-m	9		

*Standard deviation.

Table 3e: LiDAR Measurement Error for Road.

Surveys	Buffer	Area Averaged Difference Indicating Repeat Measurement Error (mm)	$\sigma^*_{\text{individual LiDAR points}}$ (mm)	%Reduction in σ due to Area Averaging of LiDAR Points
Post Feb 2011: Mar 2011 and May 2011	10-m	NA	59	[78,78]
	20-m	NA		
	50-m	46		
Post Dec 2011: Feb 2012 and Oct 2015	10-m	NA	70	[74,74]
	20-m	NA		
	50-m	52		

*Standard deviation.

Table 4a: Ground surface subsidence adjustments due to LiDAR measurement error for Patch A.

Earthquake Event(s)	$\sigma_{\text{pre-EQ LiDAR survey}}$ (mm)	$\sigma_{\text{post-EQ LiDAR survey}}$ (mm)	σ_{total} (mm)	Area Average Adjusted σ (mm) **
Sep-10	158	56	134	$\pm$116
Feb-11	56	59	59	$\pm$51
Jun-11	59	61	62	$\pm$54
Dec-11	61	70	87	$\pm$75
CES	158	70	124	$\pm$108

**Based on the highest %Reduction in Table 3a.

Table 4b: Ground surface subsidence adjustments due to LiDAR measurement error for Patch B.

Earthquake Event(s)	$\sigma_{pre\text{-}EQ\ LiDAR\ survey}$ (mm)	$\sigma_{post\text{-}EQ\ LiDAR\ survey}$ (mm)	σ_{total} (mm)	Area Average Adjusted σ (mm) **
Sep-10	158	56	134	±146
Feb-11	56	59	59	±64
Jun-11	59	61	62	±68
Dec-11	61	70	87	±94
CES	158	70	124	±135

**Based on the highest %Reduction in Table 3b.

Table 4c: Ground surface subsidence adjustments due to LiDAR measurement error for Patch C.

Earthquake Event(s)	$\sigma_{pre\text{-}EQ\ LiDAR\ survey}$ (mm)	$\sigma_{post\text{-}EQ\ LiDAR\ survey}$ (mm)	σ_{total} (mm)	Area Average Adjusted σ (mm) **
Sep-10	158	56	134	±143
Feb-11	56	59	59	±63
Jun-11	59	61	62	±66
Dec-11	61	70	87	±92
CES	158	70	124	±133

**Based on the highest %Reduction in Table 3c.

Table 4d: Ground surface subsidence adjustments due to LiDAR measurement error for Driveway.

Earthquake Event(s)	$\sigma_{pre\text{-}EQ\ LiDAR\ survey}$ (mm)	$\sigma_{post\text{-}EQ\ LiDAR\ survey}$ (mm)	σ_{total} (mm)	Area Average Adjusted σ (mm) **
Sep-10	158	56	134	±21
Feb-11	56	59	59	±9
Jun-11	59	61	62	±10
Dec-11	61	70	87	±14
CES	158	70	124	±20

**Based on the highest %Reduction in Table 3d.

Table 4e: Ground surface subsidence adjustments due to LiDAR measurement error for Road.

Earthquake Event(s)	$\sigma_{pre\text{-}EQ\ LiDAR\ survey}$ (mm)	$\sigma_{post\text{-}EQ\ LiDAR\ survey}$ (mm)	σ_{total} (mm)	Area Average Adjusted σ (mm) **
Sep-10	158	56	134	±105
Feb-11	56	59	59	±46
Jun-11	59	61	62	±48
Dec-11	61	70	87	±68
CES	158	70	124	±97

**Based on the highest %Reduction in Table 3e.

Table 5a: Raw liquefaction-related ground surface subsidence using original LiDAR points for Patch A.

	Average Ground Surface Subsidence (mm)		
Earthquake Event(s)	10-m Buffer	20-m Buffer	50-m Buffer
Sep-10	84	84	84
Feb-11	87	87	87
Jun-11	59	59	59
Dec-11	85	85	85
CES	314	314	315

Table 5b: Raw liquefaction-related ground surface subsidence using original LiDAR points for Patch B.

	Average Ground Surface Subsidence (mm)		
Earthquake Event(s)	10-m Buffer	20-m Buffer	50-m Buffer
Sep-10	NA	61	61
Feb-11	NA	134	134
Jun-11	NA	40	40
Dec-11	NA	43	43
CES	NA	277	278

Table 5c: Raw liquefaction-related ground surface subsidence using original LiDAR points for Patch C.

	Average Ground Surface Subsidence (mm)		
Earthquake Event(s)	10-m Buffer	20-m Buffer	50-m Buffer
Sep-10	NA	NA	91
Feb-11	NA	NA	135
Jun-11	NA	NA	69
Dec-11	NA	NA	70
CES	NA	NA	365

Table 5d: Raw liquefaction-related ground surface subsidence using original LiDAR points for Driveway.

	Average Ground Surface Subsidence (mm)		
Earthquake Event(s)	10-m Buffer	20-m Buffer	50-m Buffer
Sep-10	-34	84	76
Feb-11	256	246	235
Jun-11	51	48	46
Dec-11	75	73	71
CES	349	450	428

Table 5e: Raw liquefaction-related ground surface subsidence using original LiDAR points for Road.

	Average Ground Surface Subsidence (mm)		
Earthquake Event(s)	10-m Buffer	20-m Buffer	50-m Buffer
Sep-10	NA	NA	108
Feb-11	NA	NA	205
Jun-11	NA	NA	79
Dec-11	NA	NA	29
CES	NA	NA	421

Table 6a: Corrected liquefaction-related ground surface subsidence using original LiDAR points for Patch A with the calculated adjustments in Table 2.

	Average Calculated Ground Surface Subsidence (mm)		
Earthquake Event(s)	10-m Buffer	20-m Buffer	50-m Buffer
Sep-10	-19±125	-19±125	-19±125
Feb-11	110±50	110±50	110±50
Jun-11	5±50	5±50	5±50
Dec-11	20±75	20±75	20±75
CES	115±100	115±100	115±100

Notes: Plus/minus values are same as those in Table 4a, but rounded to the nearest 25; Positive overall values indicate ground surface subsidence, while negative overall values indicate ground surface uplift.

Table 6b: Corrected liquefaction-related ground surface subsidence using original LiDAR points for Patch B with the calculated adjustments in Table 2.

	Average Calculated Ground Surface Subsidence (mm)		
Earthquake Event(s)	10-m Buffer	20-m Buffer	50-m Buffer
Sep-10	NA	-42 ± 150	-42 ± 150
Feb-11	NA	107 ± 75	107 ± 75
Jun-11	NA	36 ± 75	36 ± 75
Dec-11	NA	-22 ± 100	-22 ± 100
CES	NA	78 ± 125	78 ± 125

Notes: Plus/minus values are same as those in Table 4b, but rounded to the nearest 25; Positive overall values indicate ground surface subsidence, while negative overall values indicate ground surface uplift.

Table 6c: Corrected liquefaction-related ground surface subsidence using original LiDAR points for Patch C with the calculated adjustments in Table 2.

	Average Calculated Ground Surface Subsidence (mm)		
Earthquake Event(s)	10-m Buffer	20-m Buffer	50-m Buffer
Sep-10	NA	NA	-12 ± 150
Feb-11	NA	NA	108 ± 75
Jun-11	NA	NA	65 ± 75
Dec-11	NA	NA	5 ± 100
CES	NA	NA	165 ± 125

Notes: Plus/minus values are same as those in Table 4c, but rounded to the nearest 25; Positive overall values indicate ground surface subsidence, while negative overall values indicate ground surface uplift.

Table 6d: Corrected liquefaction-related ground surface subsidence using original LiDAR points for Driveway with the calculated adjustments in Table 2.

	Average Calculated Ground Surface Subsidence (mm)		
Earthquake Event(s)	10-m Buffer	20-m Buffer	50-m Buffer
Sep-10	-137 ± 25	-19 ± 25	-27 ± 25
Feb-11	229 ± 25	219 ± 25	208 ± 25
Jun-11	47 ± 25	44 ± 25	42 ± 25
Dec-11	10 ± 25	8 ± 25	6 ± 25
CES	150 ± 25	251 ± 25	229 ± 25

Notes: Plus/minus values are same as those in Table 4d, but rounded to the nearest 25; Positive overall values indicate ground surface subsidence, while negative overall values indicate ground surface uplift.

Table 6e: Corrected liquefaction-related ground surface subsidence using original LiDAR points for Roadway with the calculated adjustments in Table 2.

	Average Calculated Ground Surface Subsidence (mm)		
Earthquake Event(s)	10-m Buffer	20-m Buffer	50-m Buffer
Sep-10	NA	NA	5 ± 100
Feb-11	NA	NA	178 ± 50
Jun-11	NA	NA	75 ± 50
Dec-11	NA	NA	-36 ± 75
CES	NA	NA	222 ± 100

Notes: Plus/minus values are same as those in Table 4e, but rounded to the nearest 25; Positive overall values indicate ground surface subsidence, while negative overall values indicate ground surface uplift.

Table 7a: Corrected liquefaction-related ground surface subsidence for Patch A using LiDAR DEMs.

	Estimated Ground Surface Subsidence (mm)								
	10-m Buffer			20-m Buffer			50-m Buffer		
Earthquake Event(s)	16th %ile	50th %ile	84th %ile	16th %ile	50th %ile	84th %ile	16th %ile	50th %ile	84th %ile
Sep-10	<50	<50	<50	<50	<50	<50	<50	<50	<50
Feb-11	150	200	250	150	200	250	150	200	250
Jun-11	50	50	50	50	50	50	50	50	50
Dec-11	<50	<50	50	<50	<50	50	<50	<50	50
CES	150	250	300	150	250	300	150	250	300

Note: These percentiles are not the exact statistical measures; they indicate the spatial variability of ground surface subsidence.

Table 7b: Corrected liquefaction-related ground surface subsidence for Patch B using LiDAR DEMs.

	Estimated Ground Surface Subsidence (mm)								
	10-m Buffer			20-m Buffer			50-m Buffer		
Earthquake Event(s)	16th %ile	50th %ile	84th %ile	16th %ile	50th %ile	84th %ile	16th %ile	50th %ile	84th %ile
Sep-10	NA	NA	NA	<50	<50	<50	<50	<50	<50
Feb-11	NA	NA	NA	150	150	150	150	150	150
Jun-11	NA	NA	NA	50	50	50	50	50	50
Dec-11	NA	NA	NA	50	50	50	50	50	50
CES	NA	NA	NA	250	250	250	250	250	250

Note: These percentiles are not the exact statistical measures; they indicate the spatial variability of ground surface subsidence.

Table 7c: Corrected liquefaction-related ground surface subsidence for Patch C using LiDAR DEMs.

	Estimated Ground Surface Subsidence (mm)								
	10-m Buffer			20-m Buffer			50-m Buffer		
Earthquake Event(s)	16th %ile	50th %ile	84th %ile	16th %ile	50th %ile	84th %ile	16th %ile	50th %ile	84th %ile
Sep-10	NA	NA	NA	NA	NA	NA	<50	<50	<50
Feb-11	NA	NA	NA	NA	NA	NA	150	150	150
Jun-11	NA	NA	NA	NA	NA	NA	50	50	50
Dec-11	NA	NA	NA	NA	NA	NA	50	50	50
CES	NA	NA	NA	NA	NA	NA	250	250	250

Note: These percentiles are not the exact statistical measures; they indicate the spatial variability of ground surface subsidence.

Table 7d: Corrected liquefaction-related ground surface subsidence for Driveway using LiDAR DEMs.

	Estimated Ground Surface Subsidence (mm)								
	10-m Buffer			20-m Buffer			50-m Buffer		
Earthquake Event(s)	16th %ile	50th %ile	84th %ile	16th %ile	50th %ile	84th %ile	16th %ile	50th %ile	84th %ile
Sep-10	<50	<50	<50	<50	<50	<50	<50	<50	<50
Feb-11	150	150	150	150	150	150	150	150	150
Jun-11	50	50	50	50	50	50	50	50	50
Dec-11	50	50	50	50	50	50	50	50	50
CES	250	250	250	250	250	250	250	250	250

Note: These percentiles are not the exact statistical measures; they indicate the spatial variability of ground surface subsidence.

Table 7e: Corrected liquefaction-related ground surface subsidence for Road using LiDAR DEMs.

	Estimated Ground Surface Subsidence (mm)								
	10-m Buffer			20-m Buffer			50-m Buffer		
Earthquake Event(s)	16th %ile	50th %ile	84th %ile	16th %ile	50th %ile	84th %ile	16th %ile	50th %ile	84th %ile
Sep-10	NA	NA	NA	NA	NA	NA	<50	<50	50
Feb-11	NA	NA	NA	NA	NA	NA	100	150	150
Jun-11	NA	NA	NA	NA	NA	NA	50	50	50
Dec-11	NA	NA	NA	NA	NA	NA	50	50	50
CES	NA	NA	NA	NA	NA	NA	250	350	350

Note: These percentiles are not the exact statistical measures; they indicate the spatial variability of ground surface subsidence.

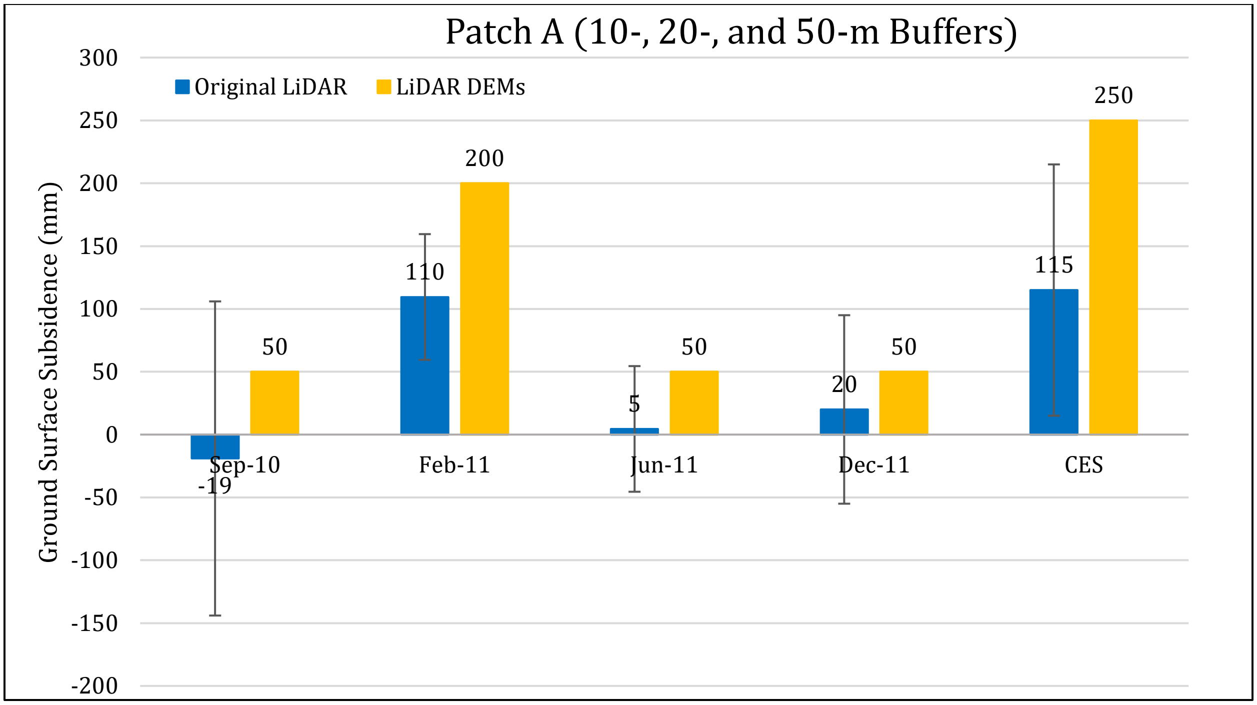

Figure 2: Comparison between ground surface subsidence determined from original LiDAR survey points and ground surface subsidence (50th %ile) estimated using LiDAR DEMs for Patch A.

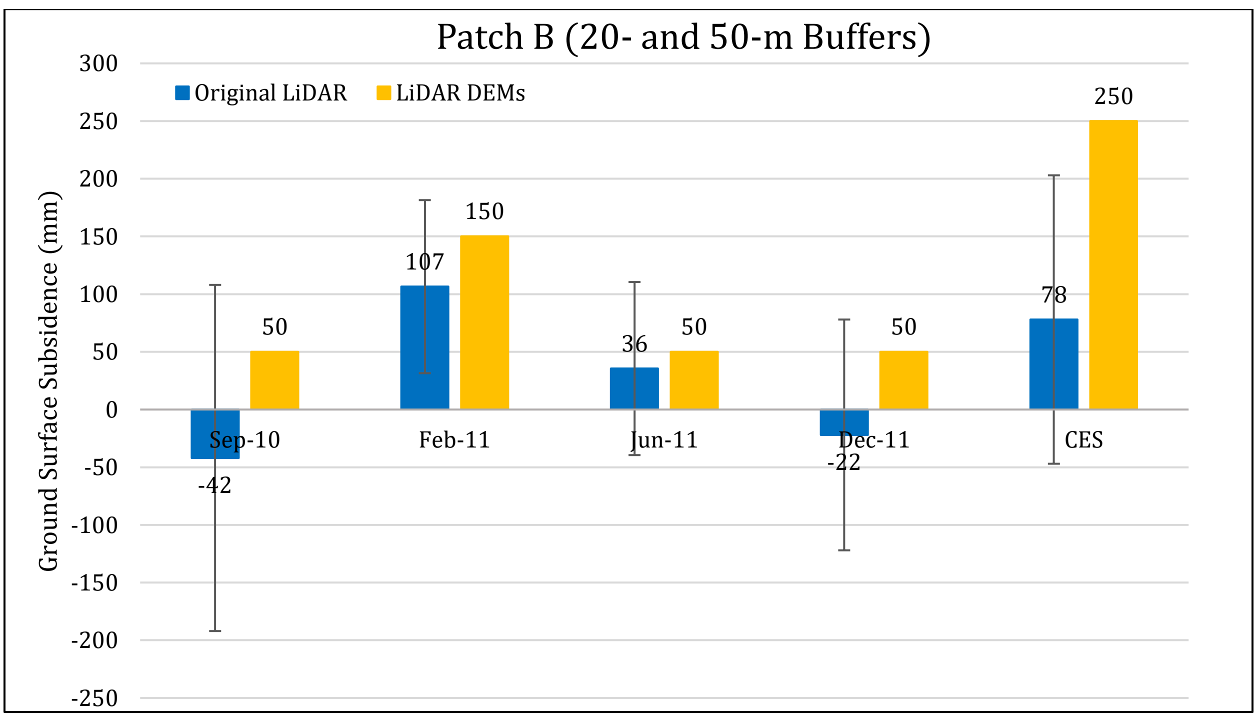

Figure 3: Comparison between ground surface subsidence determined from original LiDAR survey points and ground surface subsidence (50th %ile) estimated using LiDAR DEMs for Patch B.

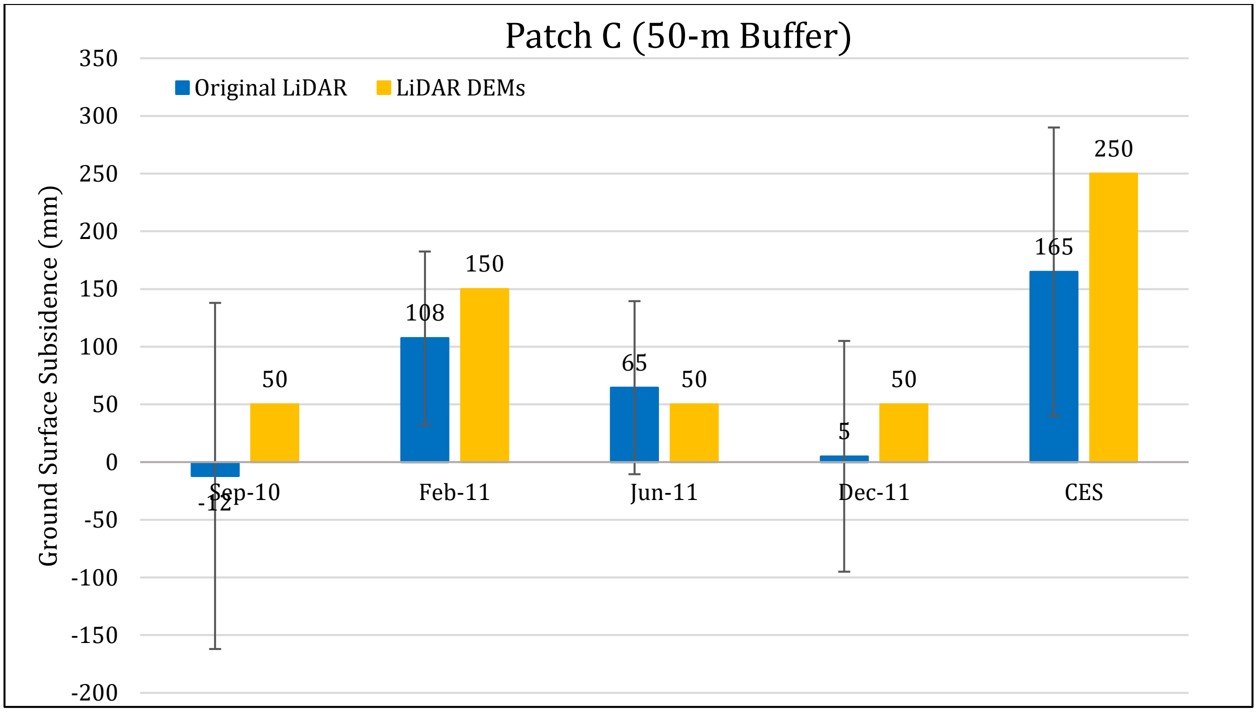

Figure 4: Comparison between ground surface subsidence determined from original LiDAR survey points and ground surface subsidence (50th %ile) estimated using LiDAR DEMs for Patch C.

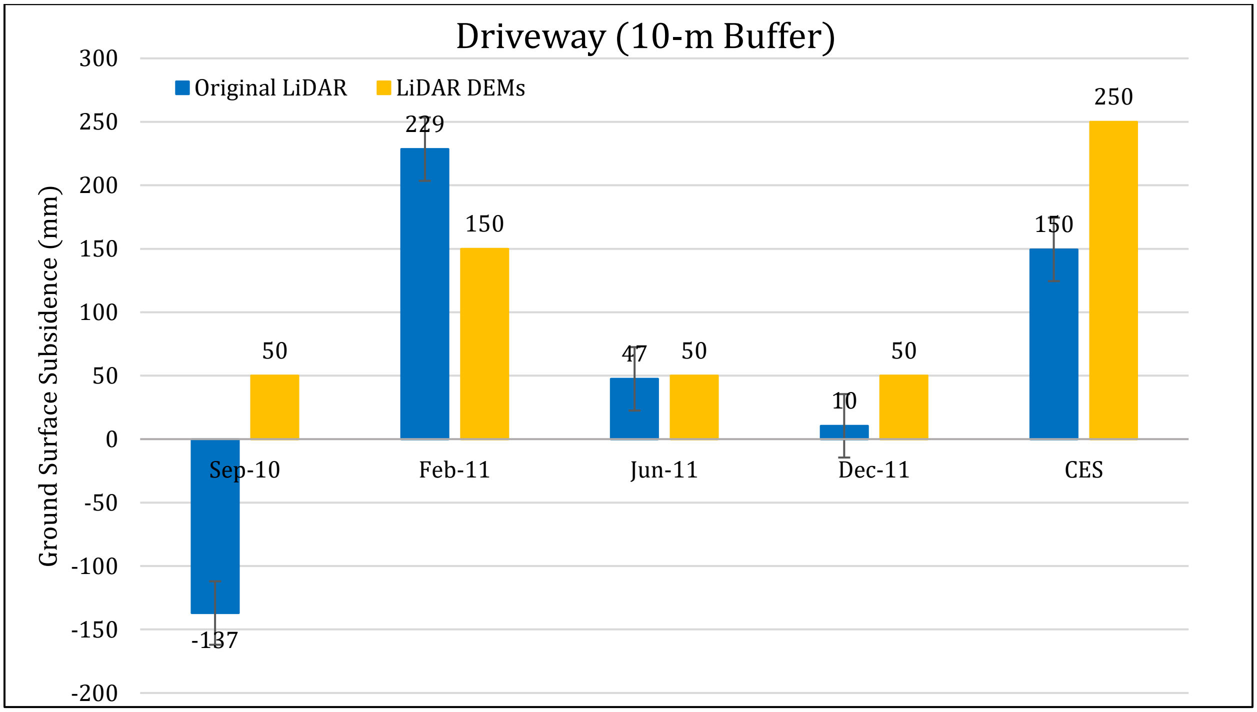

Figure 5: Comparison between ground surface subsidence determined from original LiDAR survey points and ground surface subsidence (50th %ile) estimated using LiDAR DEMs for Driveway for the 10-m buffer.

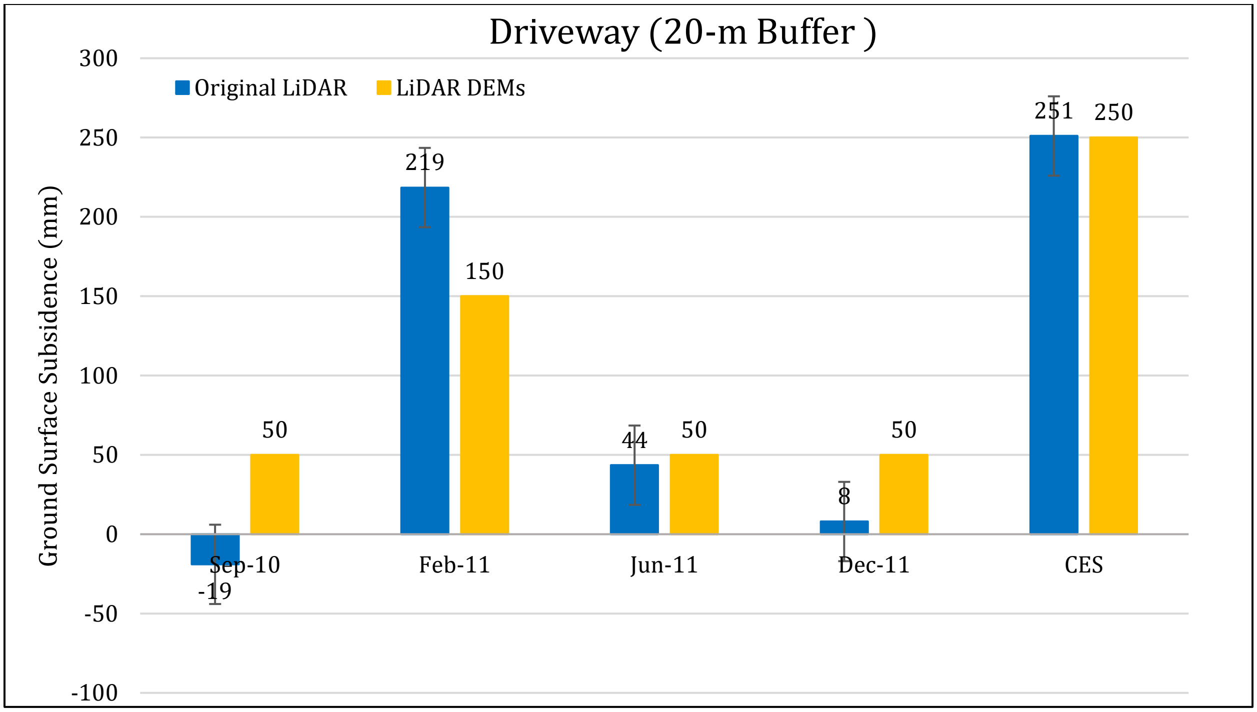

Figure 6: Comparison between ground surface subsidence determined from original LiDAR survey points and ground surface subsidence (50th %ile) estimated using LiDAR DEMs for Driveway for the 20-m buffer.

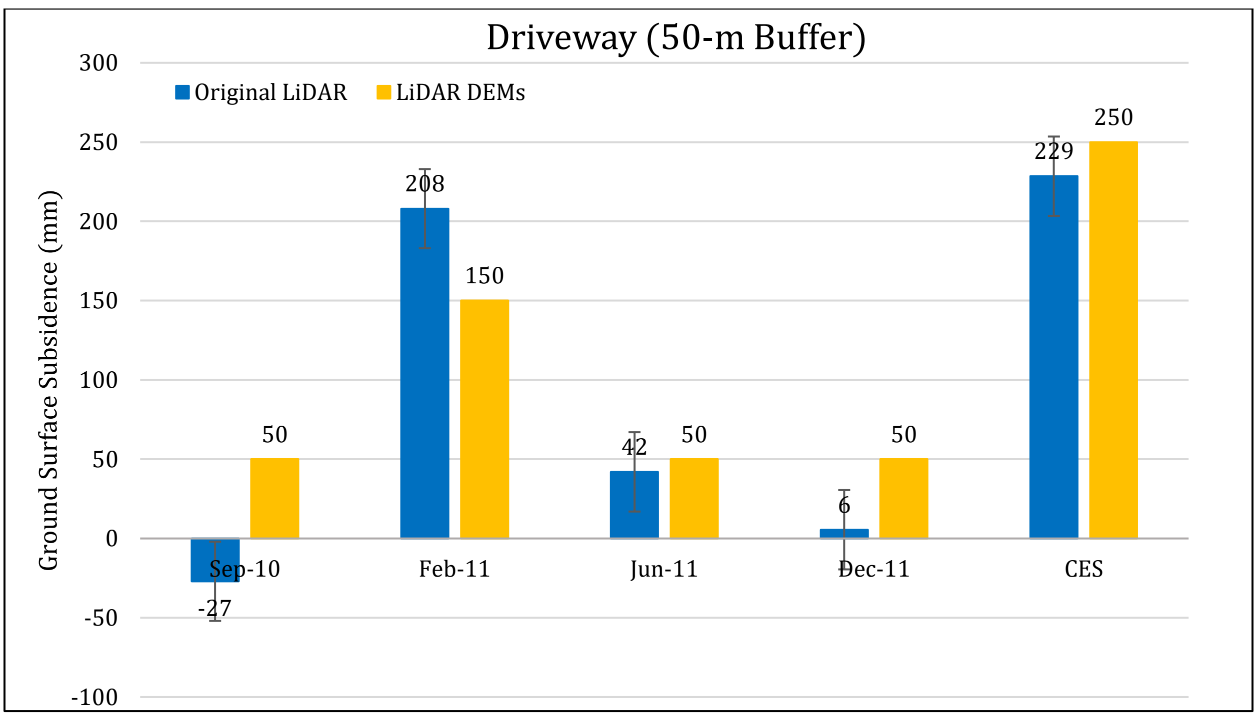

Figure 7: Comparison between ground surface subsidence determined from original LiDAR survey points and ground surface subsidence (50th %ile) estimated using LiDAR DEMs for Driveway for the 50-m buffer.

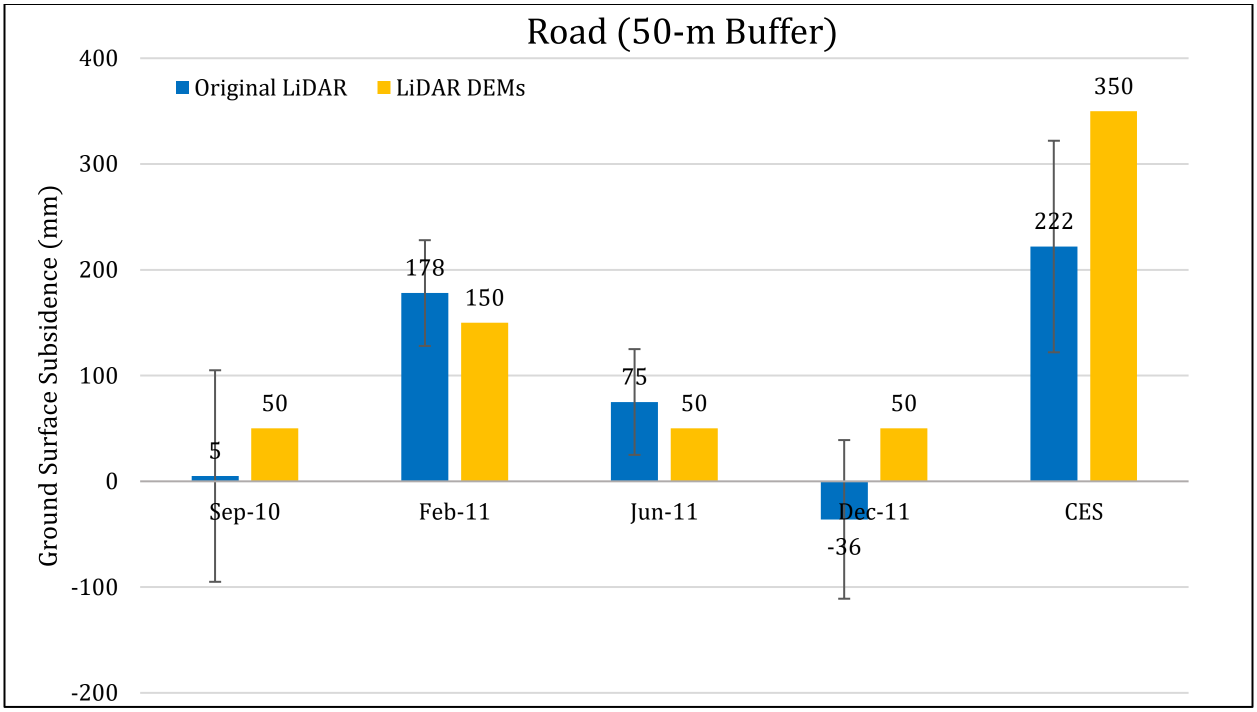

Figure 8: Comparison between ground surface subsidence determined from original LiDAR survey points and ground surface subsidence (50th %ile) estimated using LiDAR DEMs for Road.

Note 2: The ground surface subsidence values determined from original LiDAR survey points are generally similar to the ground surface subsidence values estimated using LiDAR DEMs for all earthquake events. The main discrepancy occurs for Patch A for the Feb-11 EQ wherein the LiDAR DEM estimate is ~100 mm higher than that obtained from the original LiDAR survey points.

Table 8a: Ejecta-Induced settlement for the top 20 m of the soil profile for Patch A for the 50th %ile PGA, P_L=50%, and C_{FC}=0.13 using BI-2014, ZRB-2002, and I_C cutoff of 2.6.

Earthquake Event(s)	M_W	PGA (g)	Depth to Groundwater (m)	S_T(mm)	S_{V1D} (mm)	$S_{E,L}$ (mm)
Sep-10	7.1	0.18	2.5	-19±125	17±20	-36±127
Feb-11	6.2	0.34	2.5	110±50	80±50	30±71
Jun-11	6.2	0.22	1.8	5±50	29±25	-24±56
Dec-11	6.1	0.30	1.5	20±75	87±50	-67±90

Notes: S_T = Total settlement (Table 6a); S_{V1D} = Average vertical settlement due to volumetric compression using Boulanger and Idriss (2014) (BI-2014), Zhang et al. (2002) (ZRB-2002) procedures and de Greef and Lengkeek (2018) thin-layer correction; $S_{E,L}$ = Ejecta-induced settlement as the difference between the LiDAR-based S_T and S_{V1D}.

Table 8b: Ejecta-Induced settlement for the top 20 m of the soil profile for Patch B for the 50th %ile PGA, P_L=50%, and C_{FC}=0.13 using BI-2014, ZRB-2002, and I_C cutoff of 2.6.

Earthquake Event(s)	M_W	PGA (g)	Depth to Groundwater (m)	S_T(mm)	S_{V1D} (mm)	$S_{E,L}$ (mm)
Sep-10	7.1	0.18	2.5	-42±150	16±20	-58±151
Feb-11	6.2	0.34	2.5	107±75	78±50	29±90
Jun-11	6.2	0.22	1.8	36±75	32±25	4±79
Dec-11	6.1	0.30	1.5	-22±100	76±50	-98±112

Notes: S_T = Total settlement (Table 6b); S_{V1D} = Average vertical settlement due to volumetric compression using Boulanger and Idriss (2014) (BI-2014), Zhang et al. (2002) (ZRB-2002) procedures and de Greef and Lengkeek (2018) thin-layer correction; $S_{E,L}$ = Ejecta-induced settlement as the difference between the LiDAR-based S_T and S_{V1D}.

Table 8c: Ejecta-Induced settlement for the top 20 m of the soil profile for Patch C for the 50th %ile PGA, P_L=50%, and C_{FC}=0.13 using BI-2014, ZRB-2002, and I_C cutoff of 2.6.

Earthquake Event(s)	M_W	PGA (g)	Depth to Groundwater (m)	S_T(mm)	S_{V1D} (mm)	$S_{E,L}$ (mm)
Sep-10	7.1	0.18	2.5	-12±150	16±20	-28±151
Feb-11	6.2	0.34	2.5	108±75	107±50	1±90
Jun-11	6.2	0.22	1.8	65±75	38±25	27±79
Dec-11	6.1	0.30	1.5	5±100	113±50	-108±112

Notes: S_T = Total settlement (Table 6c); S_{V1D} = Average vertical settlement due to volumetric compression using Boulanger and Idriss (2014) (BI-2014), Zhang et al. (2002) (ZRB-2002) procedures and de Greef and Lengkeek (2018) thin-layer correction; $S_{E,L}$ = Ejecta-induced settlement as the difference between the LiDAR-based S_T and S_{V1D}.

Table 8d: Ejecta-Induced settlement for the top 20 m of the soil profile for Driveway within the 20-m buffer for the 50th %ile PGA, P_L=50%, and C_{FC}=0.13 using BI-2014, ZRB-2002, and I_C cutoff of 2.6.

Earthquake Event(s)	M_W	PGA (g)	Depth to Groundwater (m)	S_T(mm)	S_{V1D} (mm)	$S_{E,L}$ (mm)
Sep-10	7.1	0.18	2.5	-19±25	17±20	-36±32
Feb-11	6.2	0.34	2.5	219±25	94±50	125±56
Jun-11	6.2	0.22	1.8	44±25	34±25	10±35
Dec-11	6.1	0.30	1.5	8±25	100±50	-92±56

Notes: S_T = Total settlement (Table 6d); S_{V1D} = Average vertical settlement due to volumetric compression using Boulanger and Idriss (2014) (BI-2014), Zhang et al. (2002) (ZRB-2002) procedures and de Greef and Lengkeek (2018) thin-layer correction; $S_{E,L}$ = Ejecta-induced settlement as the difference between the LiDAR-based S_T and S_{V1D}.

Table 8e: Ejecta-Induced settlement for the top 20 m of the soil profile for Driveway within the 50-m buffer for the 50th %ile PGA, P_L=50%, and C_{FC}=0.13 using BI-2014, ZRB-2002, and I_C cutoff of 2.6.

Earthquake Event(s)	M_W	PGA (g)	Depth to Groundwater (m)	S_T(mm)	S_{V1D} (mm)	S_E (mm)
Sep-10	7.1	0.18	2.5	-27±25	17±20	-44±32
Feb-11	6.2	0.34	2.5	208±25	94±50	114±56
Jun-11	6.2	0.22	1.8	42±25	34±25	8±35
Dec-11	6.1	0.30	1.5	6±25	100±50	-94±56

Notes: S_T = Total settlement (Table 6d); S_{V1D} = Average vertical settlement due to volumetric compression using Boulanger and Idriss (2014) (BI-2014), Zhang et al. (2002) (ZRB-2002) procedures and de Greef and Lengkeek (2018) thin-layer correction; $S_{E,L}$ = Ejecta-induced settlement as the difference between the LiDAR-based S_T and S_{V1D}.

Table 8f: Ejecta-Induced settlement for the top 20 m of the soil profile for Road within the for the 50th %ile PGA, P_L=50%, and C_{FC}=0.13 using BI-2014, ZRB-2002, and I_C cutoff of 2.6.

Earthquake Event(s)	M_W	PGA (g)	Depth to Groundwater (m)	S_T(mm)	S_{V1D} (mm)	S_E (mm)
Sep-10	7.1	0.18	2.5	5±100	16±20	-11±102
Feb-11	6.2	0.34	2.5	178±50	76±50	102±71
Jun-11	6.2	0.22	1.8	75±50	28±25	47±56
Dec-11	6.1	0.30	1.5	-36±75	74±50	-110±90

Notes: S_T = Total settlement (Table 6e); S_{V1D} = Average vertical settlement due to volumetric compression using Boulanger and Idriss (2014) (BI-2014), Zhang et al. (2002) (ZRB-2002) procedures and de Greef and Lengkeek (2018) thin-layer correction; $S_{E,L}$ = Ejecta-induced settlement as the difference between the LiDAR-based S_T and S_{V1D}.

Note 3: The uncertainty for volumetric settlement was derived based on the sensitivity of volumetric settlement to PGA, C_{FC}, and P_L for each earthquake event for VsVp 57203 *Shirley Intermediate School* and CC LIQ 1 – CPT 5586 – *Vivian St* sites. Taking the 50th percentile as the baseline case, the minimum and maximum values correspoding to the difference between the 25th percentile and the 50th percentile and the 75th percentile and the 50th percentile were determined. The arithmetic mean of the range of the minimum and maximum difference was evaluated for each patch at the two sites. The maximum arithmetic mean for each earthquake event was rounded to the nearest five and used as the uncertainty value. Accordingly, the 1-D volumetric settlement uncertainties of ±20, ±50, ±25, and ±50 mm for the Sep-10, Feb-11, Jun-11, and Dec-11 earthquake events, respectively, were used for all sites in this study.

Table 9a: Coverage area and height of ejecta estimates for Patch A using photographs.

Earthquake Event	$A_{E,thin}$ (m^2)	$H_{E,thin}$ (mm)	$A_{E,thick}$ (m^2)	$H_{E,thick}$ (mm)	$A_{E,cone}$ (m^2)	$H_{E,cone}$ (mm)	A_T (m^2)
Sep-10	0	0	0	0	0	0	98
Feb-11	13	50-100	50	100-180	7.6	200-300	98
Jun-11	41	10-30	16	50-100	0	0	98
Dec-11	2.0	20-30	11	30-50	0	0	98

Notes: $A_{E,thick/thin}$ = Coverage area of thick/thin ejecta layers; $H_{E,thick/thin}$ = Lower-upper estimate of height of thick/thin ejecta layers; Thin and thick layers correspond to light gray and dark gray colors of ejecta observed in aerial photographs; $A_{E,cone}$ = Coverage area of conically shaped ejecta layers; $H_{E,cone}$ = Lower-upper estimate of height of conically shaped ejecta layers; A_T = Total assessment area of a buffer being considered.

Table 9b: Coverage area and height of ejecta estimates for Patch B using photographs.

Earthquake Event	$H_{E,thin}$ (mm)	$A_{E,thin}$ (m^2)	$H_{E,thick}$ (mm)	$A_{E,thick}$ (m^2)	A_T (m^2)
Sep-10	0	0	0	0	20
Feb-11	10-30	20	0	0	20
Jun-11	0	0	0	0	20
Dec-11	0	0	0	0	20

Notes: $A_{E,thick/thin}$ = Coverage area of thick/thin ejecta layers; $H_{E,thick/thin}$ = Lower-upper estimate of height of thick/thin ejecta layers; Thin and thick layers correspond to light gray and dark gray colors of ejecta observed in aerial photographs; A_T = Total assessment area of a buffer being considered.

Table 9c: Coverage area and height of ejecta estimates for Patch C using photographs.

Earthquake Event	$H_{E,thin}$ (mm)	$A_{E,thin}$ (m^2)	$A_{E,thick}$ (m^2)	$H_{E,thick}$ (m)	A_T (m^2)
Sep-10	0	0	0	0	63
Feb-11	0	0	0	0	63
Jun-11	0	0	0	0	63
Dec-11	0	0	0	0	63

Notes: $A_{E,thick/thin}$ =Coverage area of thick/thin ejecta layers; $H_{E,thick/thin}$ = Lower-upper estimate of height of thick/thin ejecta layers; Thin and thick layers correspond to light gray and dark gray colors of ejecta observed in aerial photographs; A_T= Total assessment area of a buffer being considered.

Table 9d: Coverage area and height of ejecta estimates for Driveway within the 20-m buffer using photographs.

EQ Event	$H_{E,thin1}$ (mm)	$A_{E,thin1}$ (m²)	$H_{E,thin2}$ (mm)	$A_{E,thin2}$ (m²)	$H_{E,thick1}$ (mm)	$A_{E,thick1}$ (m²)	$H_{E,thick2}$ (mm)	$A_{E,thick2}$ (m²)	A_T (m²)
Sep-10	0	0	0	0	0	0	0	0	85
Feb-11	0	0	5-10	68	8-16	8	10-20	9	85
Jun-11	0	0	0	0	30-60	6.4	0	0	85
Dec-11	0	0	0	0	0	0	0	0	85

Notes: $A_{E,thick/thin}$ =Coverage area of thick/thin ejecta layers; $H_{E,thick/thin}$ = Lower-upper estimate of height of thick/thin ejecta layers; Thin and thick layers correspond to light gray and dark gray colors of ejecta observed in aerial photographs; A_T= Total assessment area of a buffer being considered.

Table 9e: Coverage area and height of ejecta estimates for Driveway within the 50-m buffer using photographs.

EQ Event	$H_{E,thin1}$ (mm)	$A_{E,thin1}$ (m²)	$H_{E,thin2}$ (mm)	$A_{E,thin2}$ (m²)	$H_{E,thick1}$ (mm)	$A_{E,thick1}$ (m²)	$H_{E,thick2}$ (mm)	$A_{E,thick2}$ (m²)	A_T (m²)
Sep-10	0	0	0	0	0	0	0	0	124
Feb-11	2-4	23	5-10	84	8-16	8	10-20	9	124
Jun-11	0	0	0	0	30-60	6.4	0	0	124
Dec-11	0	0	0	0	0	0	0	0	124

Notes: $A_{E,thick/thin}$ =Coverage area of thick/thin ejecta layers; $H_{E,thick/thin}$ = Lower-upper estimate of height of thick/thin ejecta layers; Thin and thick layers correspond to light gray and dark gray colors of ejecta observed in aerial photographs; A_T= Total assessment area of a buffer being considered.

Table 9f: Coverage area and height of ejecta estimates for Road within the 50-m buffer using photographs.

EQ Event	$H_{E,thick}$ (mm)	$A_{E,thick}$ (m²)	$H_{E,thin2}$ (mm)	$A_{E,thin2}$ (m²)	$H_{E,thin1}$ (mm)	$A_{E,thin1}$ (m²)	$H_{E,pyr/prism}$ (mm)	$V_{E,pyr+prism}$ (m³)	A_T (m²)
Sep-10	0	0	0	0	0	0	0	0	874
Feb-11	40-80	4.8	10-20	1.8	3-6	700	0	0	768
Jun-11	20-40	7.7	4-8	24	0	0	0	0	894
Dec-11	0	0	0	0	0	0	15-65	0.28-0.55	880

Notes: $A_{E,thick/thin}$ =Coverage area of thick/thin ejecta layers; $H_{E,thick/thin}$ = Lower-upper estimate of height of thick/thin ejecta layers; Thin and thick layers correspond to light gray and dark gray colors of ejecta observed in aerial photographs; $H_{E,prism+pyr}$ = Lower-upper estimate of ejecta height near the curb based on 2-4% cross slope of normal crown; $V_{E,prism+pyr}$ = Lower-upper estimate of total volume of prismatic- and pyramidal-shape ejecta; A_T= Total assessment area of a buffer being considered.

Note 4: The values in Table 9 correspond to the coverage area of ejecta outlined in aerial photographs (Figures 101 through 105) and the lower and upper estimates of ejecta height based on geometry, ground photographs (Figures 106 through 109), and EQC LDAT property inspection notes (Figures 110 through 112) and reports from August 2011 (up to 200 mm in height of ejected material within Patch A, traces of ejecta within Patch B). The ejecta-induced settlement using photographs and engineering judgment, $S_{E,P}$, is estimated as

$$S_{E,P} = \frac{\sum_{i=1}^{a} A_{E,thick,i} * H_{E,thick,i} + \sum_{j=1}^{b} A_{E,thin,j} * H_{E,thin,j}}{A_T} + \frac{\frac{1}{3}\sum_{m=1}^{e} A_{E,cone,m} * H_{E,cone,m} + \frac{1}{2}\sum_{n=1}^{f} W_{E,prism,n} * H_{E,prism,n} * L_{E,prism,n}}{A_T} + \frac{\frac{1}{3}\sum_{p=1}^{g} W_{E,pyramid,p} * H_{E,pyramid} * L_{E,pyramid}}{A_T} = \frac{\sum_{i=1}^{a} V_{E,thick,i} + \sum_{j=1}^{b} V_{E,thin,j}}{A_T} + \frac{\sum_{m=1}^{e} V_{E,cone,m} + \sum_{n=1}^{f} V_{E,prism,n} + \sum_{p=1}^{g} V_{E,pyramid,p}}{A_T}$$

where

- $A_{E,thick,i}$ and $H_{E,thick,i}$ are the area and the height of a thick ejecta layer, respectively;
- $A_{E,thin,j}$ and $H_{E,thin,j}$ are the area and the height of a thin ejecta layer, respectively;
- $A_{E,cone,m}$ and $H_{E,cone,m}$ are the aerea and the height of a conically shaped ejecta, respectively;
- $W_{E,prism,n}$ and $L_{E,prism,n}$ are the width and the length of the coverage area of a prismatically shaped ejecta layer, respectively, and $H_{E,prism,n}$ is the height of a prism-like ejecta layer;
- $W_{E,pyr,p}$ and $L_{E,pyr,p}$ are the width and the length of the coverage area of a pyramid-like ejecta layer, respectively, and $H_{E,pyr,p}$ is the height of a pyramid-like ejecta layer;
- A_T is the total assessment area for a buffer being considered (Figure 1).

Table 10a: Ejecta-induced settlement estimates for Patches A, B, and C based on photographs.

Earthquake Event	Patch A		Patch B		Patch C	
	$S_{E,P,lower}$ (mm)	$S_{E,P,upper}$ (mm)	$S_{E,P,lower}$ (mm)	$S_{E,P,lower}$ (mm)	$S_{E,P,lower}$ (mm)	$S_{E,P,upper}$ (mm)
Sep-10	0	0	0	0	0	0
Feb-11	63	113	10	30	0	0
Jun-11	12	29	0	0	0	0
Dec-11	4	6	0	0	0	0

Note: $S_{E,P,lower}$ and $S_{E,P,upper}$ correspond to lower and upper estimates of $S_{E,P}$, respectively.

Table 10b: Ejecta-induced settlement estimates for Driveway and Road based on photographs.

Earthquake Event	Driveway (20-m buffer)		Driveway (50-m buffer)		Road (50-m buffer)	
	$S_{E,P,lower}$ (mm)	$S_{E,P,upper}$ (mm)	$S_{E,P,lower}$ (mm)	$S_{E,P,upper}$ (mm)	$S_{E,P,lower}$ (mm)	$S_{E,P,upper}$ (mm)
Sep-10	0	0	0	0	0	0
Feb-11	6	12	5	10	3	6
Jun-11	2	5	2	3	≈0	1
Dec-11	0	0	0	0	≈0	1

Note: $S_{E,P,lower}$ and $S_{E,P,upper}$ correspond to lower and upper estimates of $S_{E,P}$, respectively.

Table 11a: Best final estimates of ejecta-induced settlement for Patches A, B, and C.

EQ Event	Patch A			Patch B			Patch C		
	$S_{E,L}$ (mm)	$S_{E,P}$ (mm)	$S_{E,final}$ (mm)	$S_{E,L}$ (mm)	$S_{E,P}$ (mm)	$S_{E,final}$ (mm)	$S_{E,L}$ (mm)	$S_{E,P}$ (mm)	$S_{E,final}$ (mm)
Sep-10	-36±127	0	0	-58±151	0	0	-28±151	0	0
Feb-11	30±71	88±25	90±25	29±90	20±10	20±10	1±90	0	0
Jun-11	-24±56	21±8	20±10	4±79	0	0	27±79	0	0
Dec-11	-67±90	5±1	5±5	-98±112	0	0	-108±112	0	0

Notes: $S_{E,L}$ = Ejecta-induced settlement based on LiDAR data reported in Table 8; $S_{E,P}$ = Median ejecta-induced settlement for the range of values reported in Table 10; $S_{E,final}$ = Best final estimate of ejecta-induced settlement rounded to the nearest 5; Final plus/minus values are also rounded to the nearest 5.

Table 11b: Best final estimates of ejecta-induced settlement for Driveway and Road.

EQ Event	Driveway (20-m buffer)			Driveway (50-m buffer)			Road (50-m buffer)		
	$S_{E,L}$ (mm)	$S_{E,P}$ (mm)	$S_{E,final}$ (mm)	$S_{E,L}$ (mm)	$S_{E,P}$ (mm)	$S_{E,final}$ (mm)	$S_{E,L}$ (mm)	$S_{E,P}$ (mm)	$S_{E,final}$ (mm)
Sep-10	-36±32	0	0	-44±32	0	0	-11±102	0	0
Feb-11	125±56	9±3	10±5	114±56	7.5±2.5	10±5	102±71	4.5±1.5	5±5
Jun-11	10±35	3.5±1.5	5±5	8±35	2.5±0.5	5±5	47±56	0.5±0.5	<5
Dec-11	-92±56	0	0	-94±56	0	0	-110±90	0.5±0.5	<5

Notes: $S_{E,L}$ = Ejecta-induced settlement based on LiDAR data reported in Table 8; $S_{E,P}$ = Median ejecta-induced settlement for the range of values reported in Table 10; $S_{E,final}$ = Best final estimate of ejecta-induced settlement rounded to the nearest 5; Final plus/minus values are also rounded to the nearest 5.

Note 5:

- $S_{E,final}$ for Patches A, B, and C, Driveway, and Road is based solely on $S_{E,P}$ for all earthquake events. The uncertainty associated with $S_{E,final}$ is also based on $S_{E,P}$-related uncertainty only.
- The weights are based on the LiDAR error bands, LPI prediction error (Maurer et al. 2014[3]), presence of ejecta at the site at the time of LiDAR surveys, discrepancy between visual evidence and LiDAR-based ejecta-induced settlement estimates, and completeness of visual evidence (i.e., ground and aerial photographs and EQC LDAT property inspection reports for the site). The Parnwell St and Bassett St site is in the apparent zone of higher ground surface subsidence for the Sep-10 EQ (i.e., the overestimate of the ground surface elevation by the Jul-03 LiDAR survey). The site is also in the zone of slight to moderate LPI overprediction of liquefaction severity for the Sep-10 and Feb-11 EQs. The LDAT property inspection reports and ground photographs are available for Patches A and B and partially for Patch C. There are no ground photographs of the driveway and the road.

<u>**Summary 1**</u>:

- **The best estimate of the ejecta-induced free-field ground settlement at the Parnwell St and Bassett St site for the SEP 2010, JUN 2011, and DEC 2011 earthquake is 0 mm, 20±10 mm,**

[3] Maurer, B. W., Green, R. A., Cubrinovski, M., & Bradley, B. A. (2014). Evaluation of the Liquefaction Potential Index for Assessing Liquefaction Hazard in Christchurch, New Zealand. *Journal of Geotechnical and Geoenvironmental Engineering*, 140(7), 04014032-1-11. doi:10.1061/(asce)gt.1943-5606.0001117

and 5±5 mm, respectively. During the FEB 2011 earthquake, about 30% of the site's unobstructed area experienced the ejecta-induced ground settlement of 90±25 mm.

- **The best estimate of the ejecta-induced free-field ground settlement of the road at the Parnwell St and Bassett St site for the SEP 2010, FEB 2011, JUN 2011, and DEC 2011 earthquake is 0 mm, 5±5 mm, <5 mm, and <5 mm, respectively.**

Note 6: CPT 27709 was initially named as CC LIQ 2.

Figure 9: Location of the site.

Figure 10: Position of the site relative to nearby buildings, vegetation, and free-face features.

Figure 11: Street view of the flat land.

Figure 12: Satellite image of the site taken in Dec 2004.

Figure 13: Satellite image of the site taken in Mar 2009.

Figure 14: Satellite image of the site taken on 8 Mar 2011.

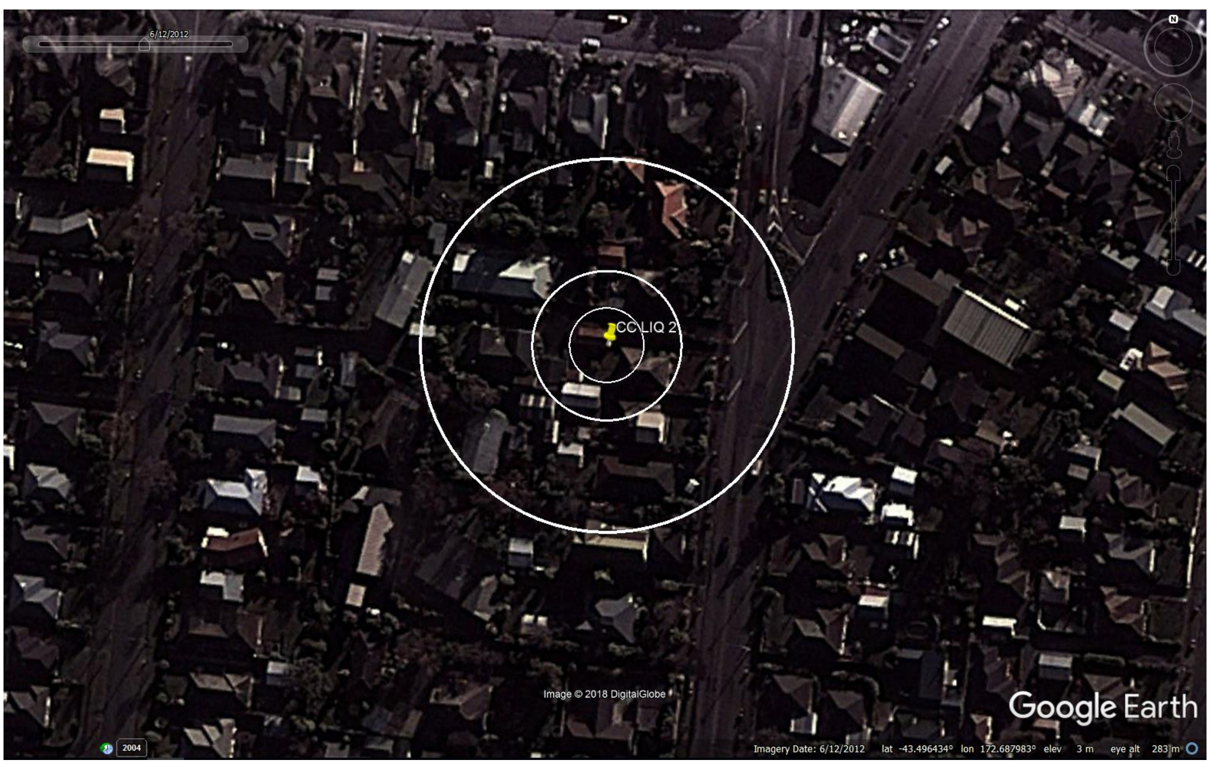

Figure 15: Satellite image of the site taken in Jun 2012.

Figure 16: Satellite image of the site taken in Oct 2012.

Figure 17: Satellite image of the site taken in Jul 2015.

Figure 18: Satellite image of the site taken in Jul 2015.

Figure 19: Satellite image of the site taken in Sep 2015.

Figure 20: Satellite image of the site taken in Nov 2015.

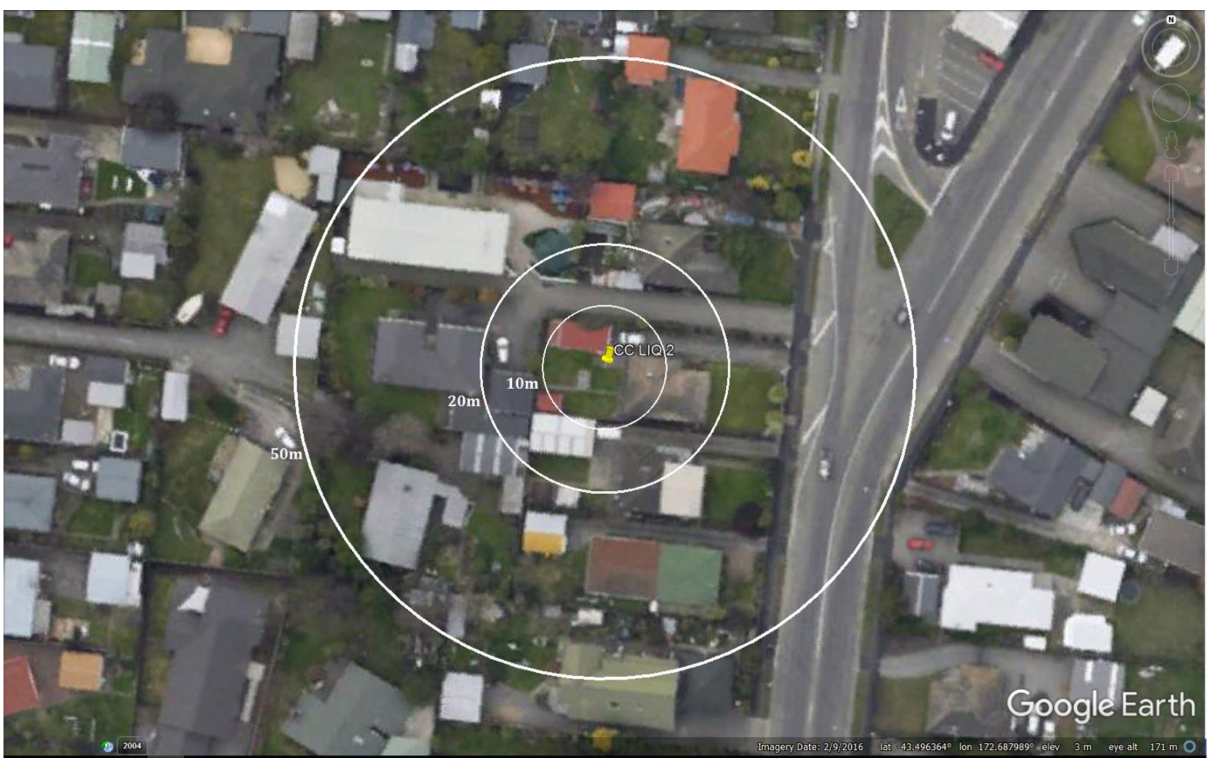

Figure 21: Aerial photograph of the site taken on Sep 4, 2010.

Figure 22: Aerial photograph of the site taken on Feb 24, 2011.

Figure 23: Aerial photograph of the site taken on June 14-15, 2011.

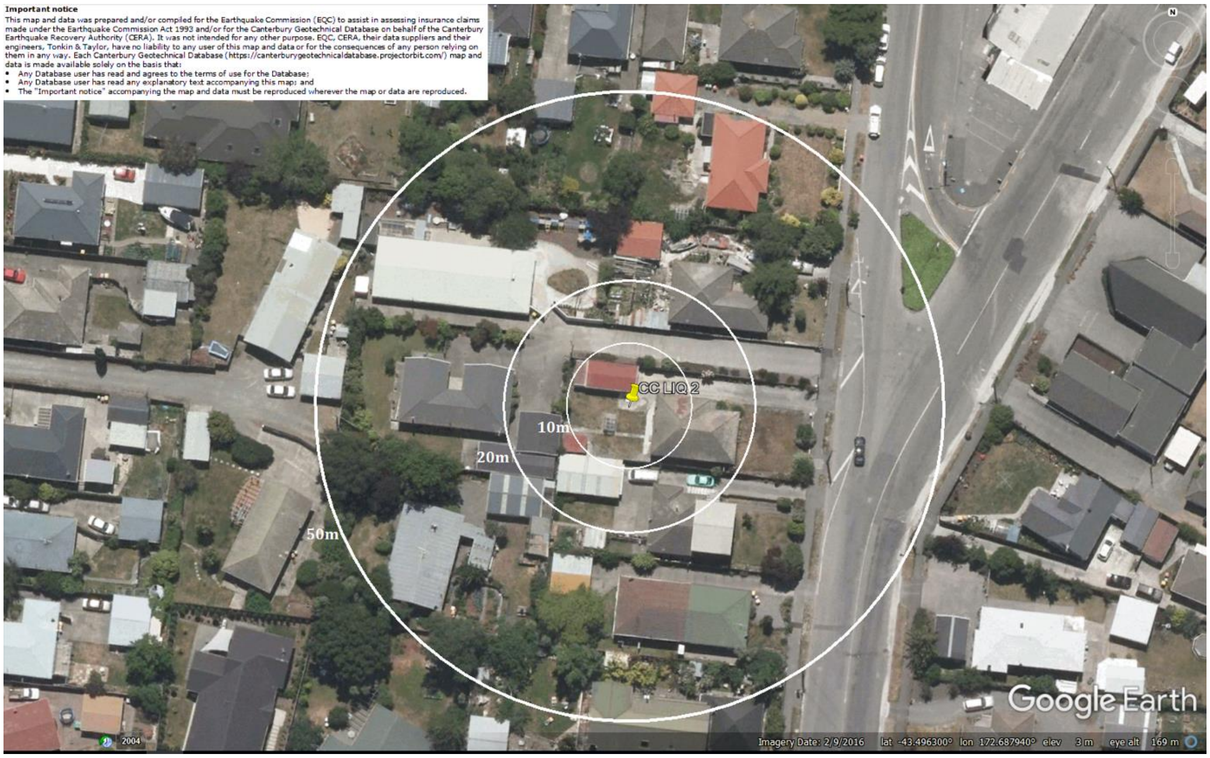

Figure 24: Aerial photograph of the site taken on Dec 24, 2012.

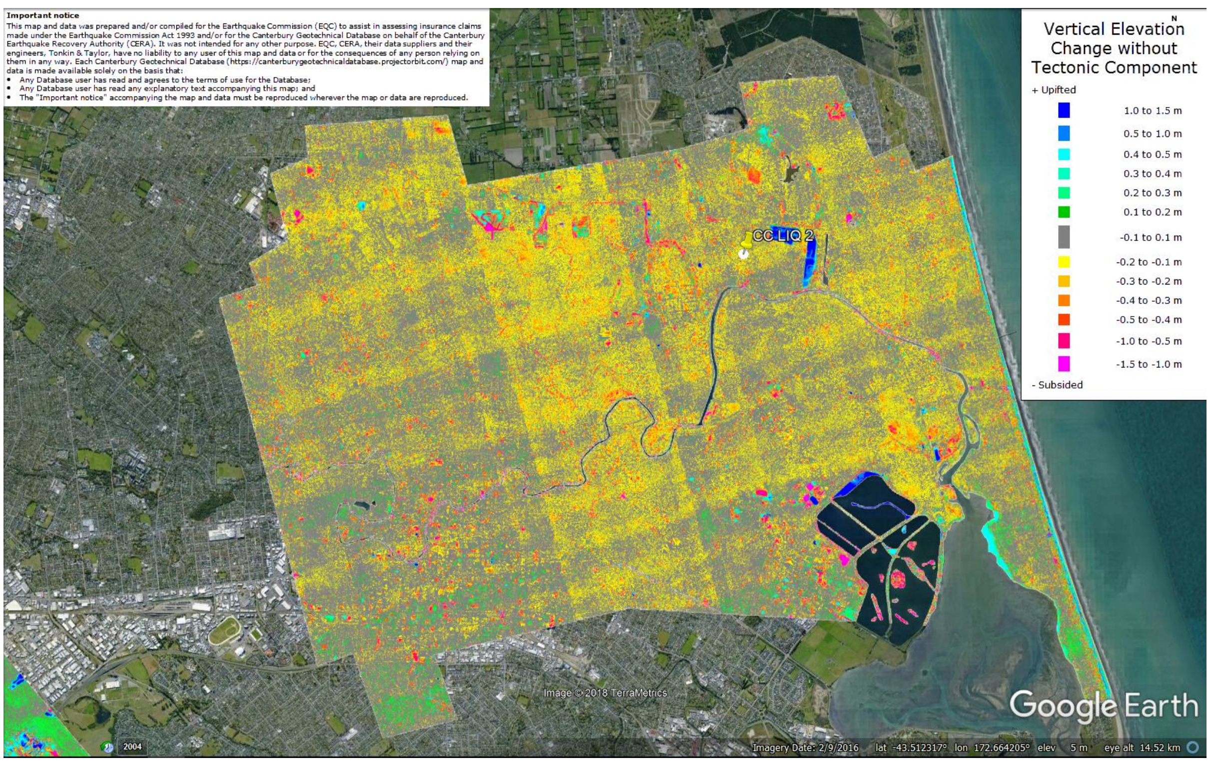

Figure 25: Vertical Ground Movements (Surface – Tectonic) for Sep 2010 Earthquake – the site is in the apparent zone of overestimated ground surface subsidence (i.e., flight error band for July 2003).

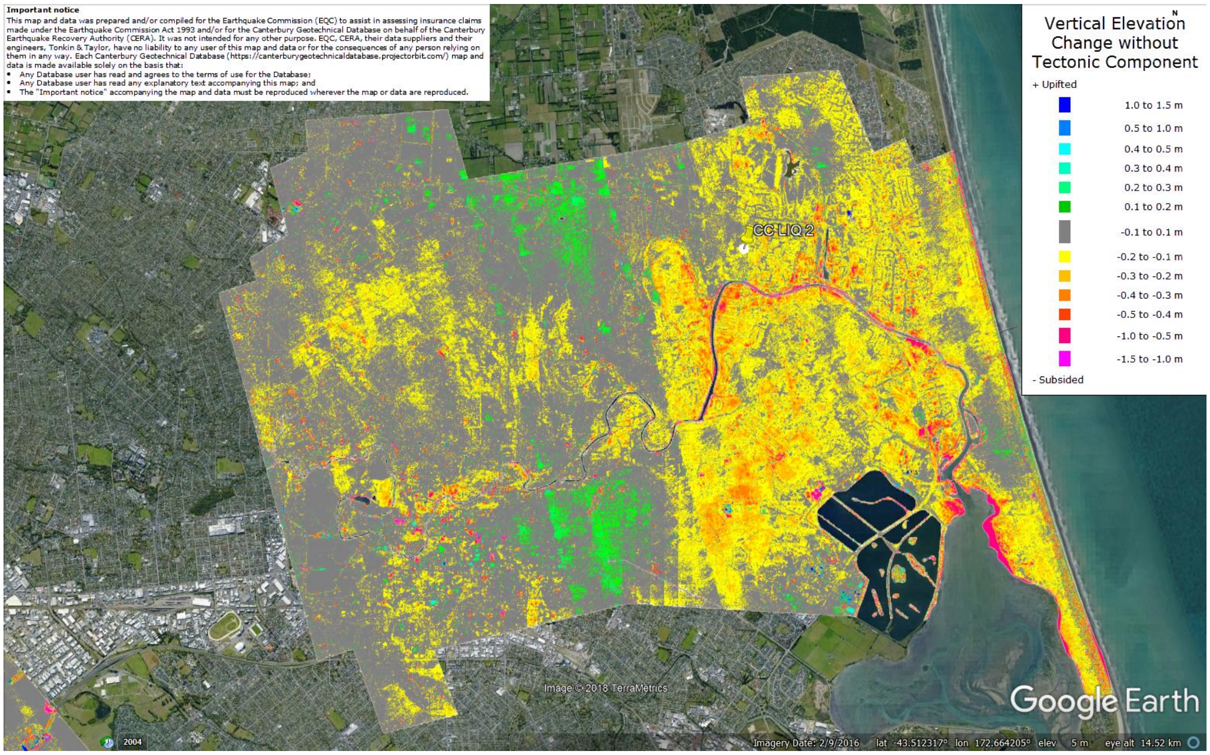

Figure 26: Vertical Ground Movements (Surface – Tectonic) for Feb 2011 Earthquake – the site is not in the apparent zone of underestimated ground surface subsidence.

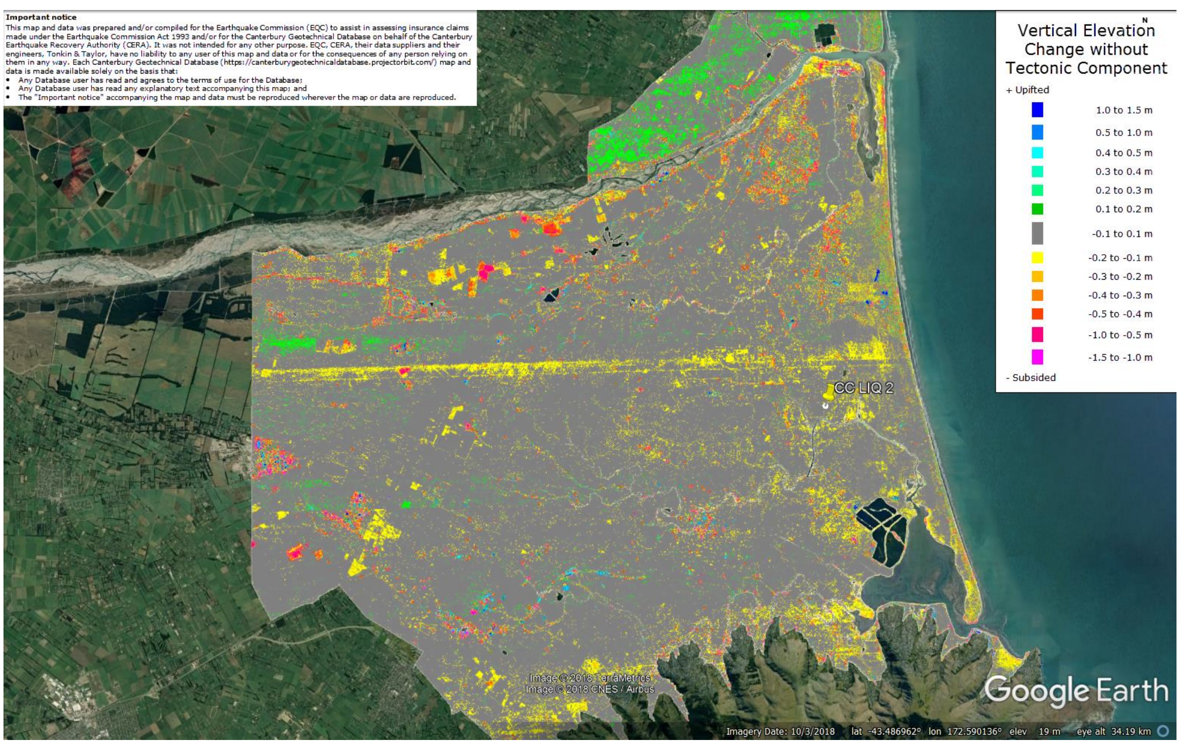

Figure 27: Vertical Ground Movements (Surface – Tectonic) for June 2011 Earthquake – the site is not in the apparent zone of overestimated or underestimated ground surface subsidence.

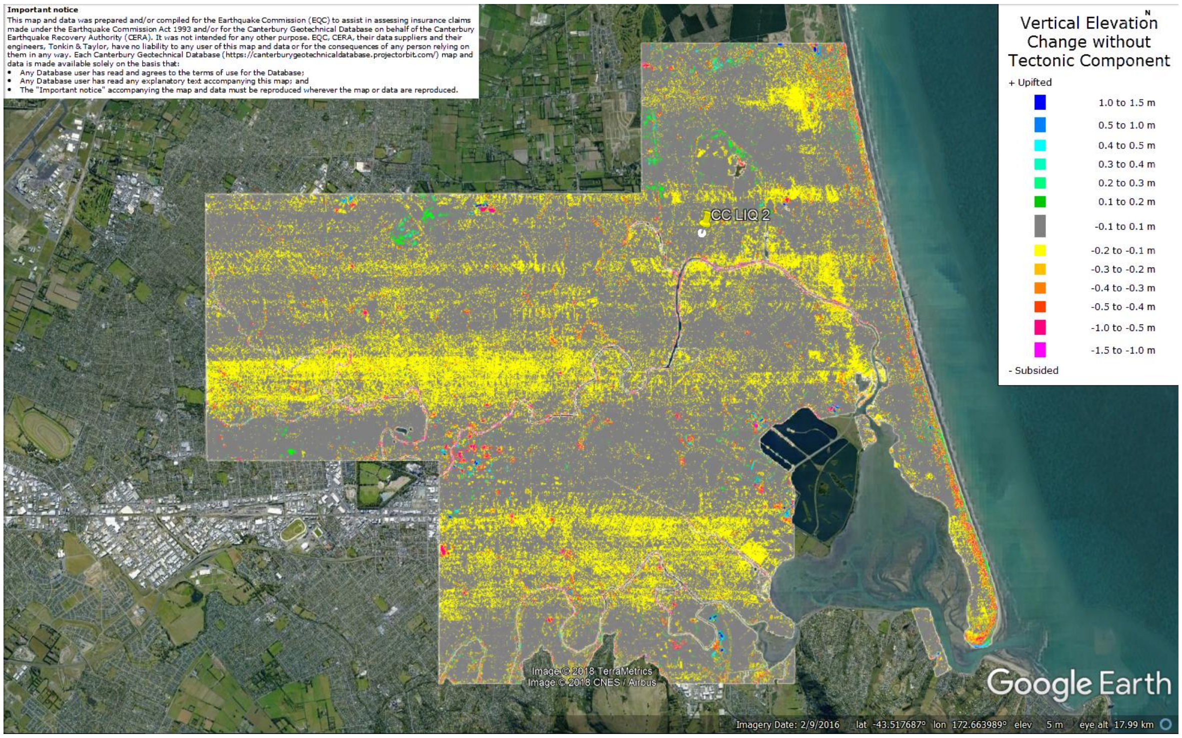

Figure 28: Vertical Ground Movements (Surface – Tectonic) for Dec 2011 Earthquake – the site is not in the apparent zone of overestimated or underestimated ground surface subsidence.

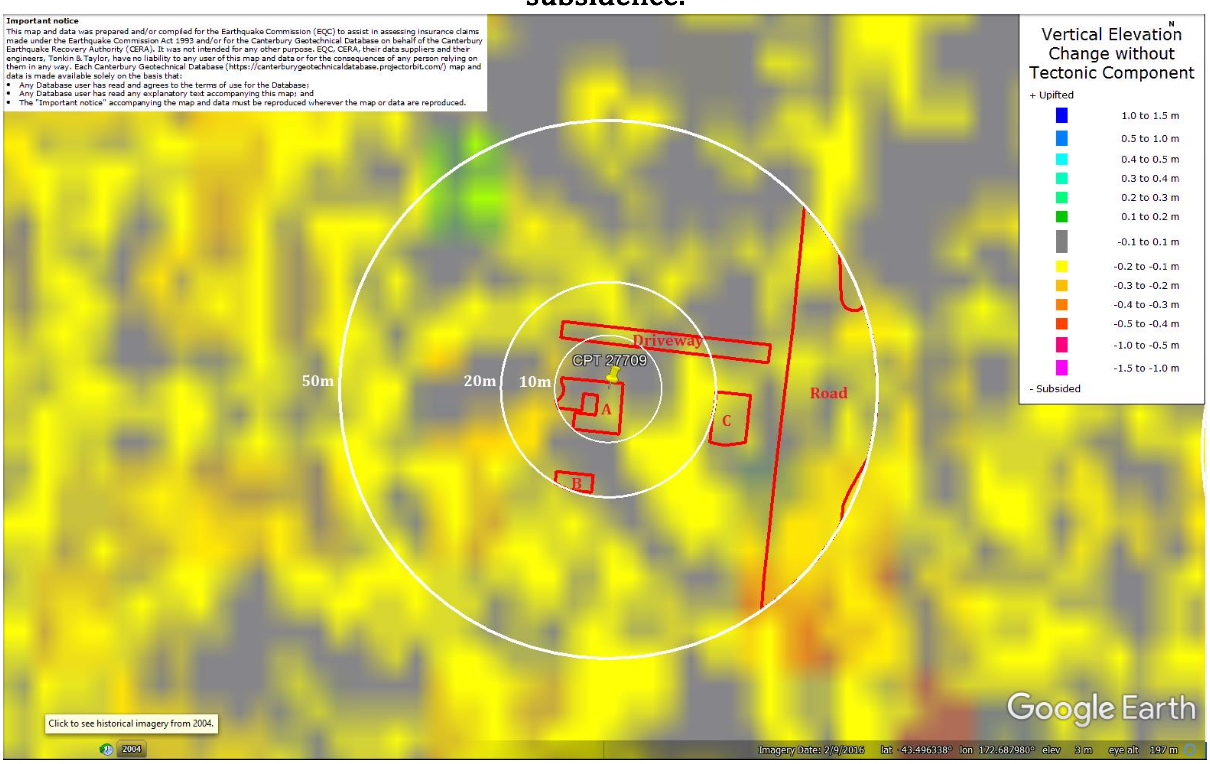

Figure 29: Ground surface subsidence without tectonic component for Sep 2010 Earthquake according to the LiDAR DEM.

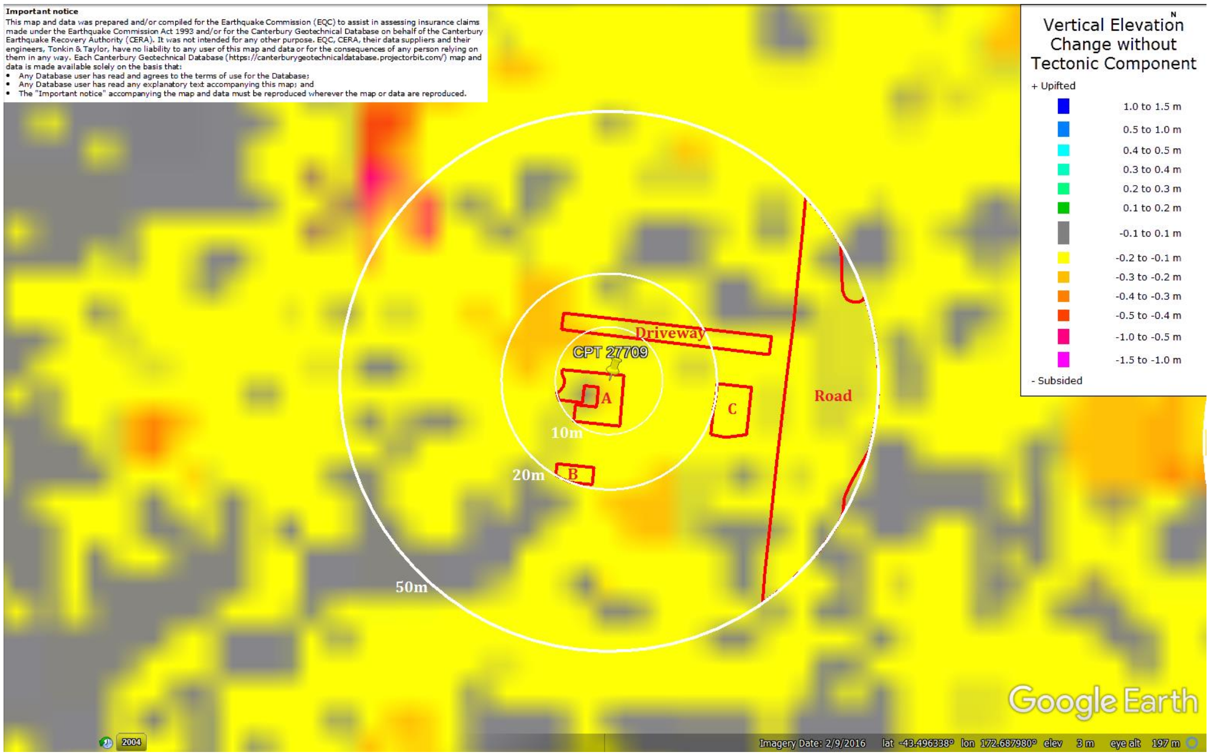

Figure 30: Ground surface subsidence without tectonic component for Feb 2011 Earthquake according to the LiDAR DEM.

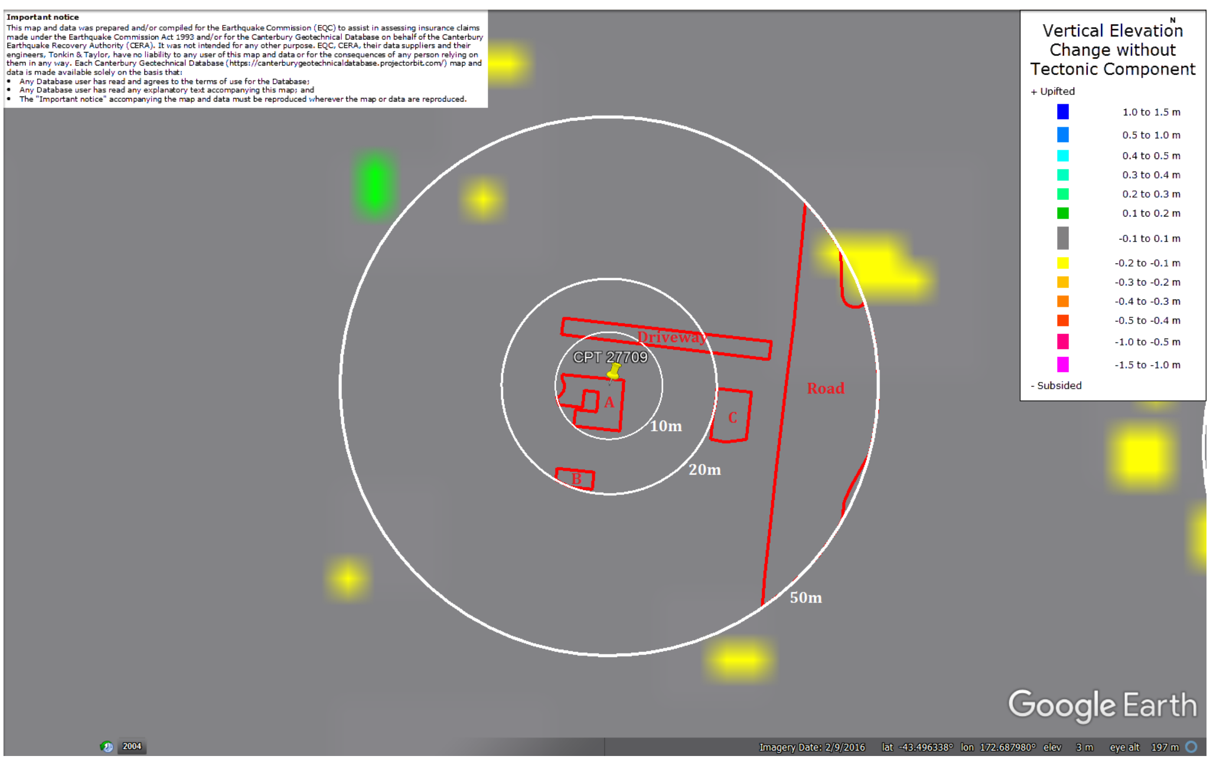

Figure 31: Ground surface subsidence without tectonic component for Jun 2011 Earthquake according to the LiDAR DEM.

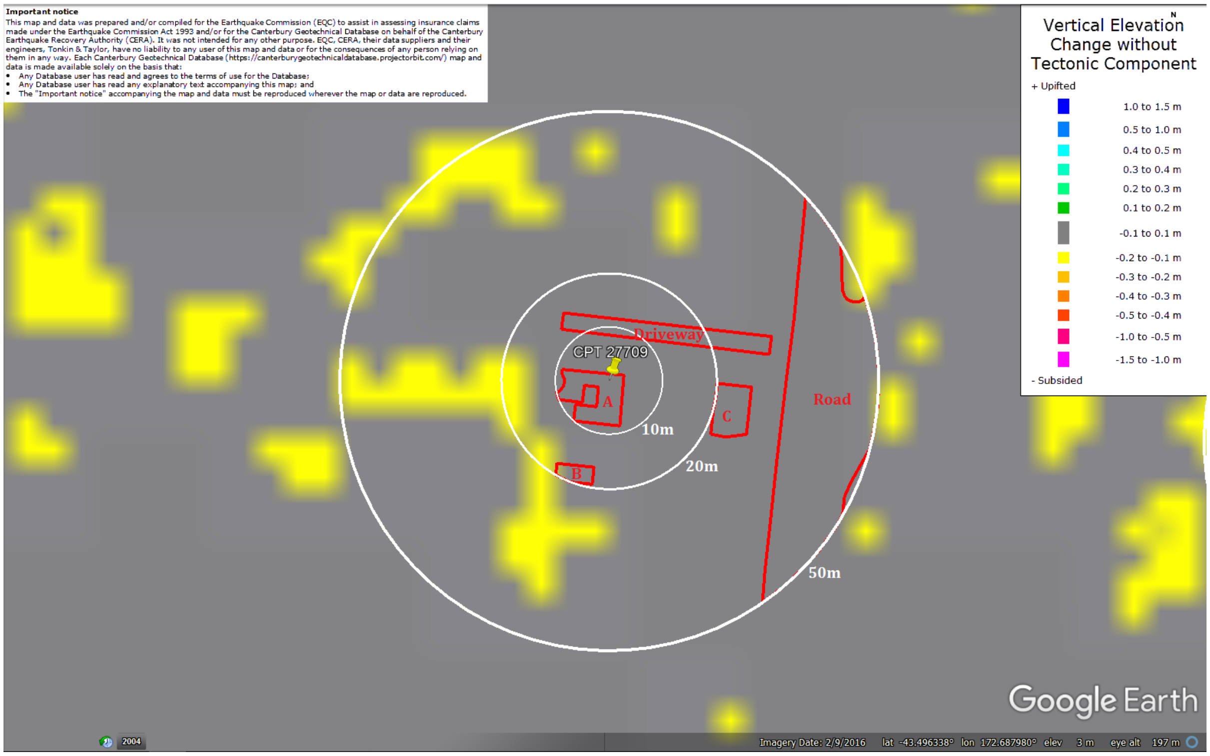

Figure 32: Ground surface subsidence without tectonic component for Dec 2011 Earthquake according to the LiDAR DEM.

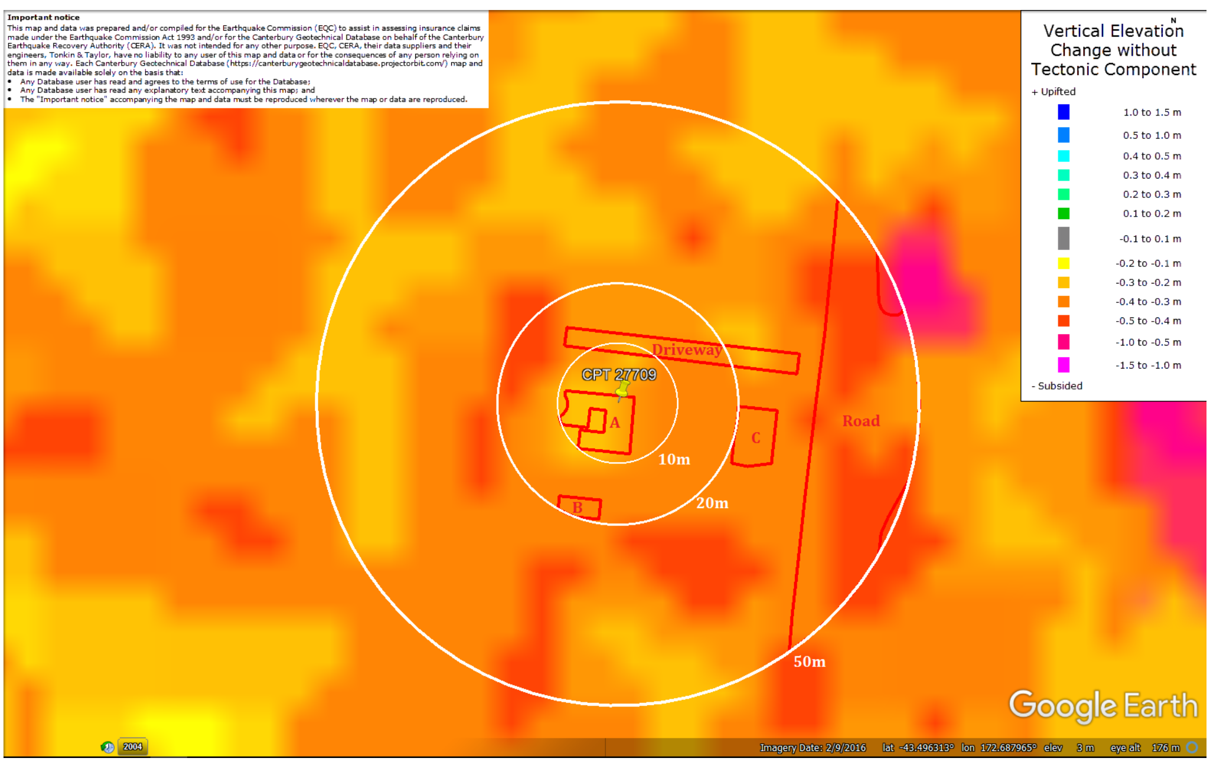

Figure 33: Ground surface subsidence without tectonic component for Canterbury Earthquake Sequence according to the LiDAR DEM.

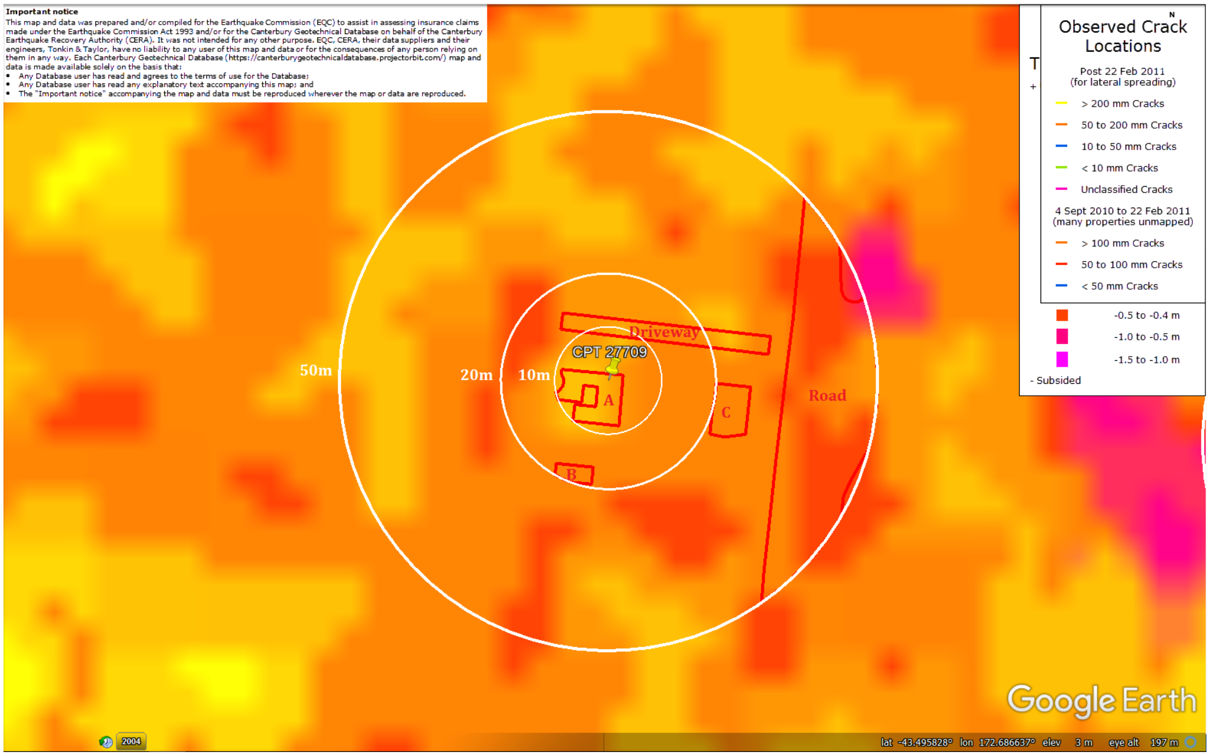

Figure 34: Absence of ground cracks indicating no lateral spreading for Canterbury Earthquake Sequence.

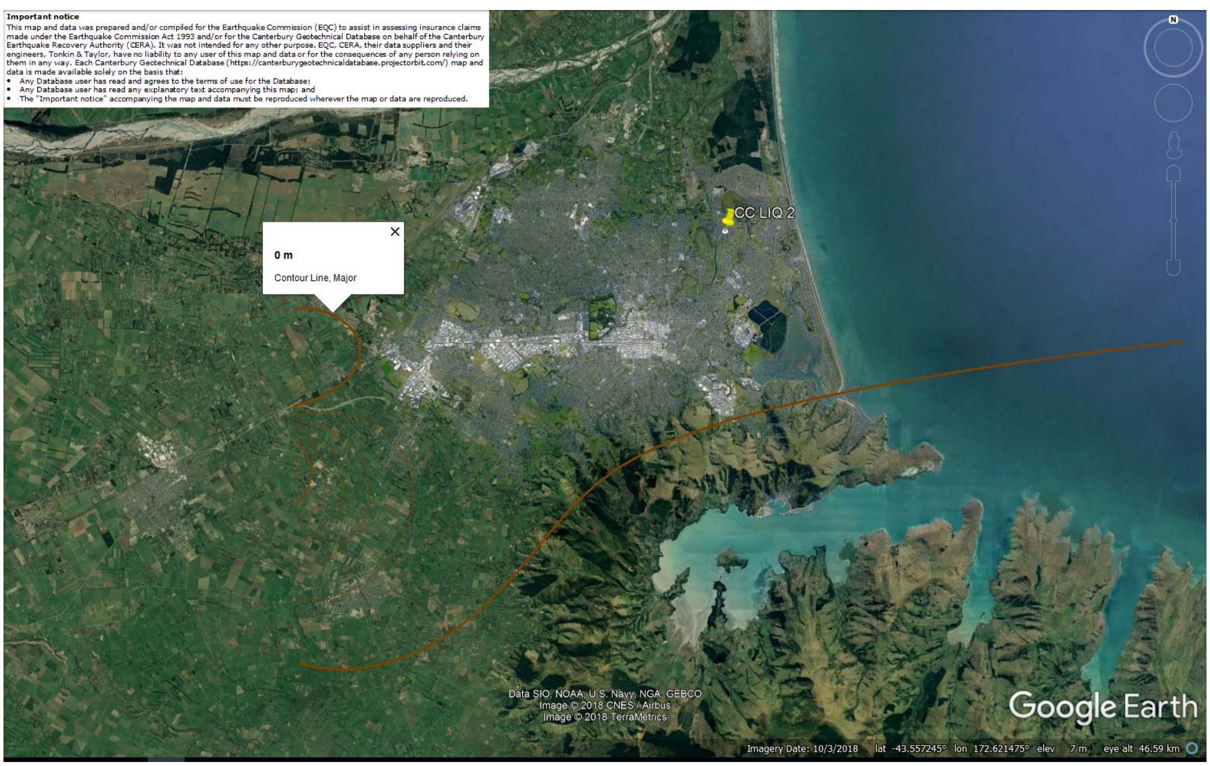

Figure 35: Vertical tectonic movements for Sep 2010 Earthquake.

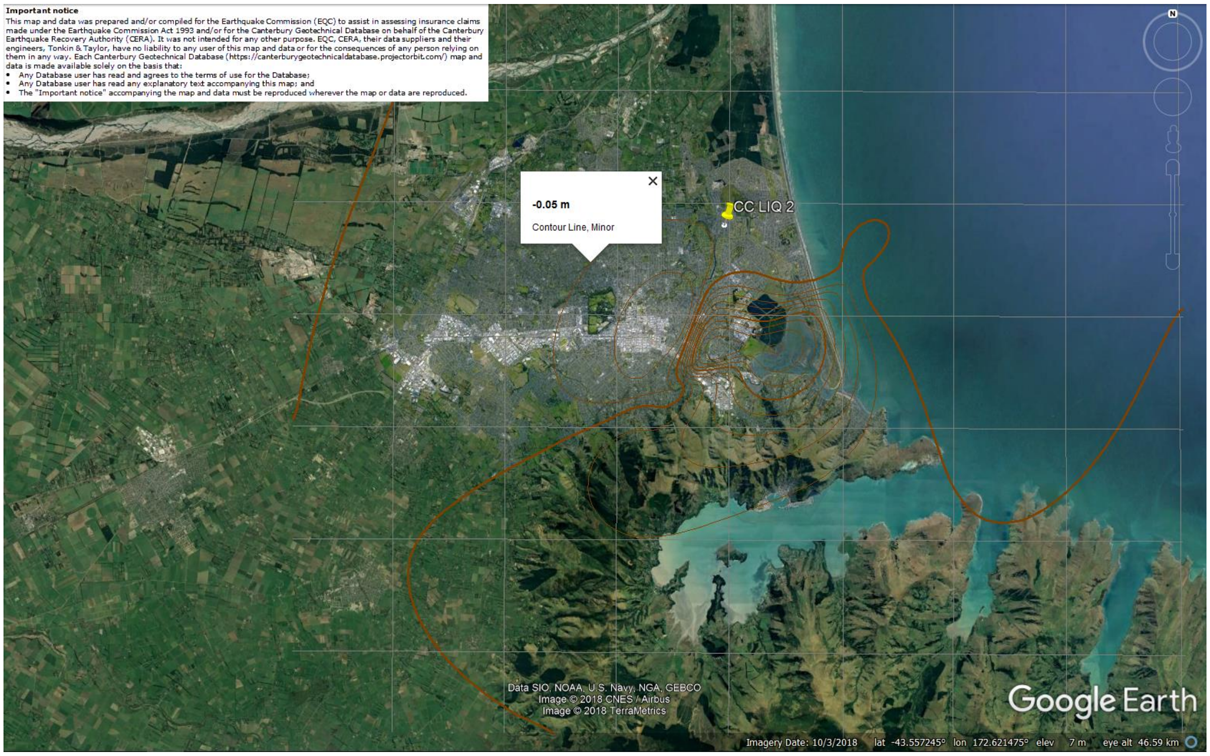

Figure 36: Vertical tectonic movements for Feb 2011 Earthquake.

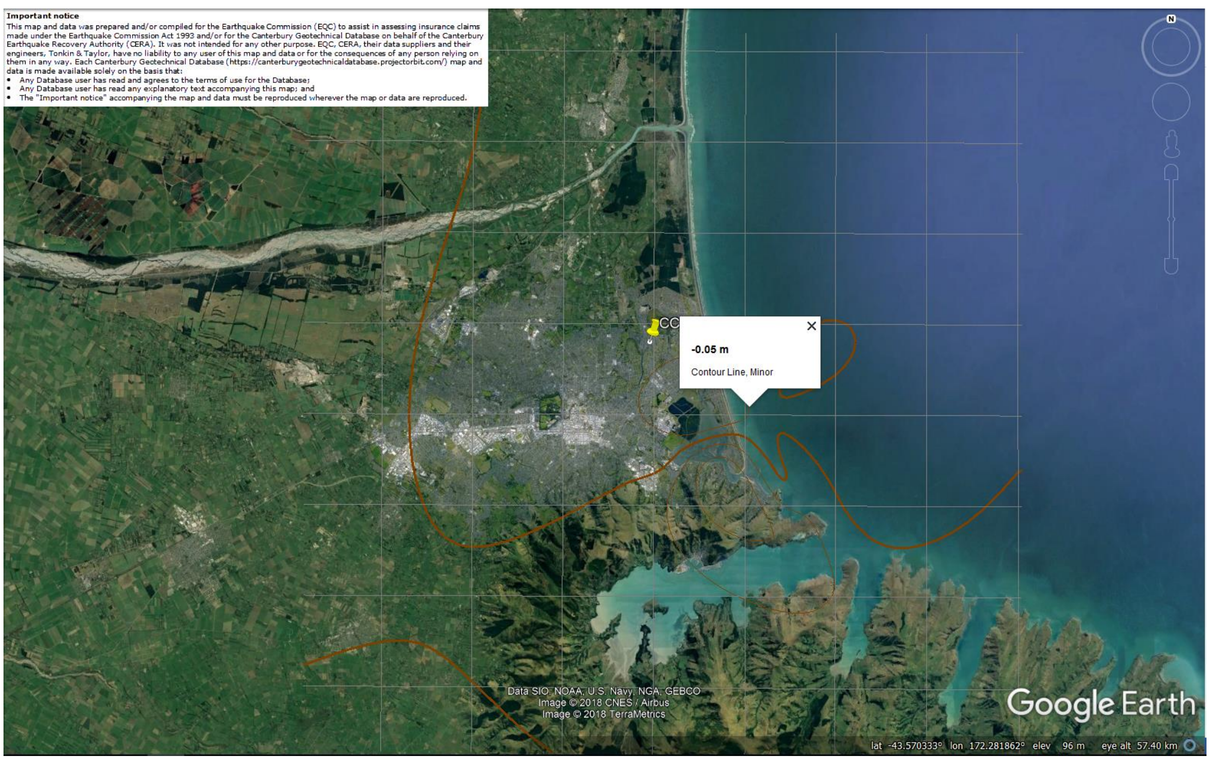

Figure 37: Vertical tectonic movements for June 2011 Earthquake.

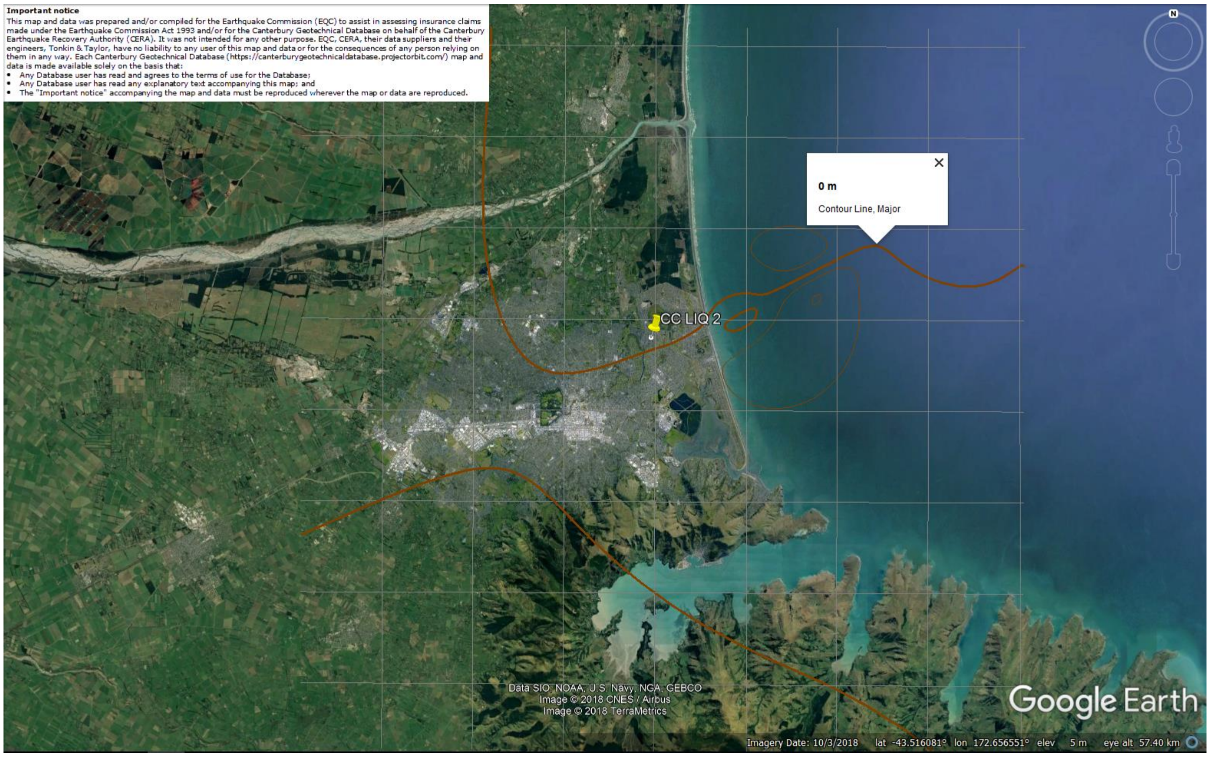

Figure 38: Vertical tectonic movements for Dec 2011 Earthquake.

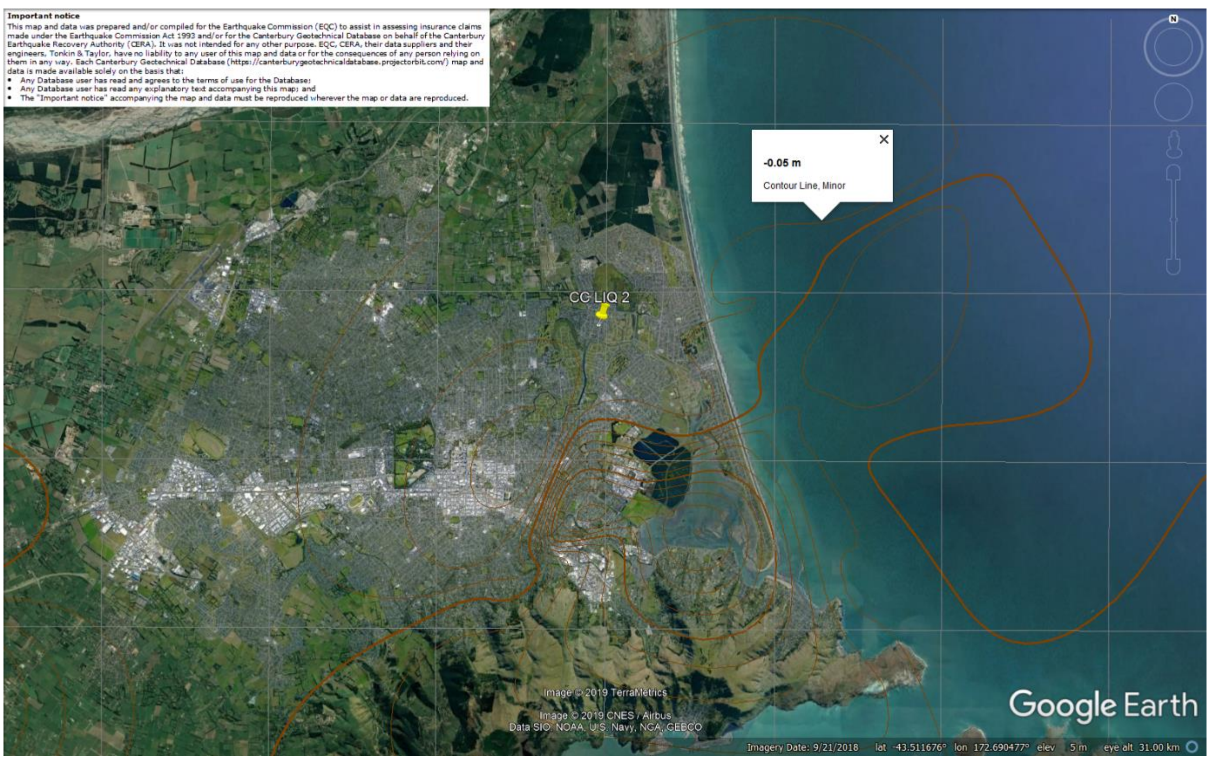

Figure 39: Vertical tectonic movements for Canterbury Earthquake Sequence.

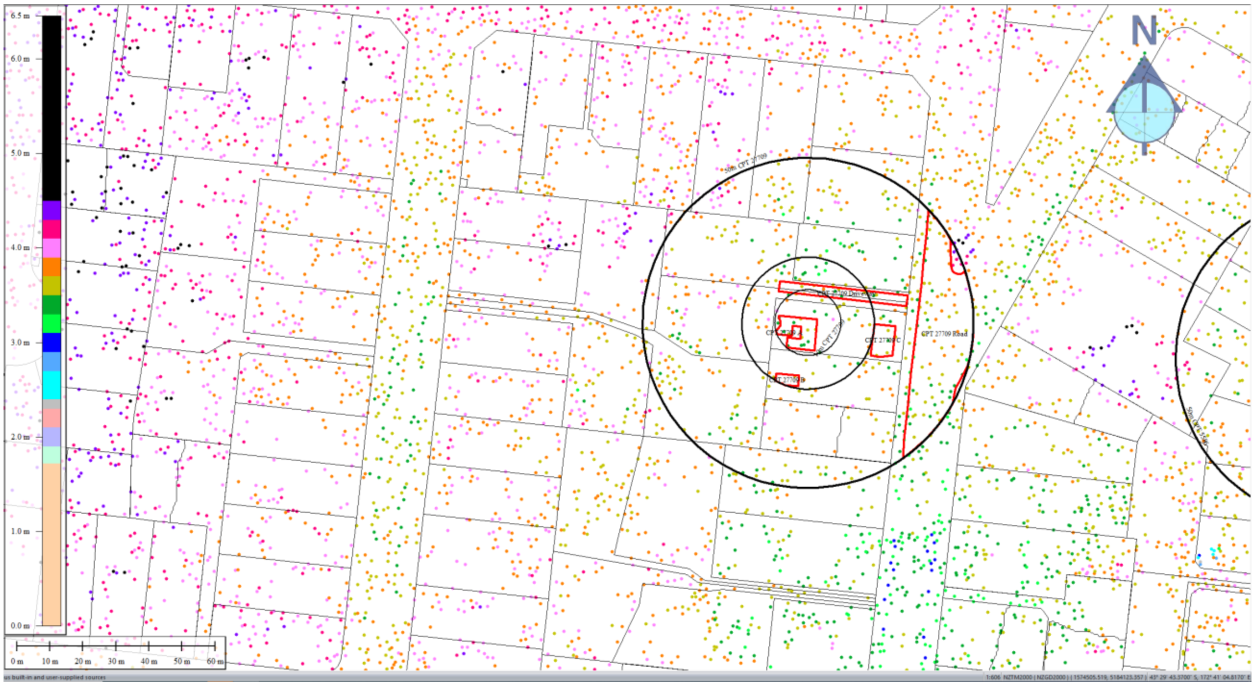

Figure 40: Jul 2003 LiDAR survey.

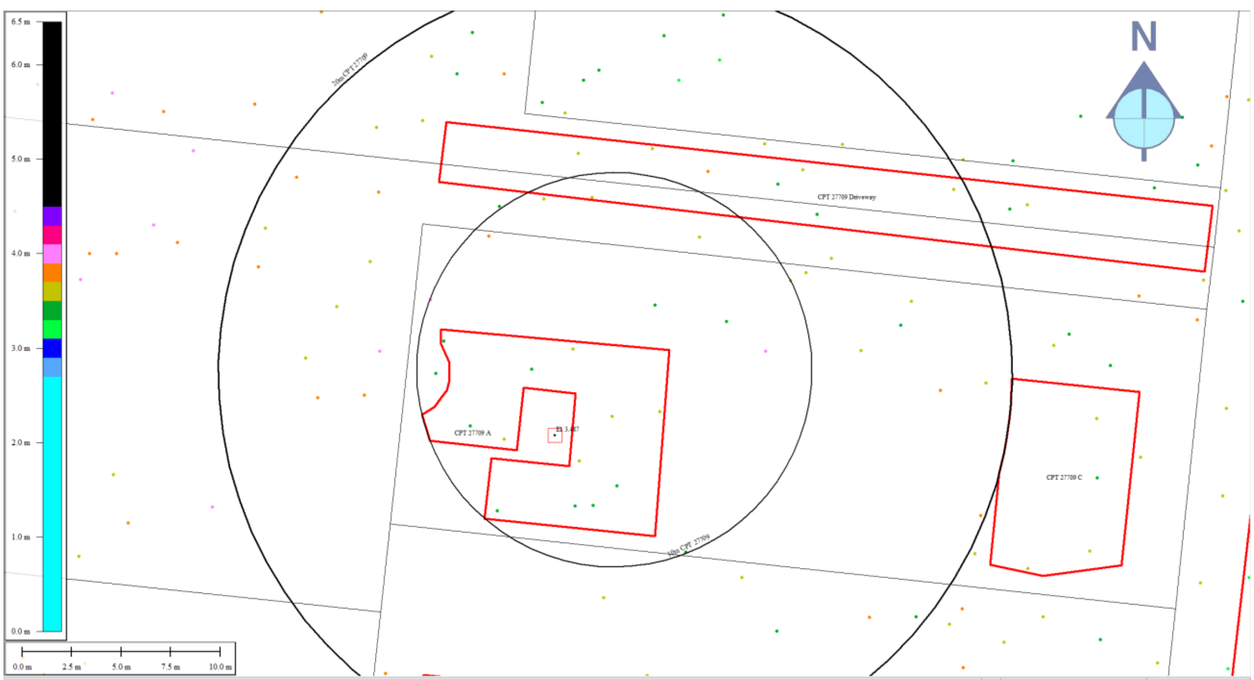

Figure 41: Ground surface elevation averaged over 10-m, 20-m, and 50-m buffers for Patch A for Jul 2003 LiDAR survey.

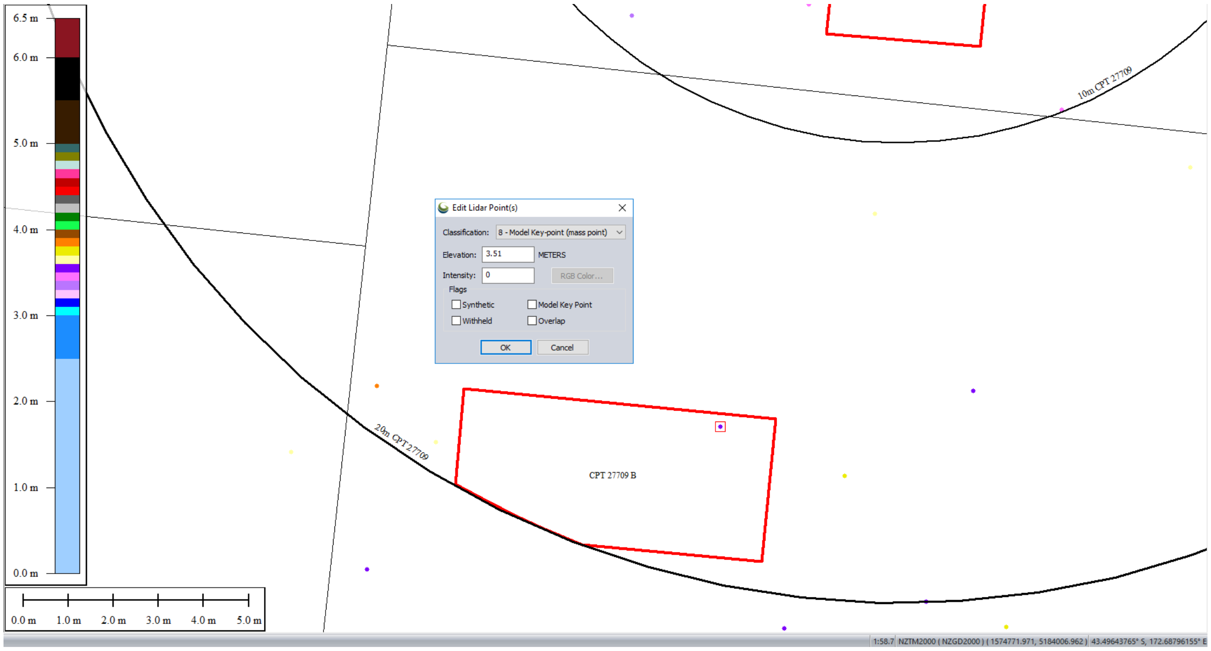

Figure 42: Ground surface elevation for 20-m and 50-m buffers for Patch B for Jul 2003 LiDAR survey.

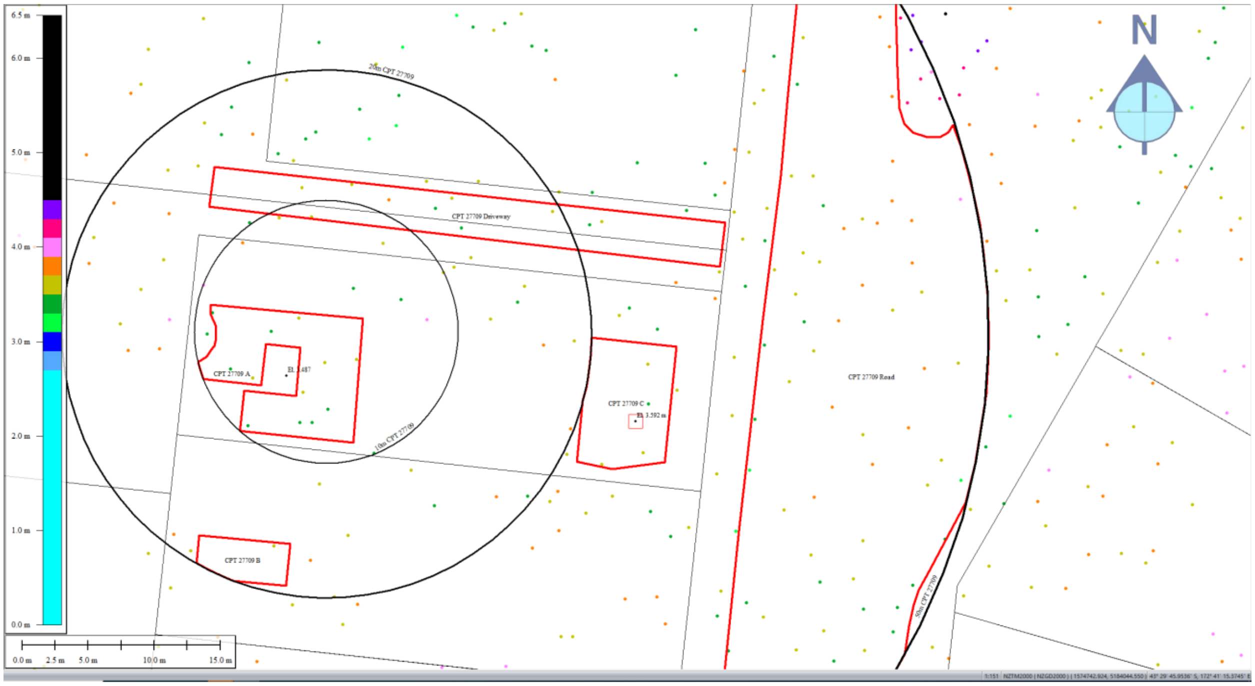

Figure 43: Ground surface elevation averaged over 50-m buffer for Patch C for Jul 2003 LiDAR survey.

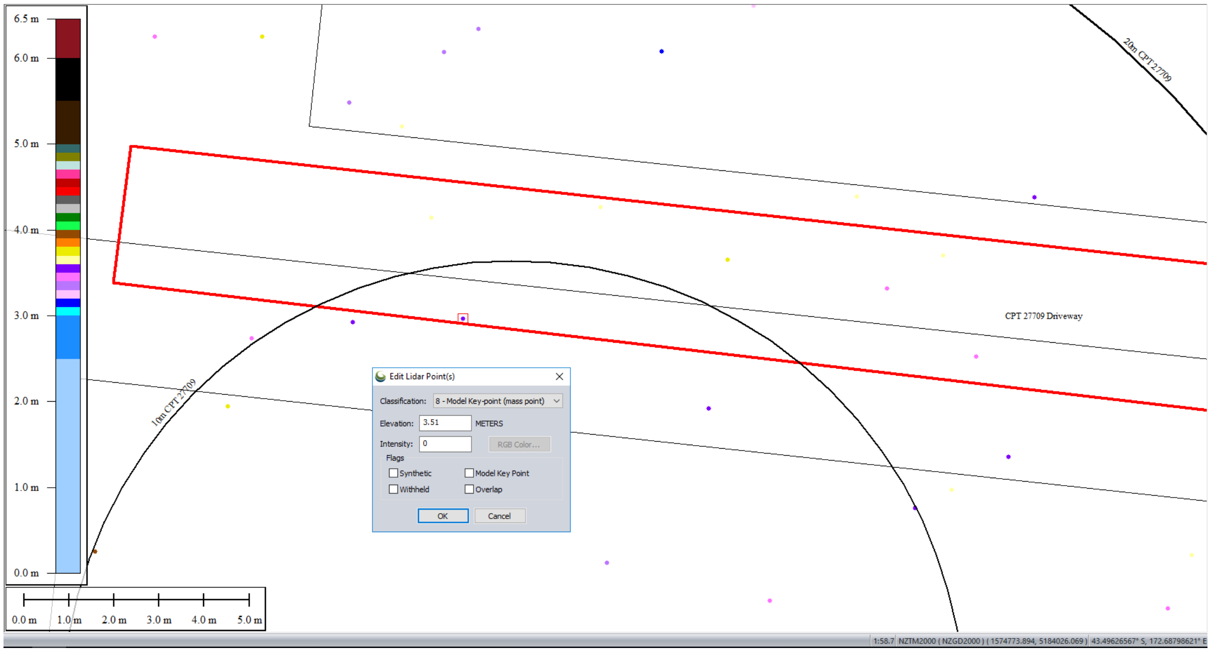

Figure 44: Ground surface elevation averaged over 10-m buffer for Driveway for Jul 2003 LiDAR survey.

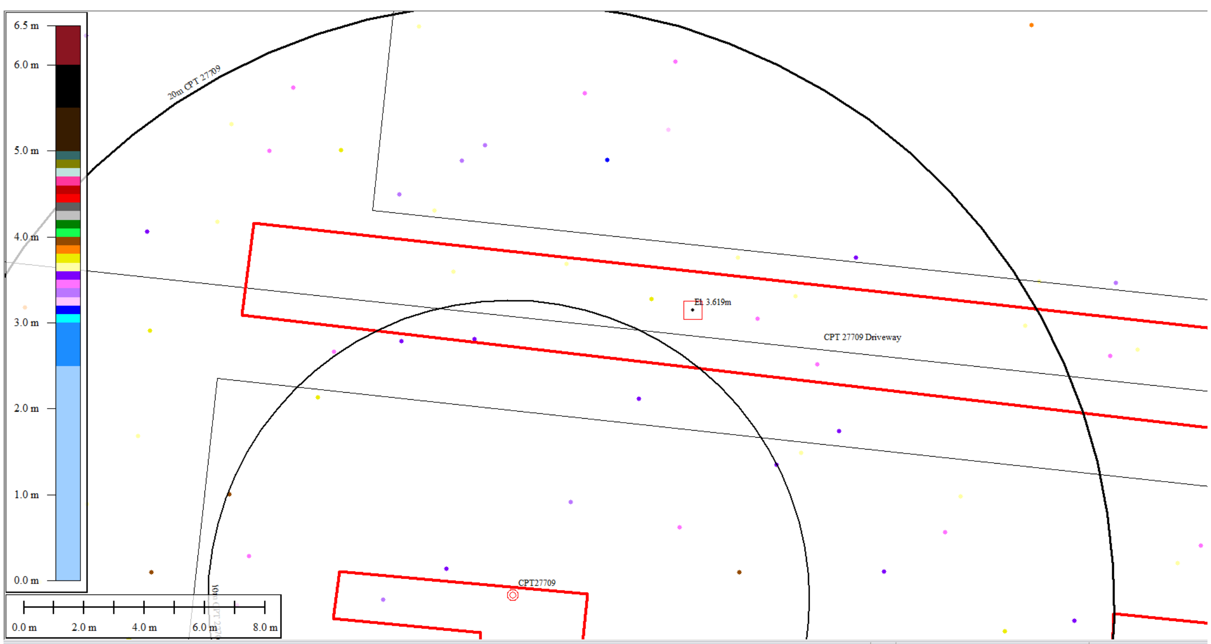

Figure 45: Ground surface elevation averaged over 20-m buffer for Driveway for Jul 2003 LiDAR survey.

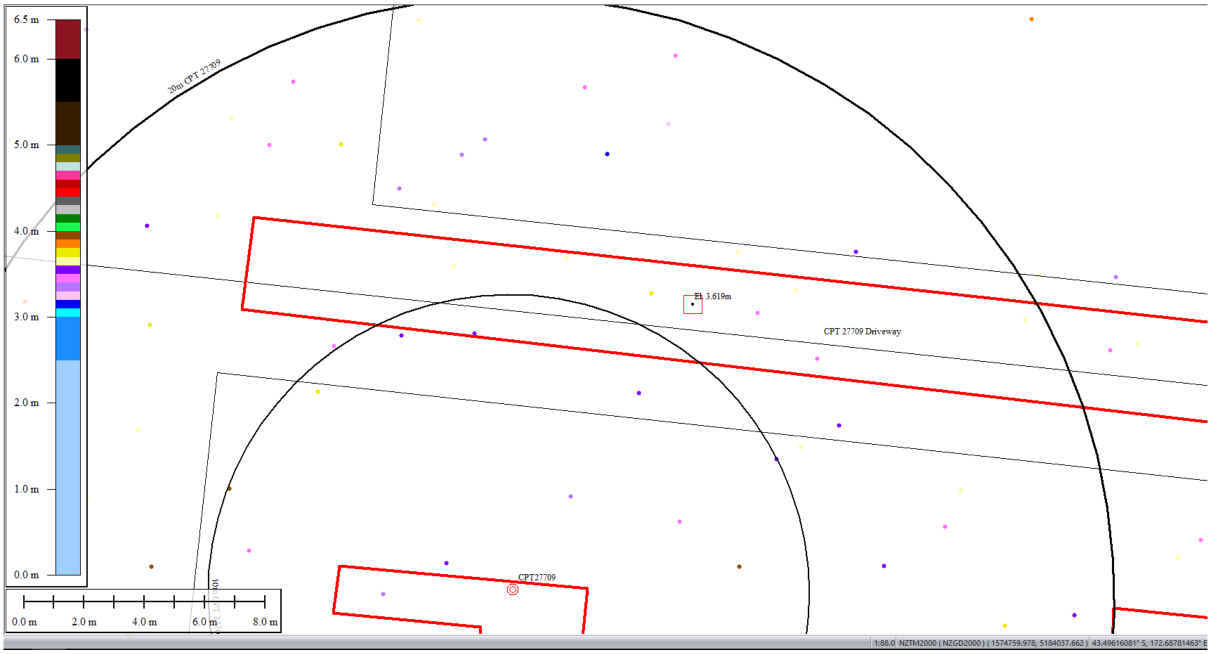

Figure 46: Ground surface elevation averaged over 50-m buffer for Driveway for Jul 2003 LiDAR survey.

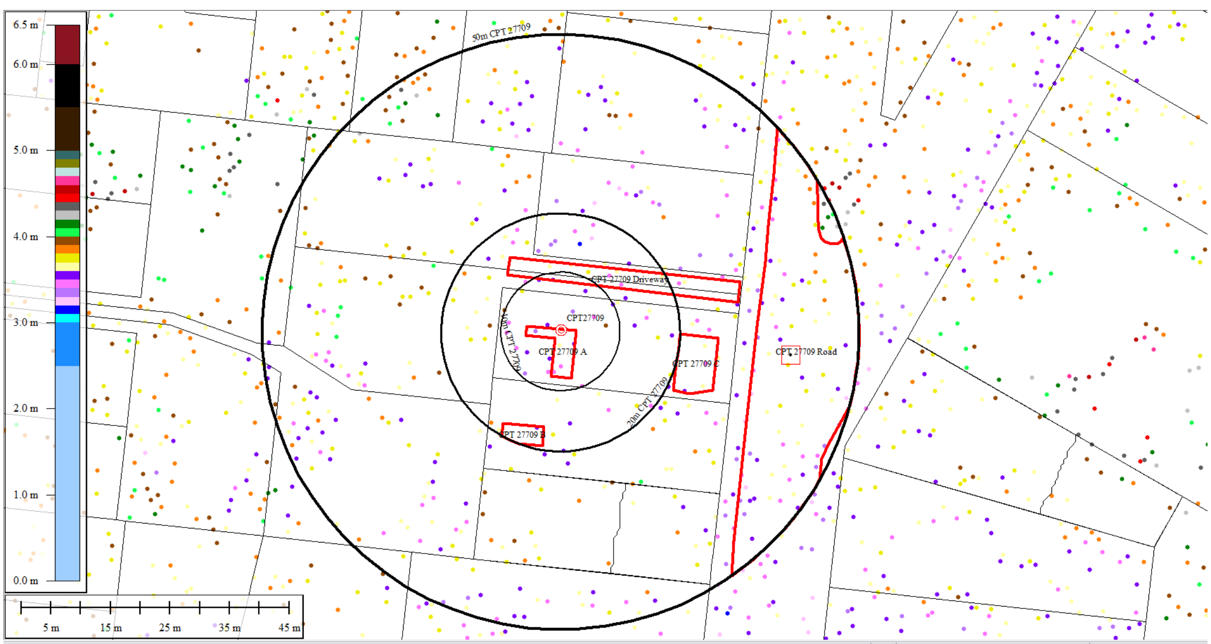

Figure 47: Ground surface elevation averaged over 50-m buffer for Road for Jul 2003 LiDAR survey.

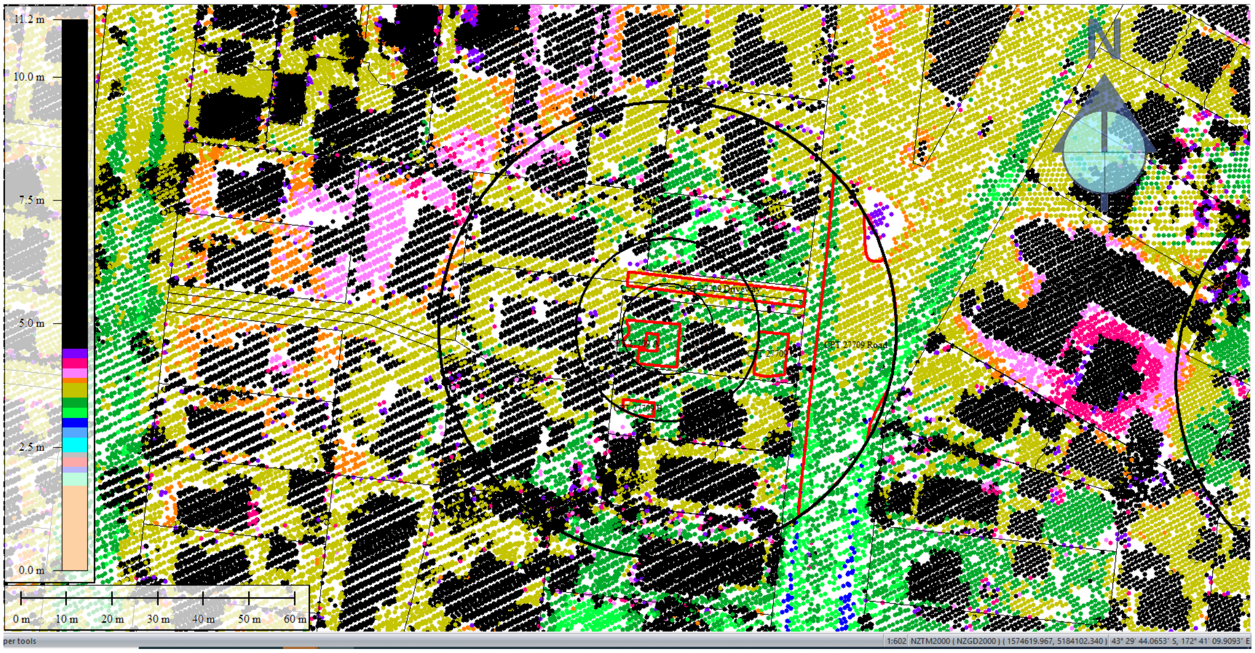

Figure 48: Sep 5, 2010 LiDAR survey.

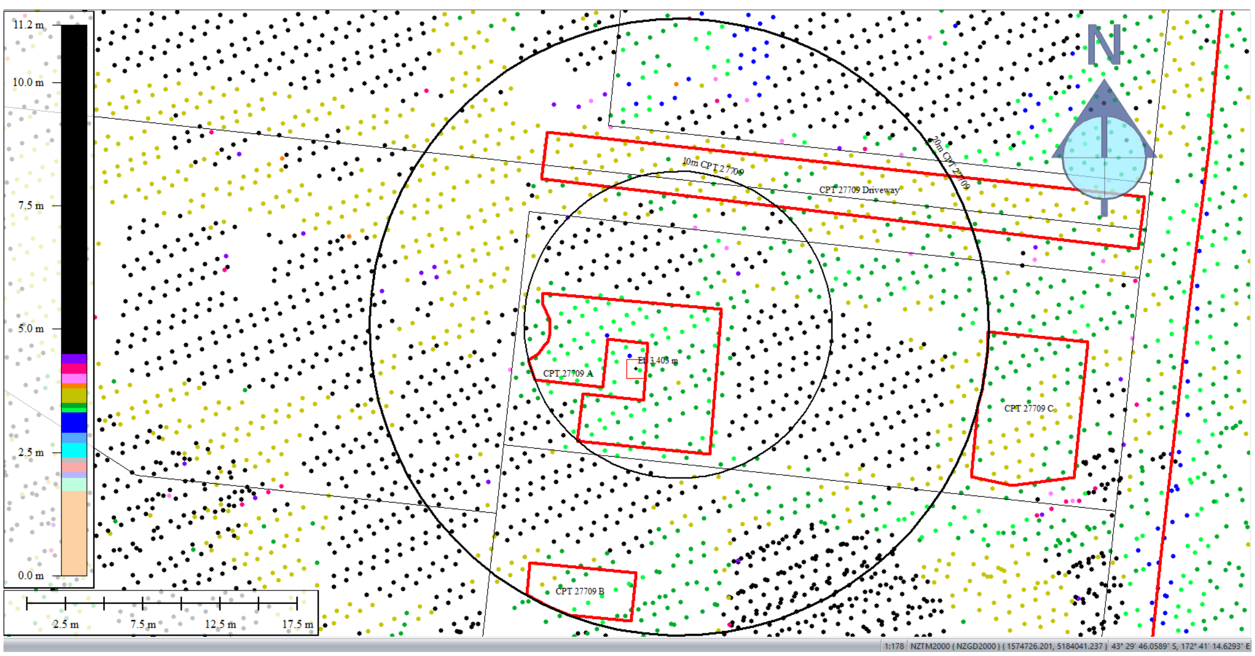

Figure 49: Ground surface elevation averaged over 10-m, 20-m, and 50-m buffers for Patch A for Sep 5, 2010 LiDAR survey.

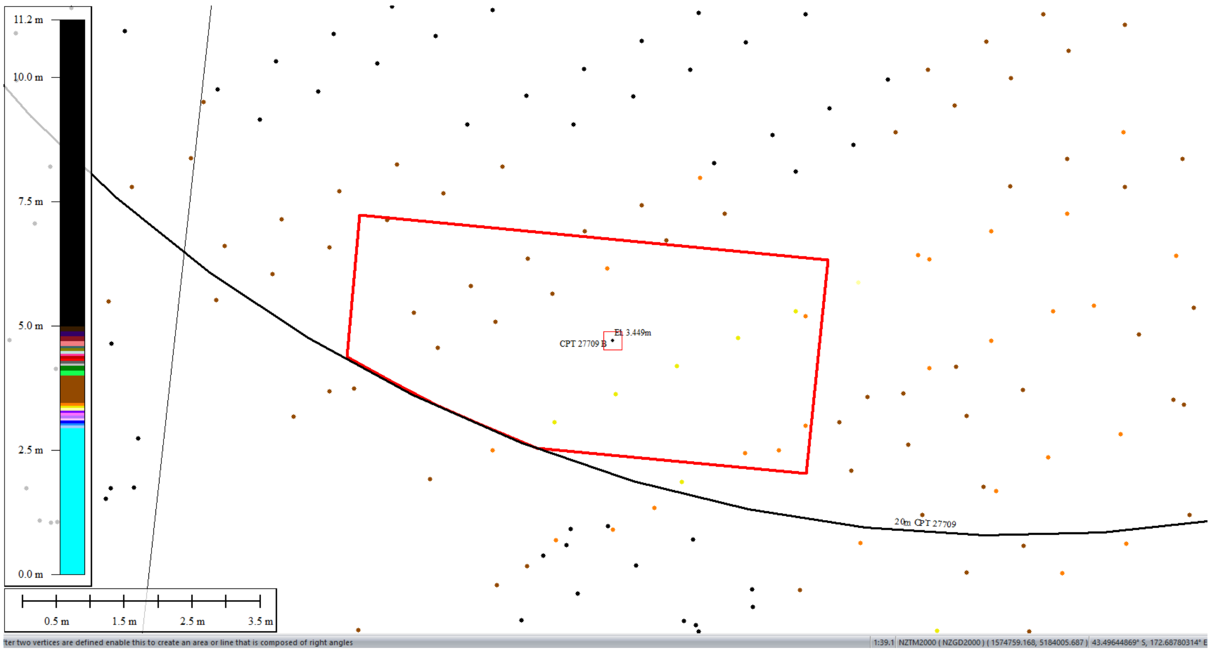

Figure 50: Ground surface elevation averaged over 20-m and 50-m buffers for Patch B for Sep 5, 2010 LiDAR survey.

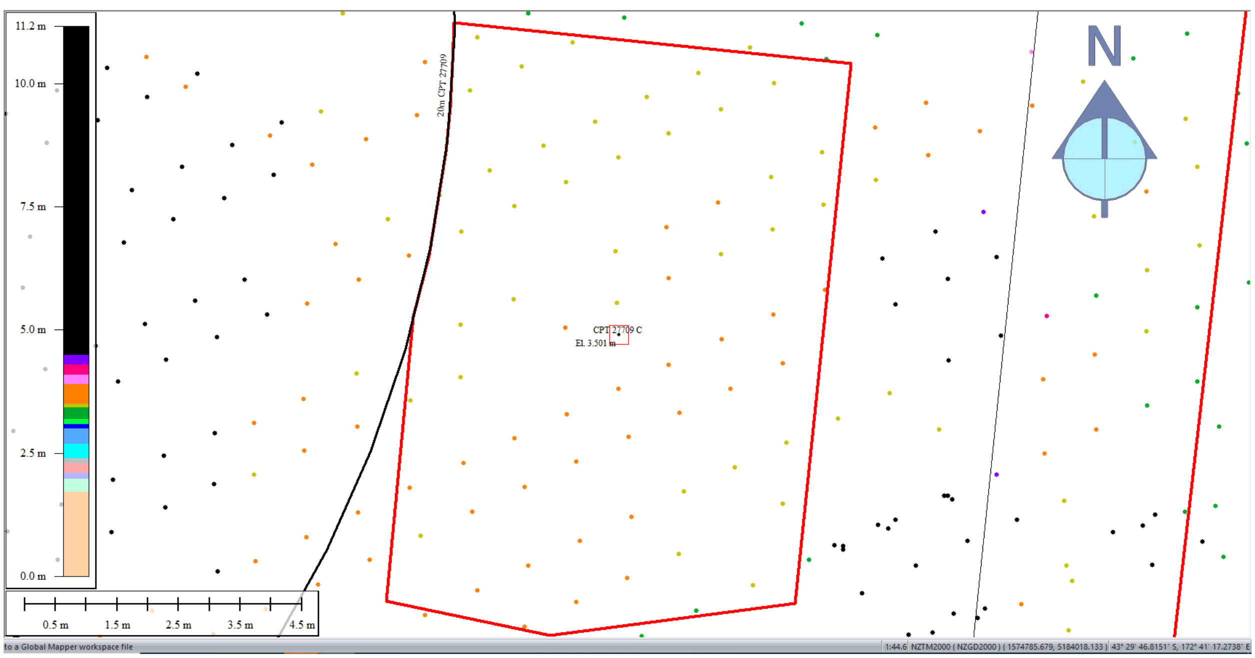

Figure 51: Ground surface elevation averaged over 50-m buffer for Patch C for Sep 5, 2010 LiDAR survey.

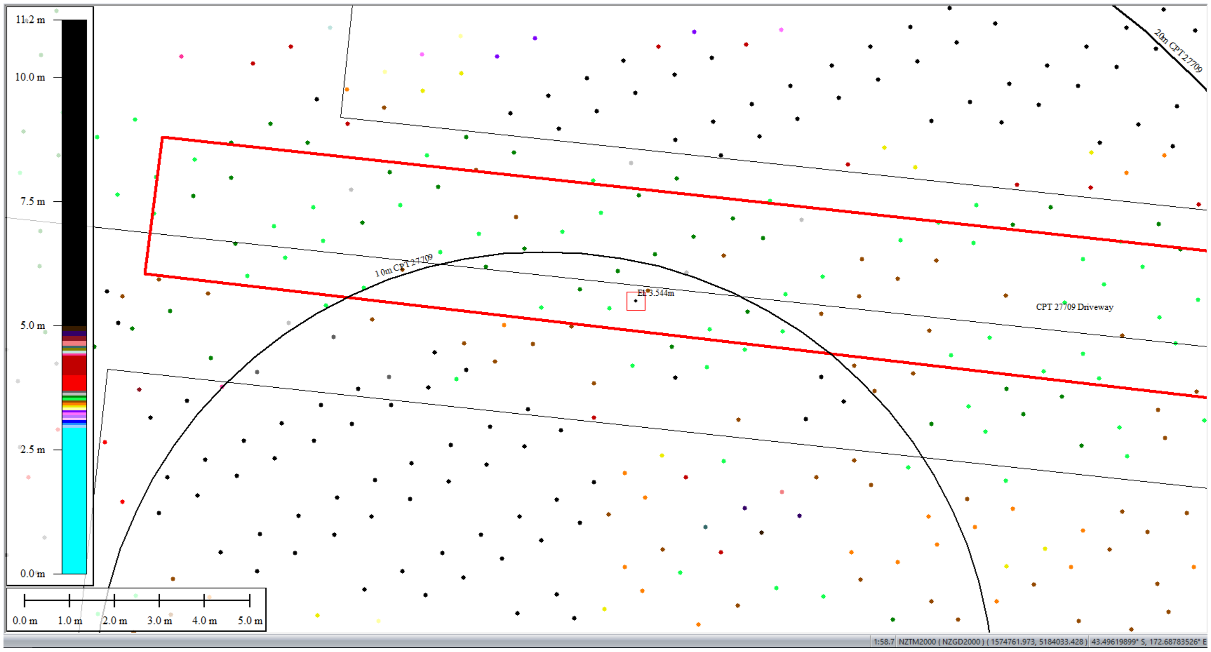

Figure 52: Ground surface elevation averaged over 10-m buffer for Driveway for Sep 5, 2010 LiDAR survey.

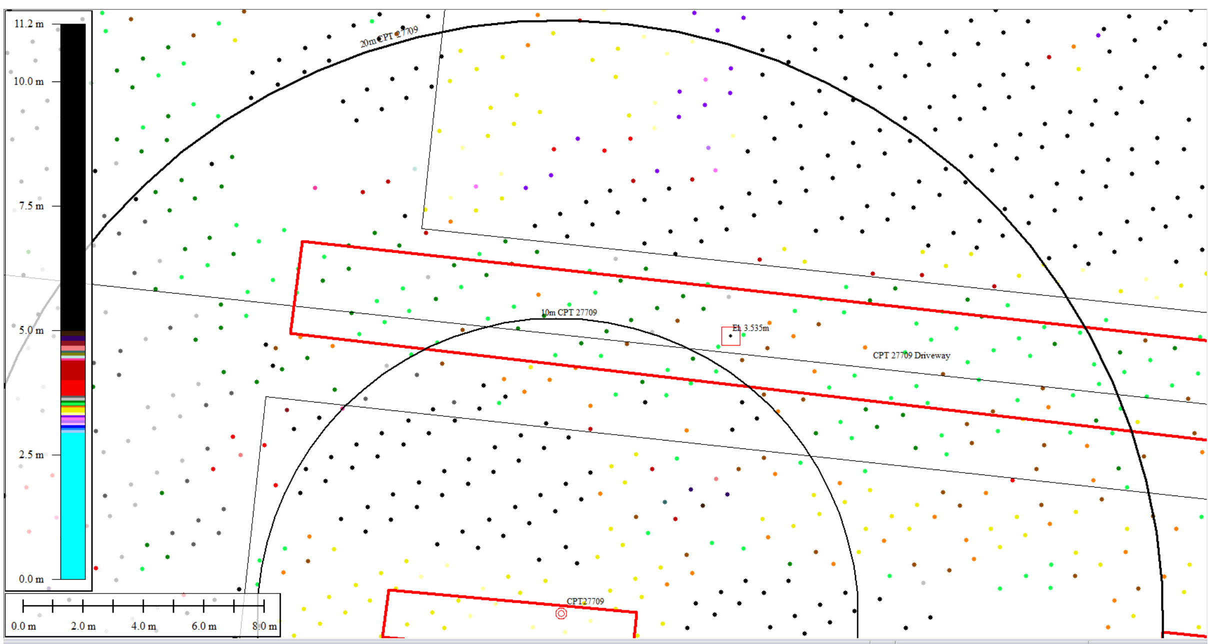

Figure 53: Ground surface elevation averaged over 20-m buffer for Driveway for Sep 5, 2010 LiDAR survey.

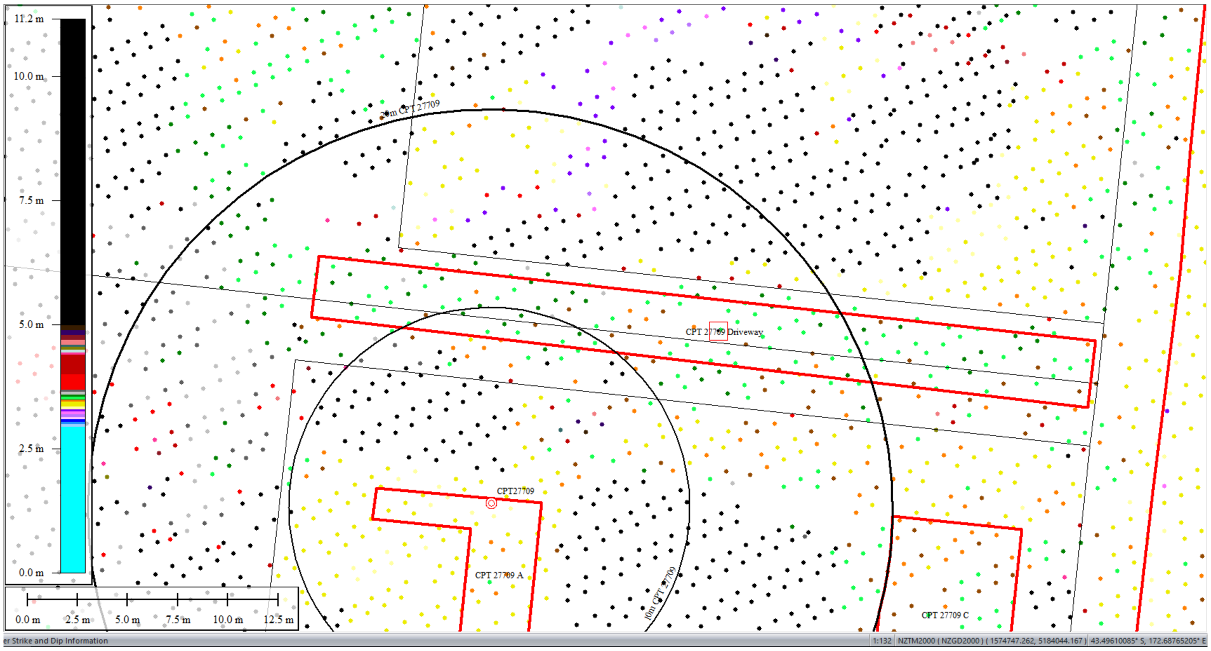

Figure 54: Ground surface elevation averaged over 50-m buffer for Driveway for Sep 5, 2010 LiDAR survey.

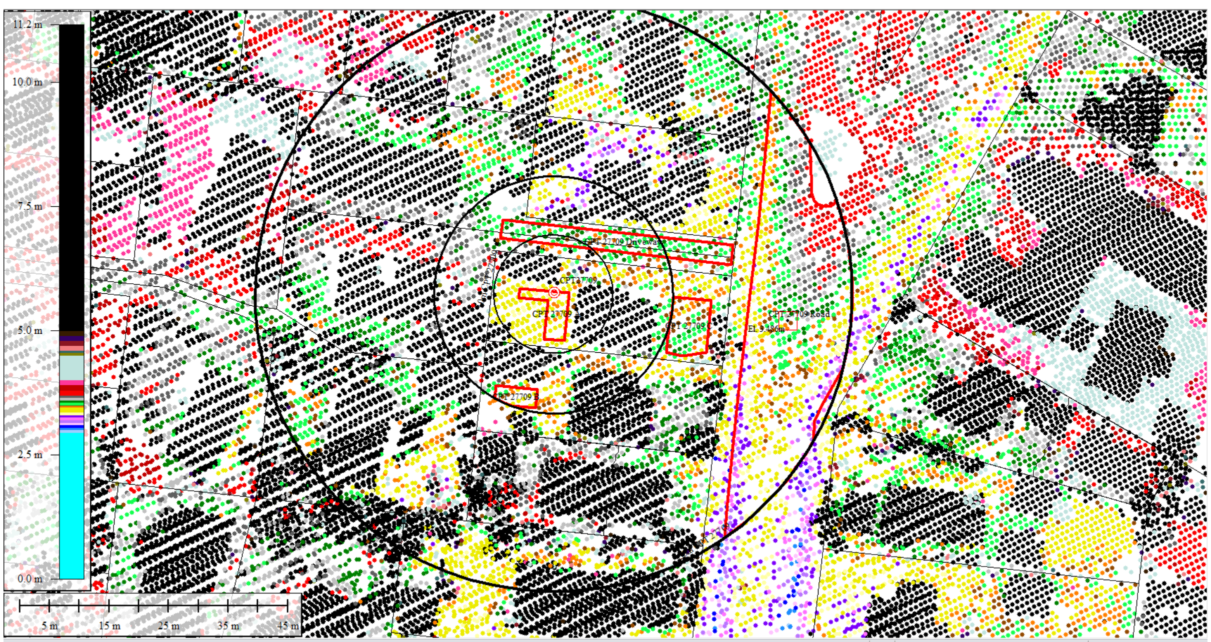

Figure 55: Ground surface elevation averaged over 50-m buffer for Road for Sep 5, 2010 LiDAR survey.

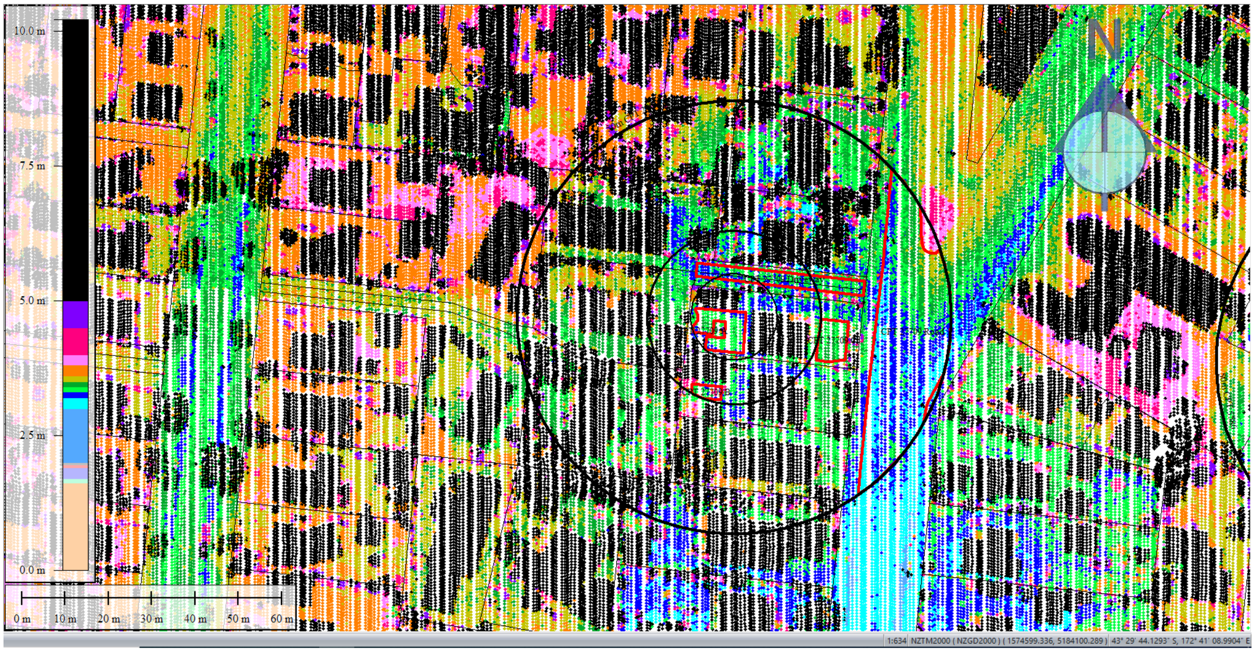

Figure 56: Mar 2011 LiDAR survey.

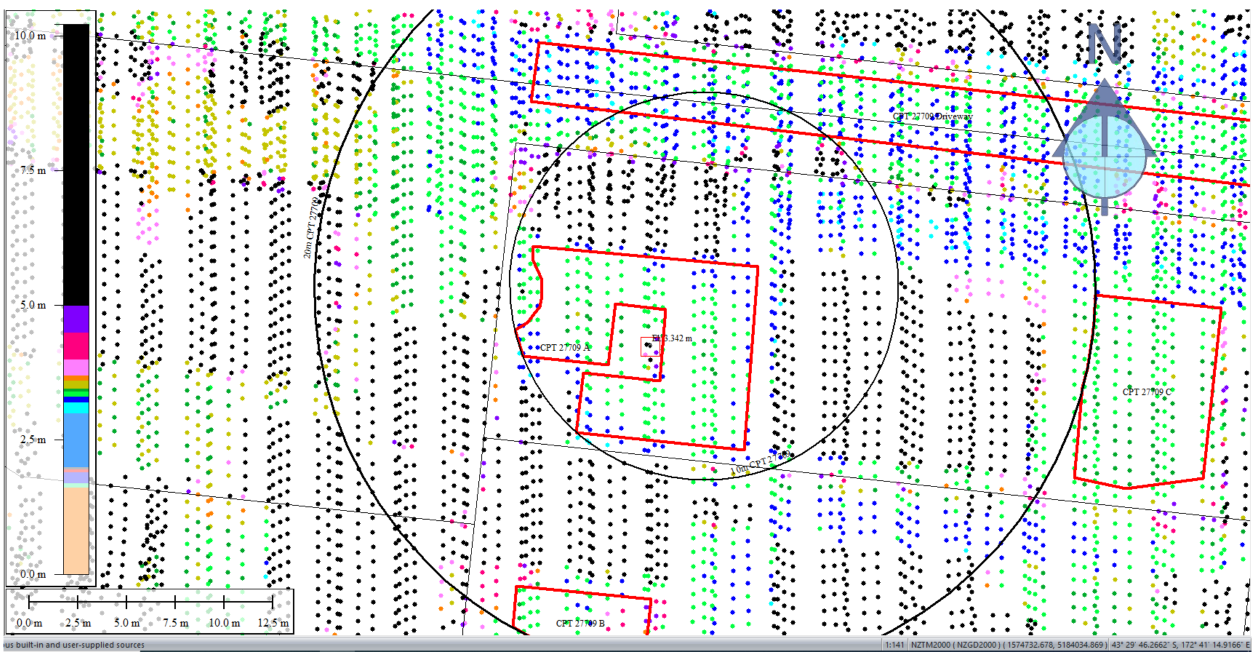

Figure 57: Ground surface elevation averaged over 10-m, 20-m, and 50-m buffers for Patch A for Mar 2011 LiDAR survey.

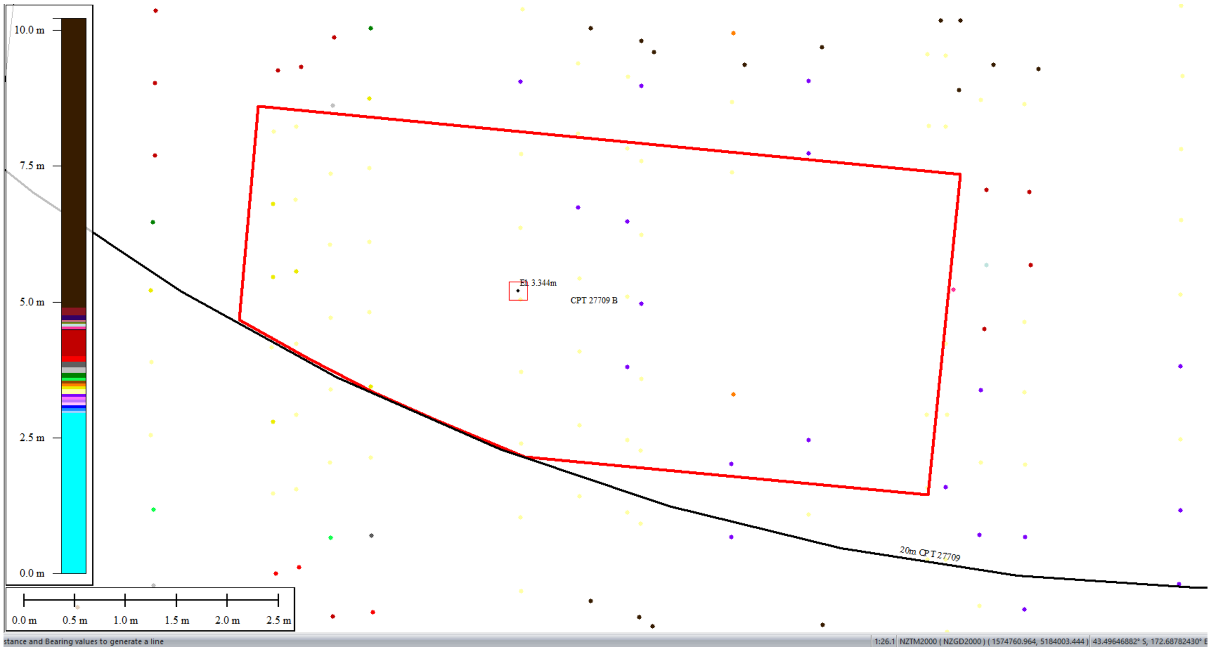

Figure 58: Ground surface elevation averaged over 20-m and 50-m buffers for Patch B for Mar 2011 LiDAR survey.

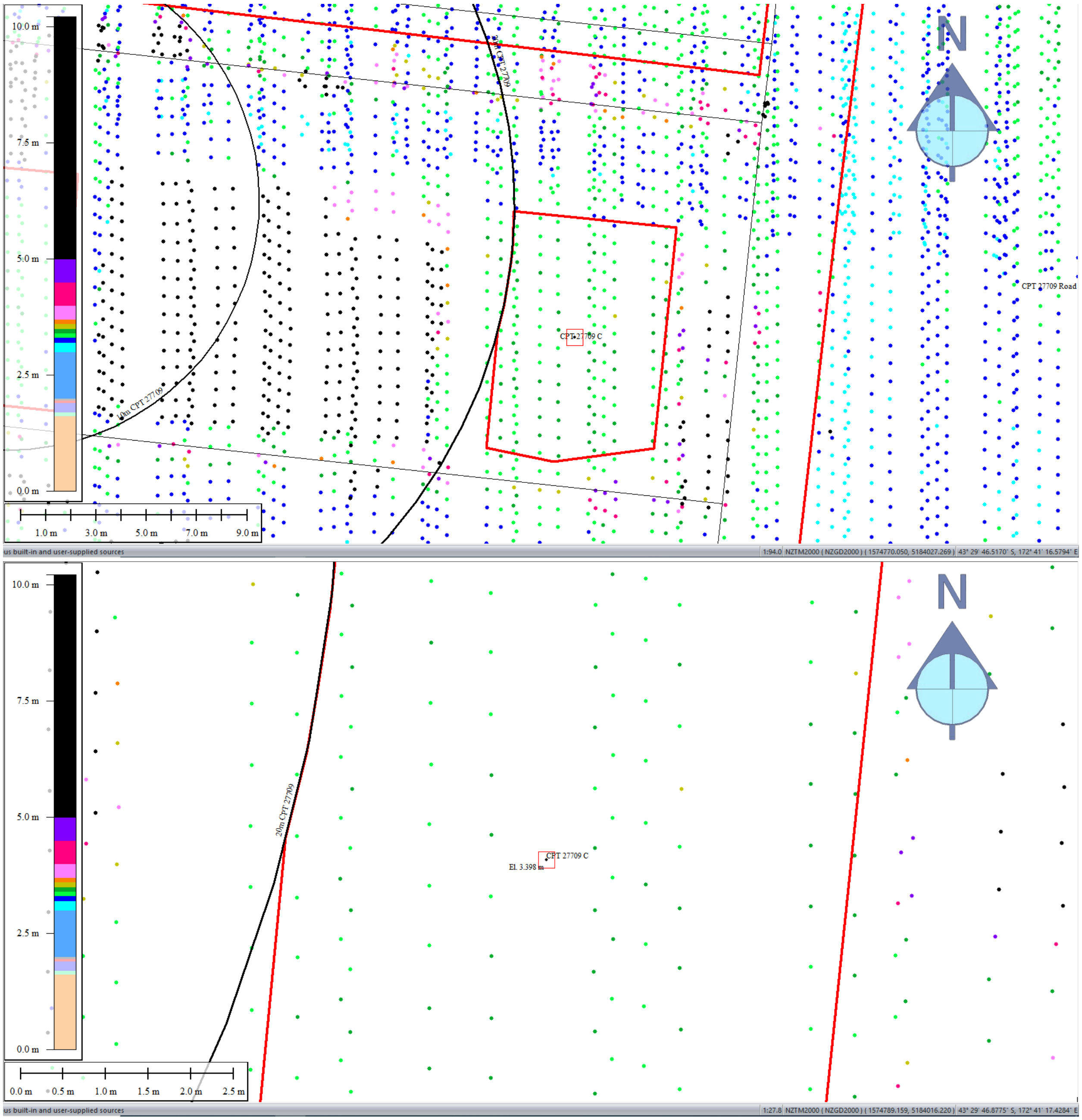

Figure 59: Ground surface elevation averaged over 50-m buffer for Patch C for Mar 2011 LiDAR survey.

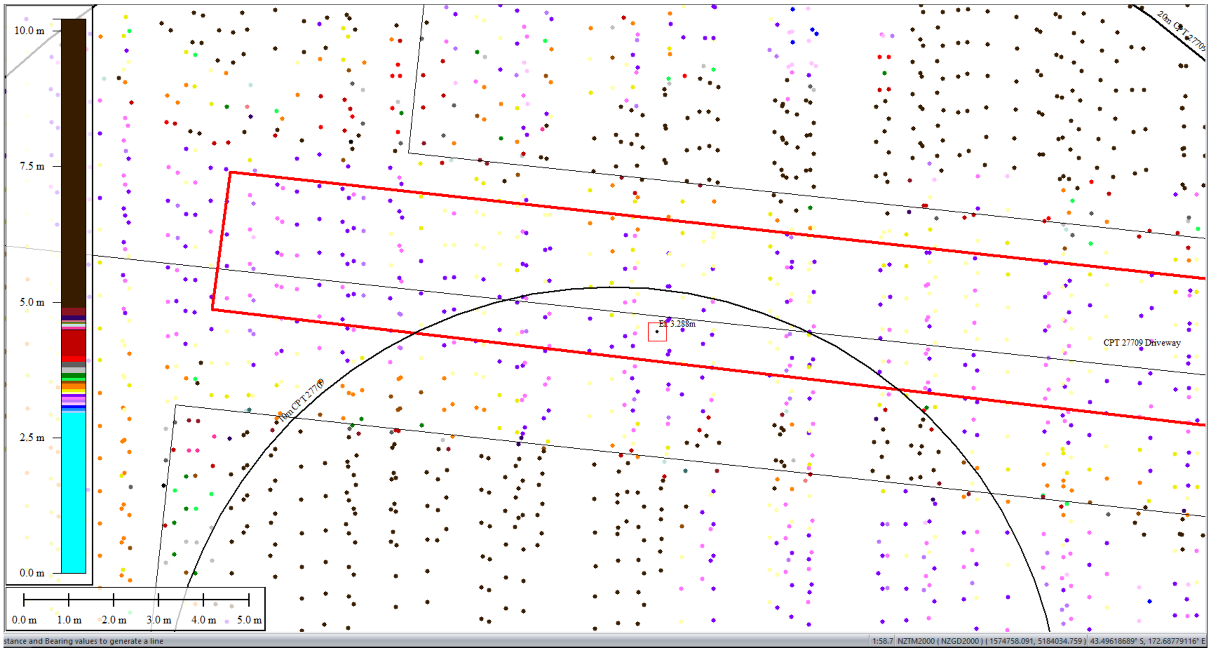

Figure 60: Ground surface elevation averaged over 10-m buffer for Driveway for Mar 2011 LiDAR survey.

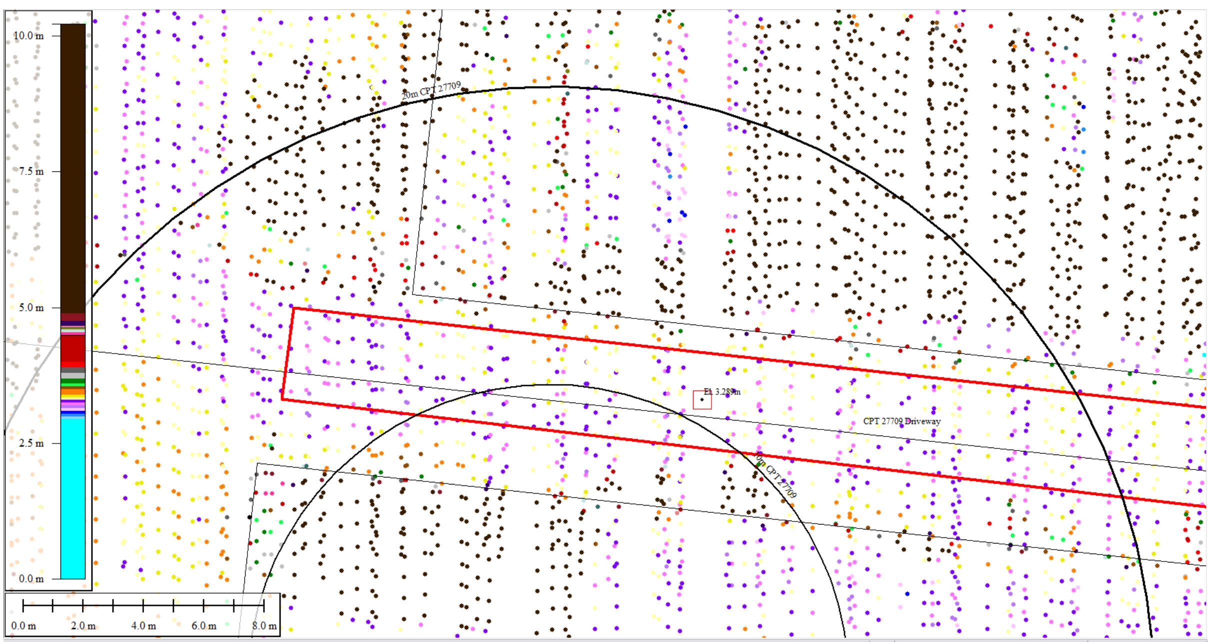

Figure 61: Ground surface elevation averaged over 20-m buffer for Driveway for Mar 2011 LiDAR survey.

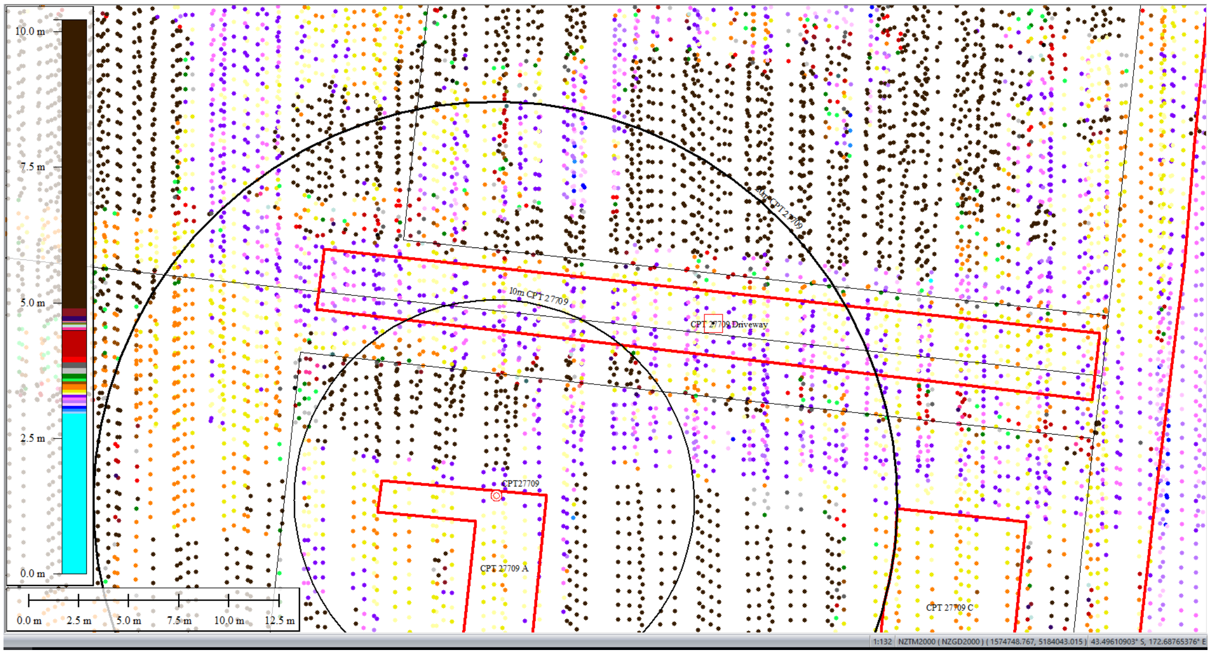

Figure 62: Ground surface elevation averaged over 50-m buffer for Driveway for Mar 2011 LiDAR survey.

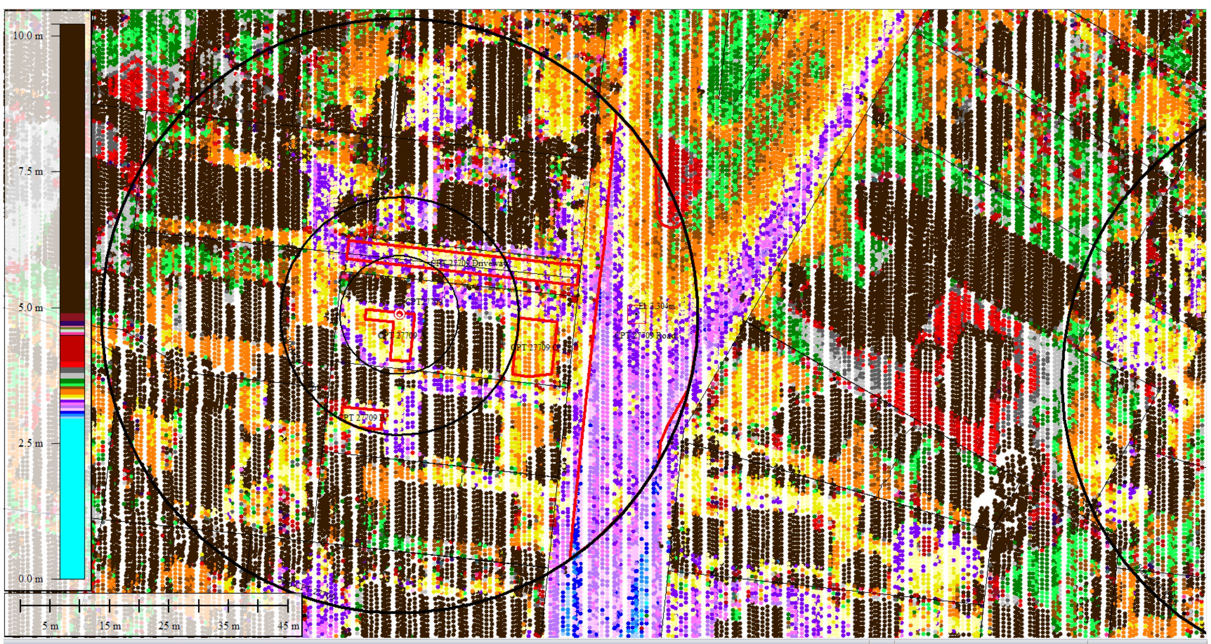

Figure 63: Ground surface elevation averaged over 50-m buffer for Road for Mar 2011 LiDAR survey.

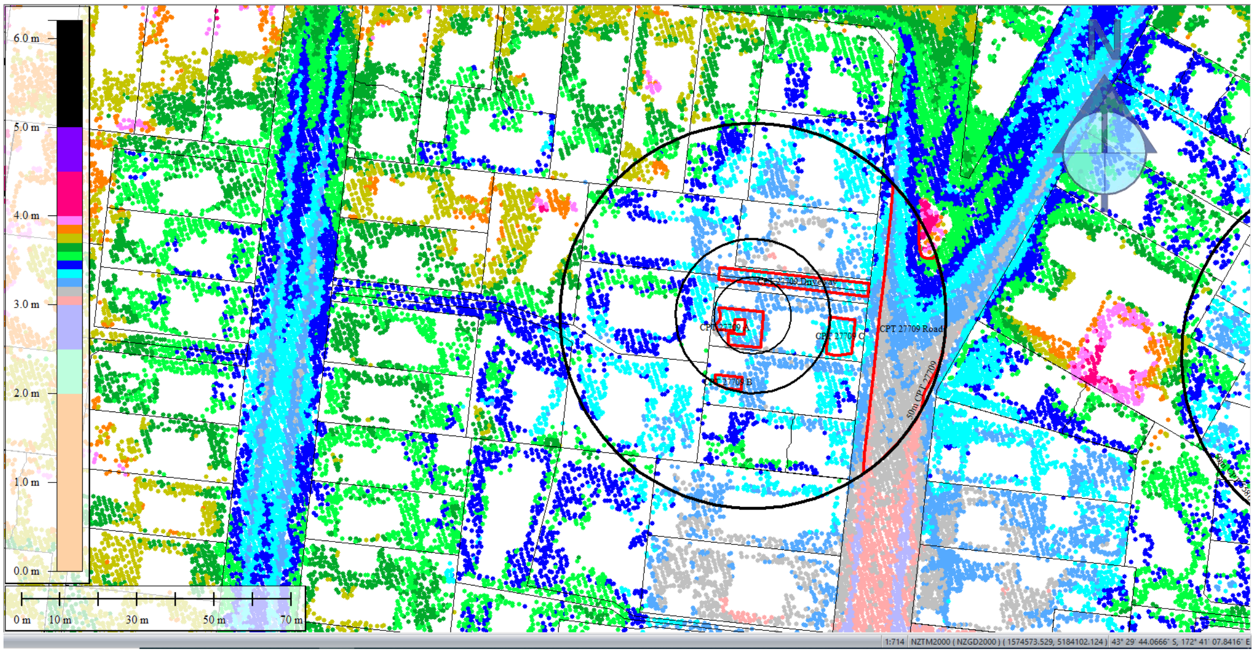

Figure 64: May 2011 LiDAR survey.

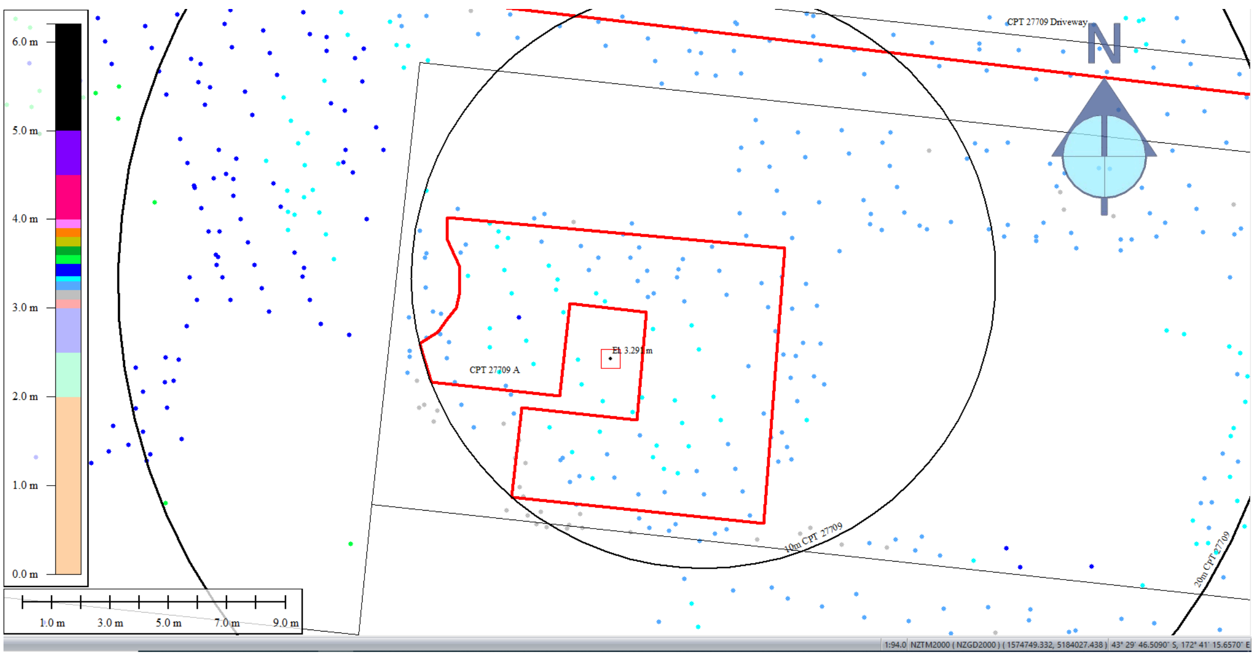

Figure 65: Ground surface elevation averaged over 10-m, 20-m, and 50-m buffers for Patch A for May 2011 LiDAR survey.

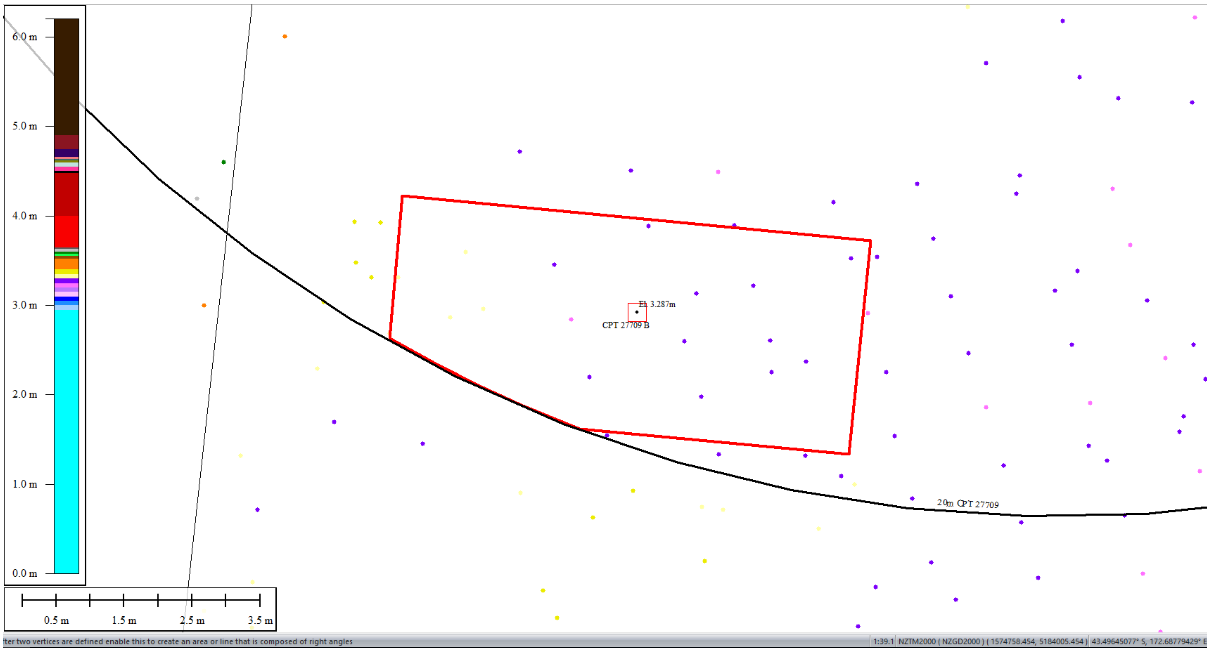

Figure 66: Ground surface elevation averaged over 20-m and 50-m buffers for Patch B for May 2011 LiDAR survey.

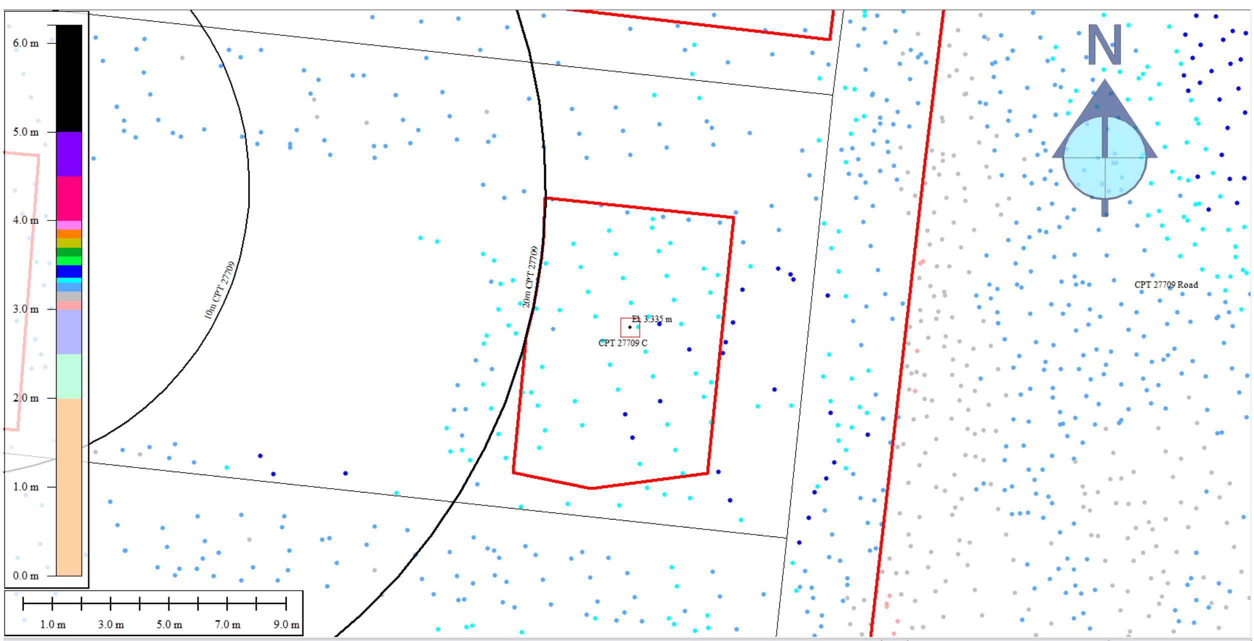

Figure 67: Ground surface elevation averaged over 50-m buffer for Patch C for May 2011 LiDAR survey.

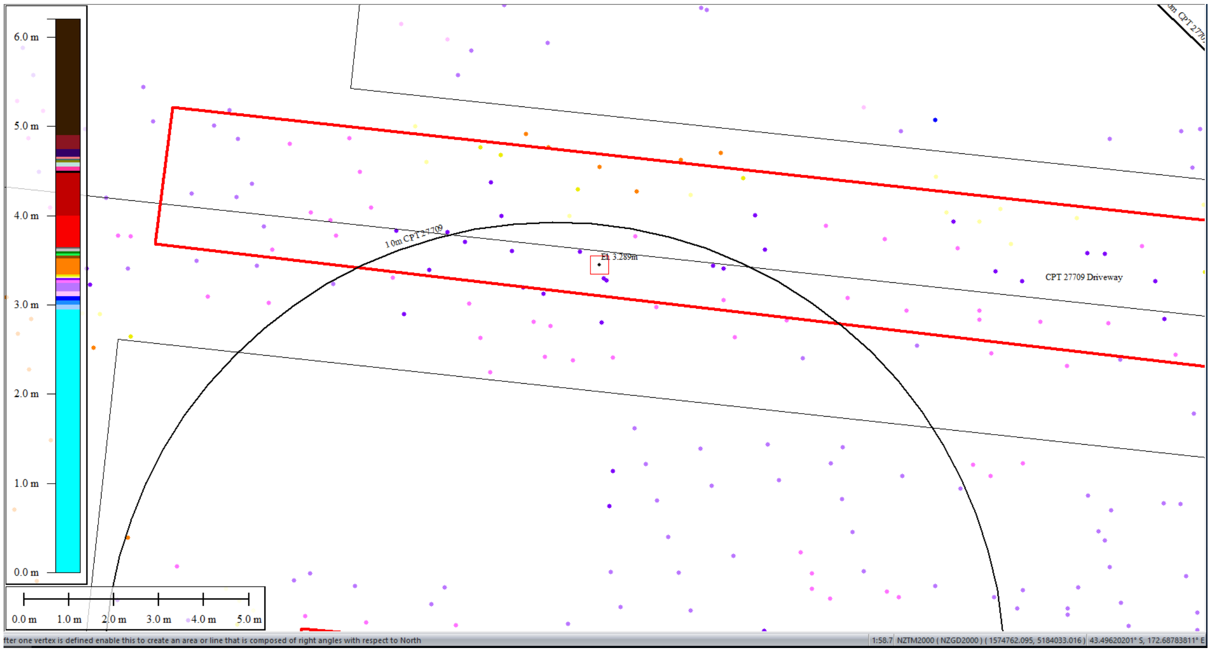

68: Ground surface elevation averaged over 10-m buffer for Driveway for May 2011 LiDAR survey.

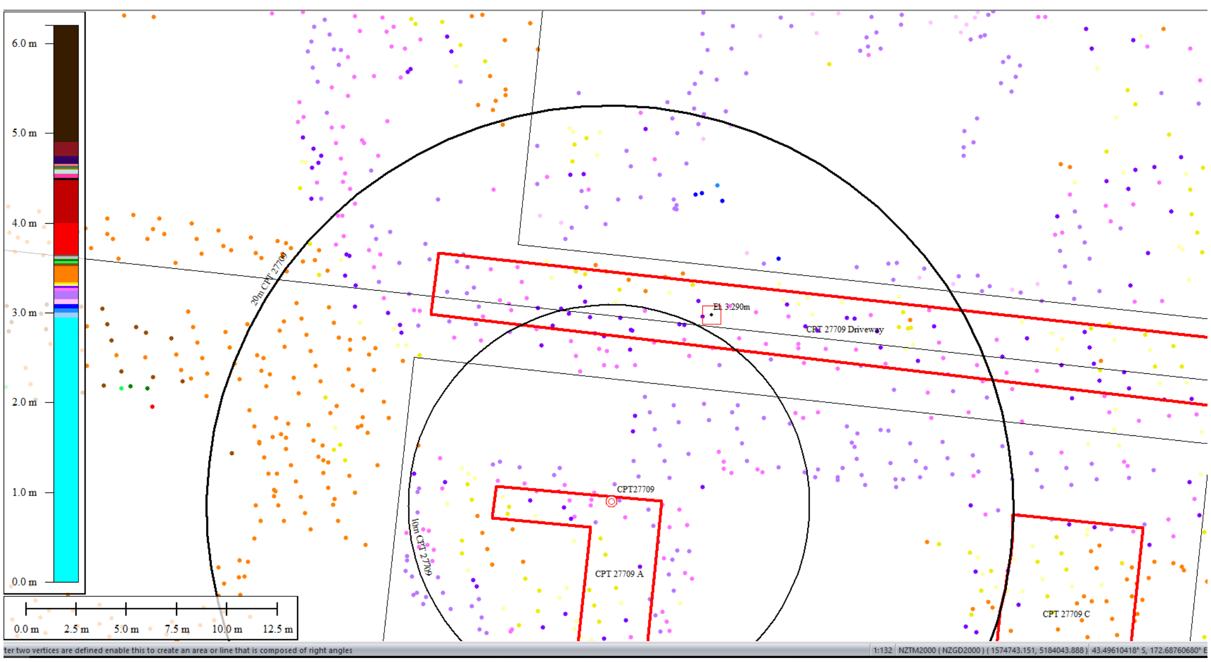

Figure 69: Ground surface elevation averaged over 20-m buffer for Driveway for May 2011 LiDAR survey.

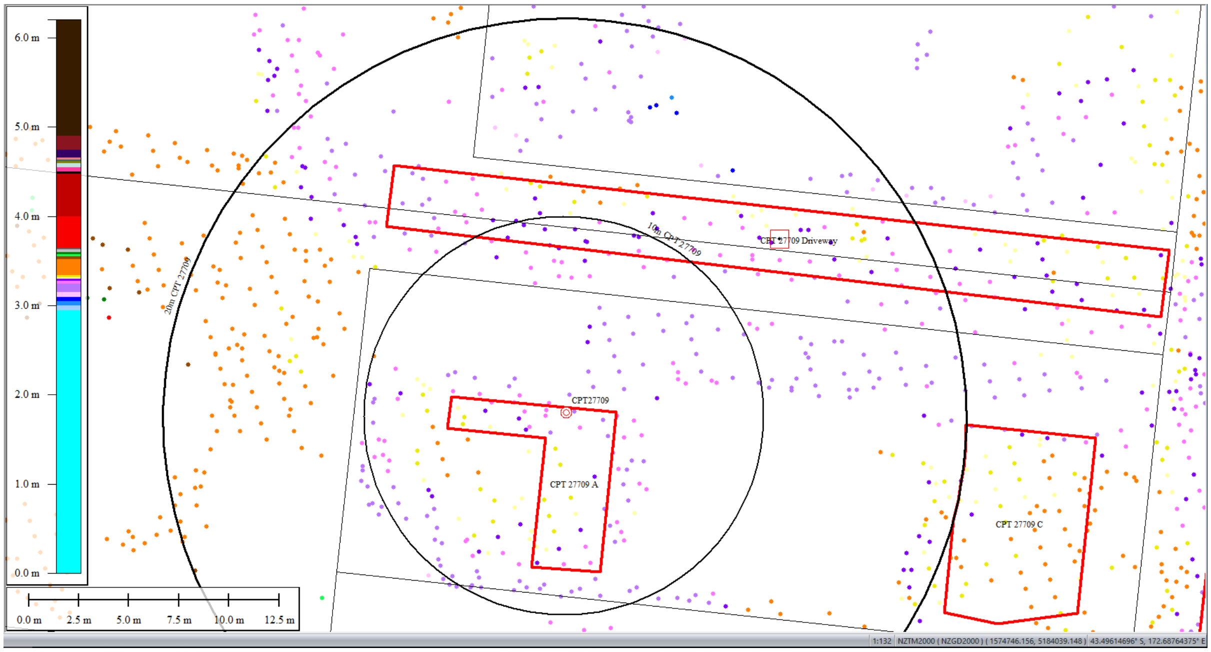

Figure 70: Ground surface elevation averaged over 50-m buffer for Driveway for May 2011 LiDAR survey.

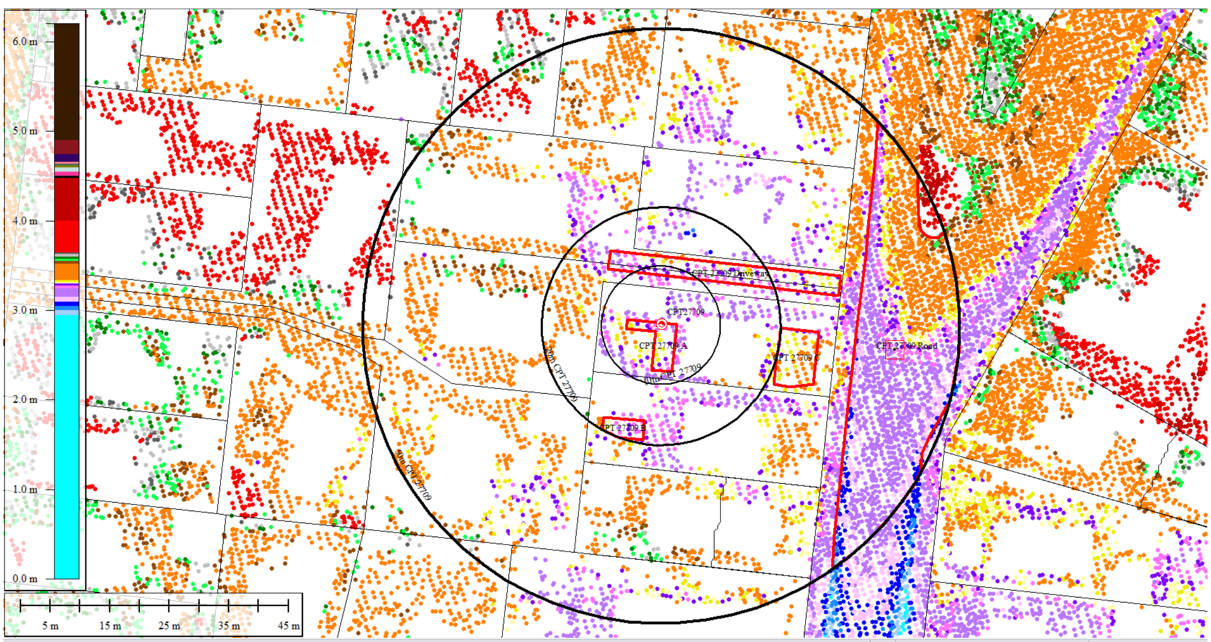

Figure 71: Ground surface elevation averaged over 50-m buffer for Road for May 2011 LiDAR survey.

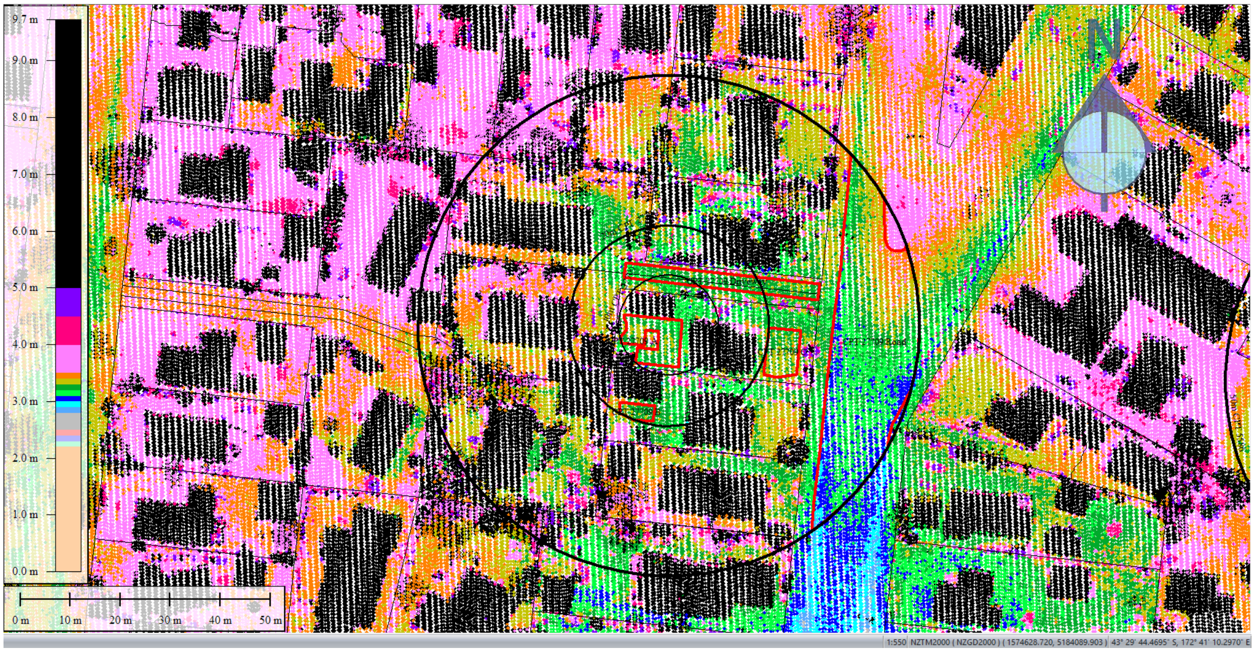

Figure 72: Sep 2011 LiDAR survey.

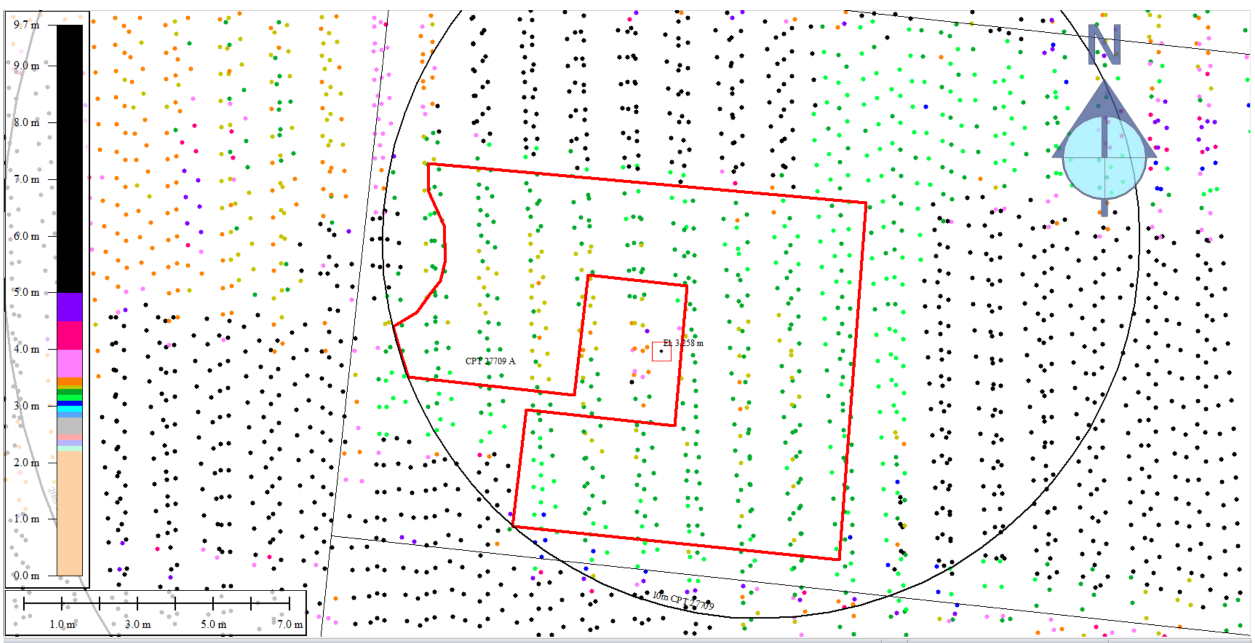

Figure 73: Ground surface elevation averaged over 10-m, 20-m, and 50-m buffers for Patch A for Sep 2011 LiDAR survey.

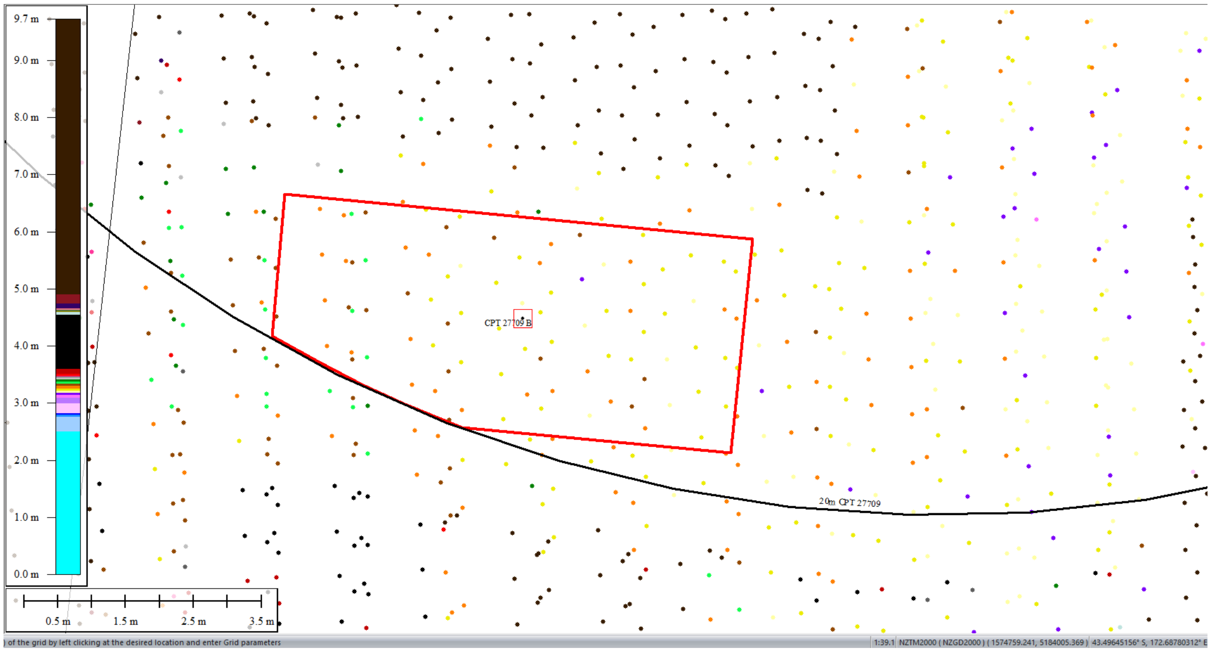

Figure 74: Ground surface elevation averaged over 20-m and 50-m buffers for Patch B for Sep 2011 LiDAR survey.

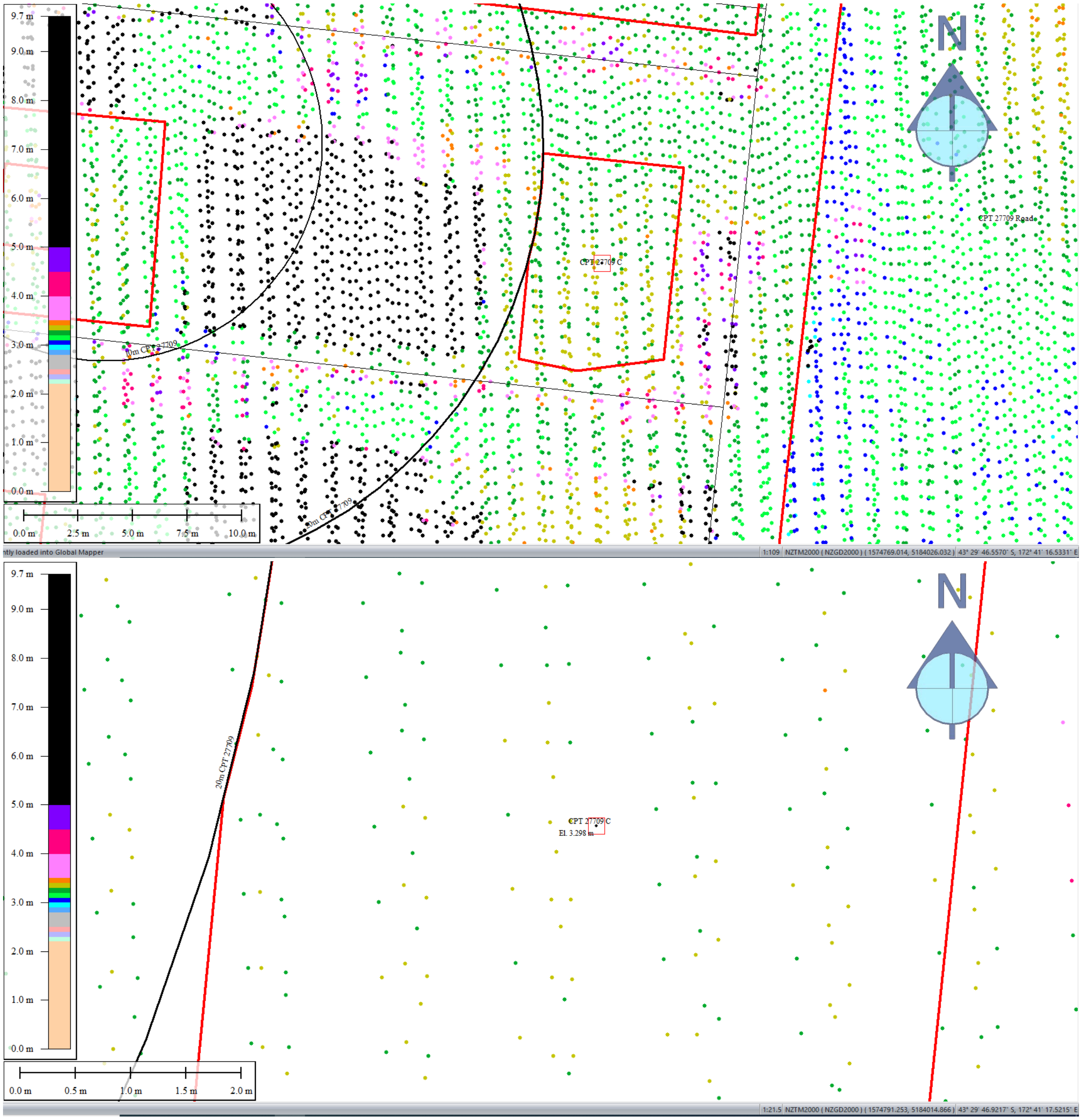

Figure 75: Ground surface elevation averaged over 50-m buffer for Patch C for Sep 2011 LiDAR survey.

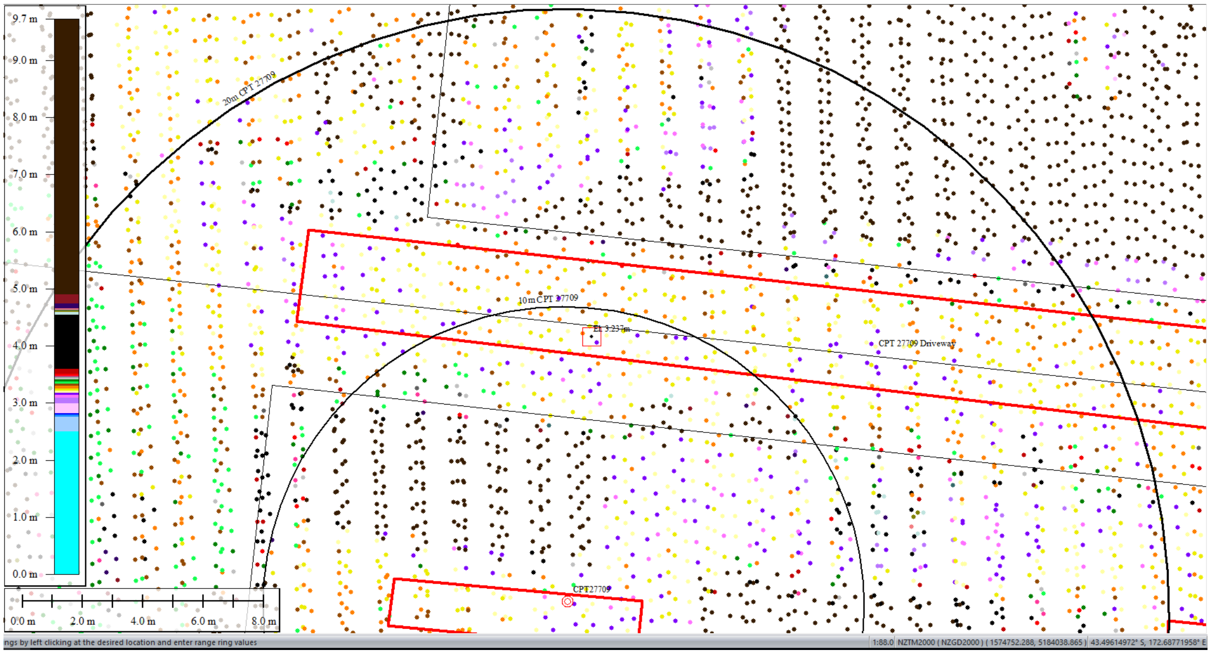

Figure 76: Ground surface elevation averaged over 10-m buffer for Driveway for Sep 2011 LiDAR survey.

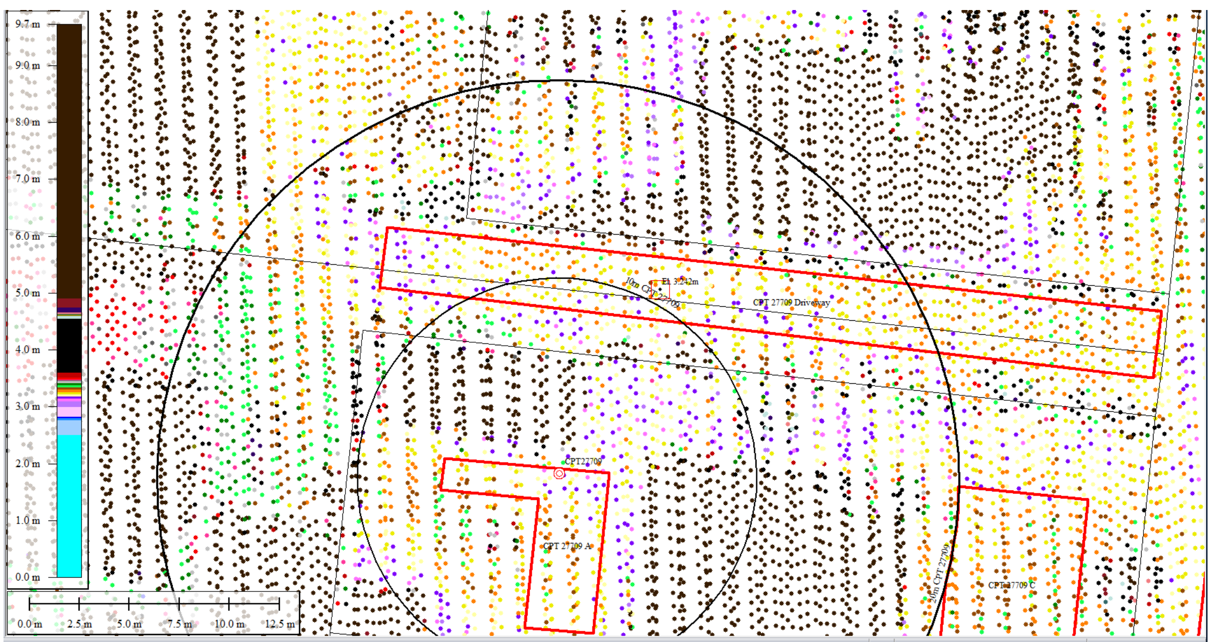

Figure 77: Ground surface elevation averaged over 20-m buffer for Driveway for Sep 2011 LiDAR survey.

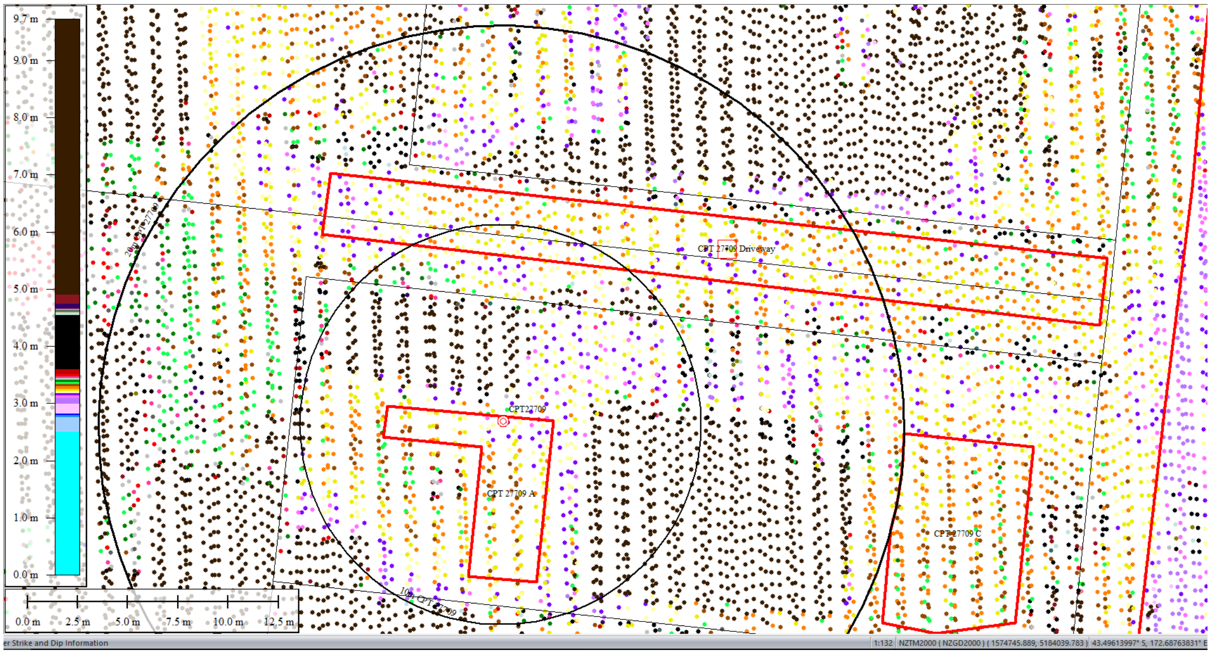

Figure 78: Ground surface elevation averaged over 50-m buffer for Driveway for Sep 2011 LiDAR survey.

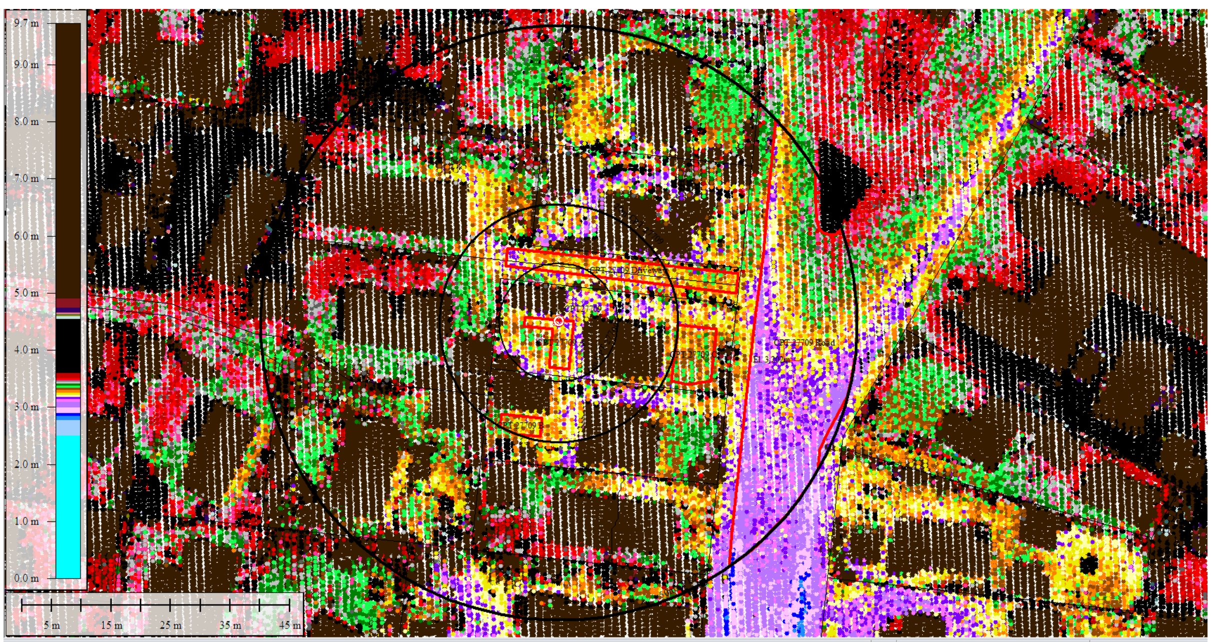

Figure 79: Ground surface elevation averaged over 50-m buffer for Road for Sep 2011 LiDAR survey.

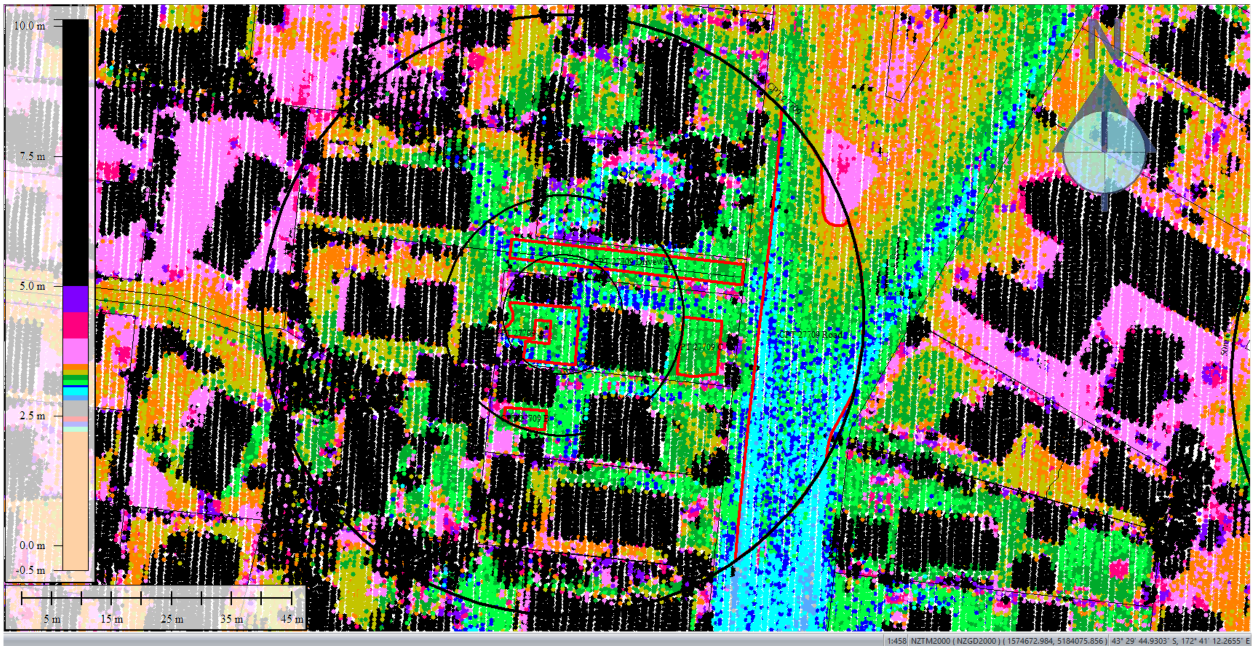

Figure 80: Feb 2012 LiDAR survey.

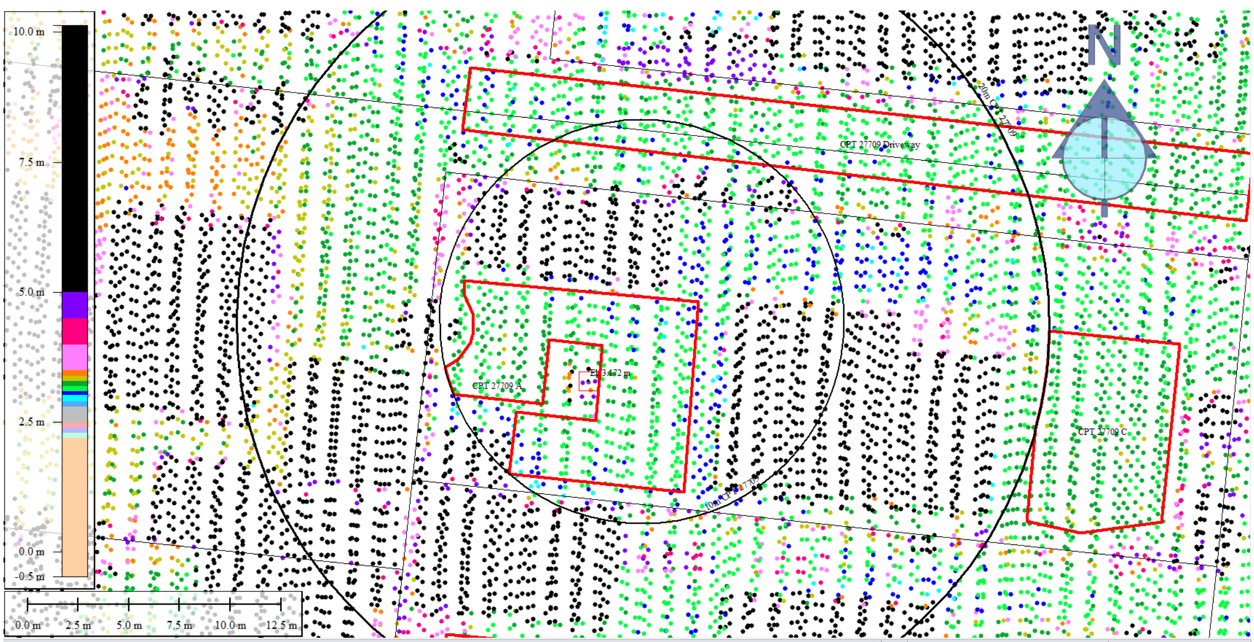

Figure 81: Ground surface elevation averaged over 10-m, 20-m, and 50-m buffers for Patch A for Feb 2012 LiDAR survey.

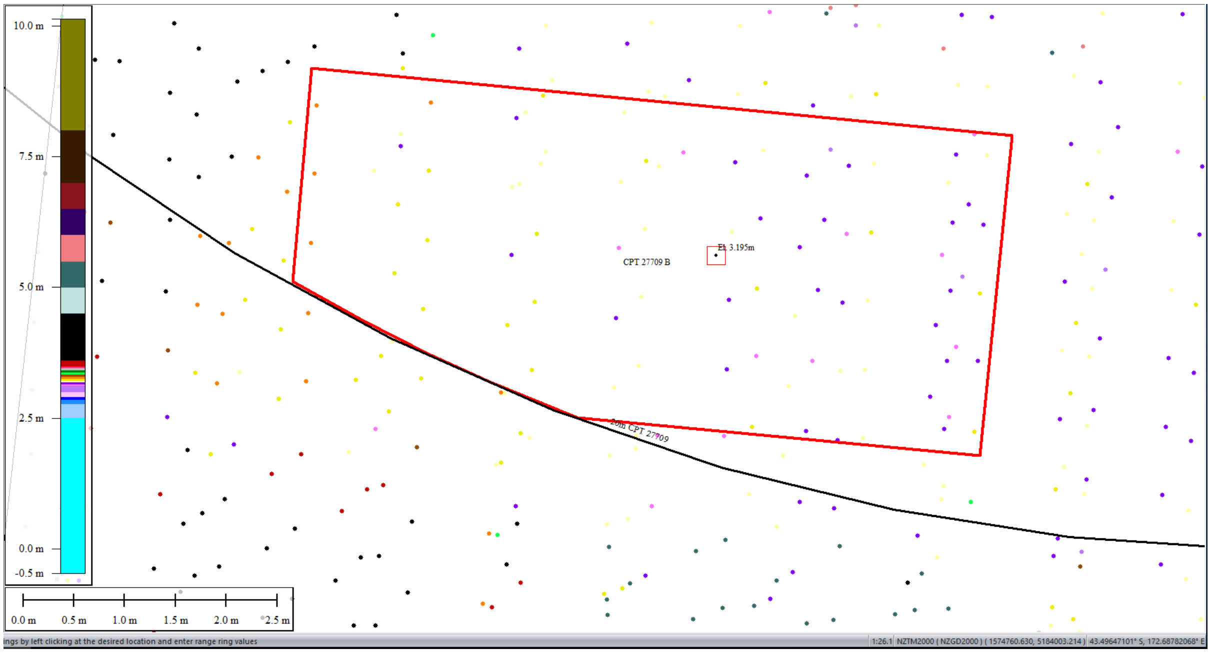

Figure 82: Ground surface elevation averaged over 20-m and 50-m buffers for Patch B for Feb 2012 LiDAR survey.

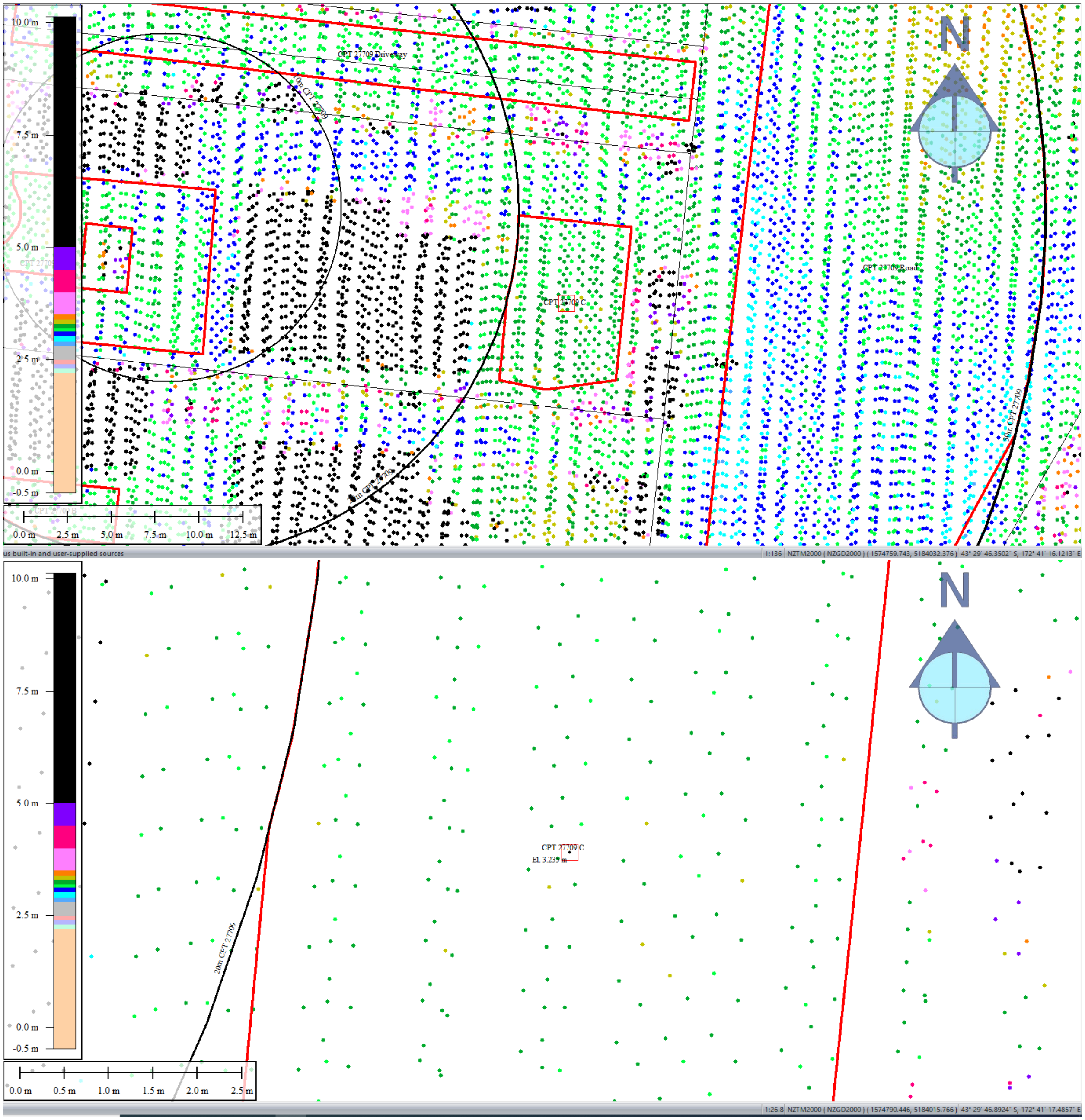

Figure 83: Ground surface elevation averaged over 50-m buffer for Patch C for Feb 2012 LiDAR survey.

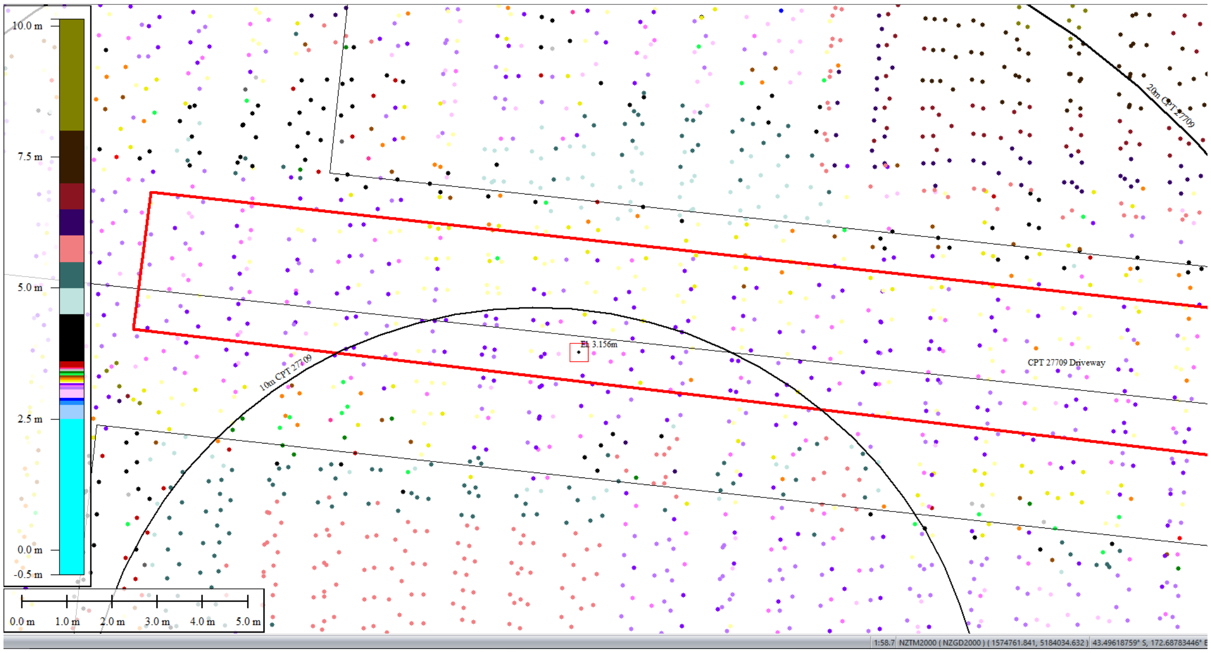

Figure 84: Ground surface elevation averaged over 10-m buffer for Driveway for Feb 2012 LiDAR survey.

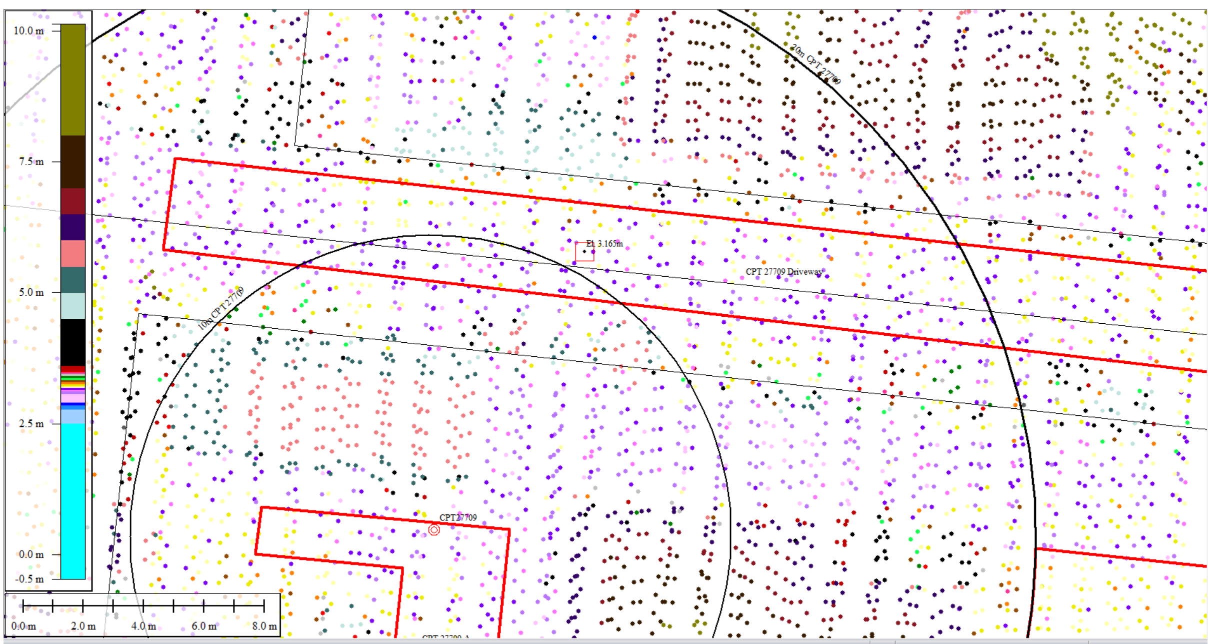

Figure 85: Ground surface elevation averaged over 20-m buffer for Driveway for Feb 2012 LiDAR survey.

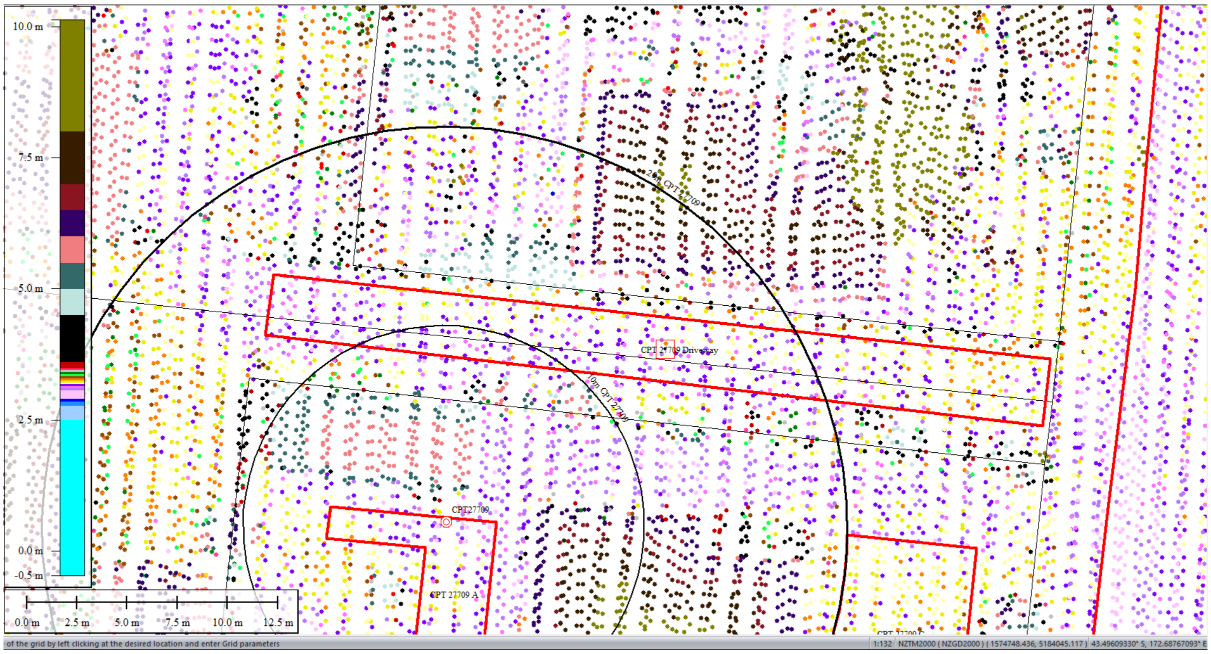

Figure 86: Ground surface elevation averaged over 50-m buffer for Driveway for Feb 2012 LiDAR survey.

Figure 87: Ground surface elevation averaged over 50-m buffer for Road for Feb 2012 LiDAR survey.

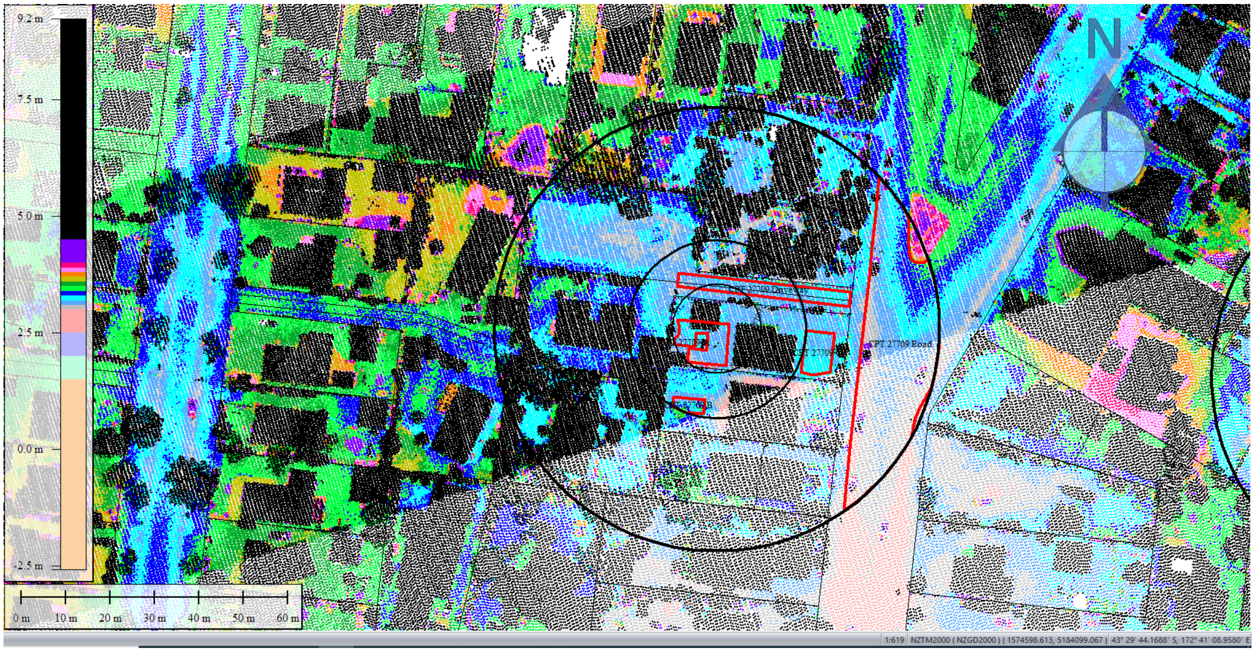

Figure 88: Oct 2015 LiDAR survey.

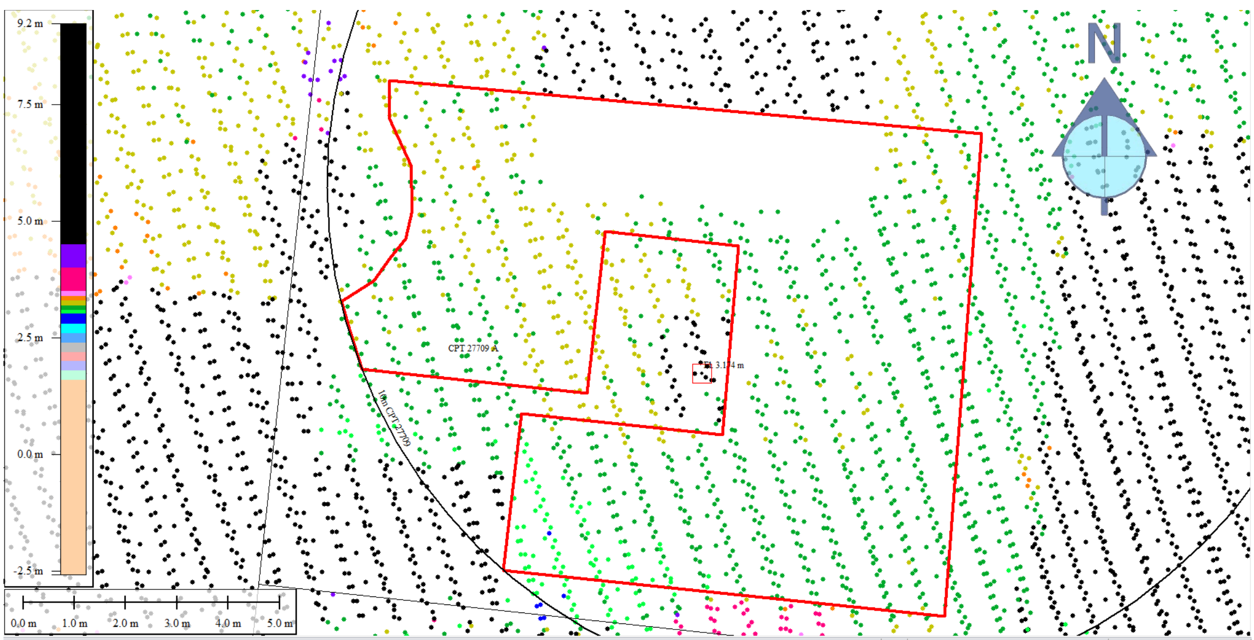

Figure 89: Ground surface elevation averaged over 10-m, 20-m, and 50-m buffers for Patch A for Oct 2015 LiDAR survey.

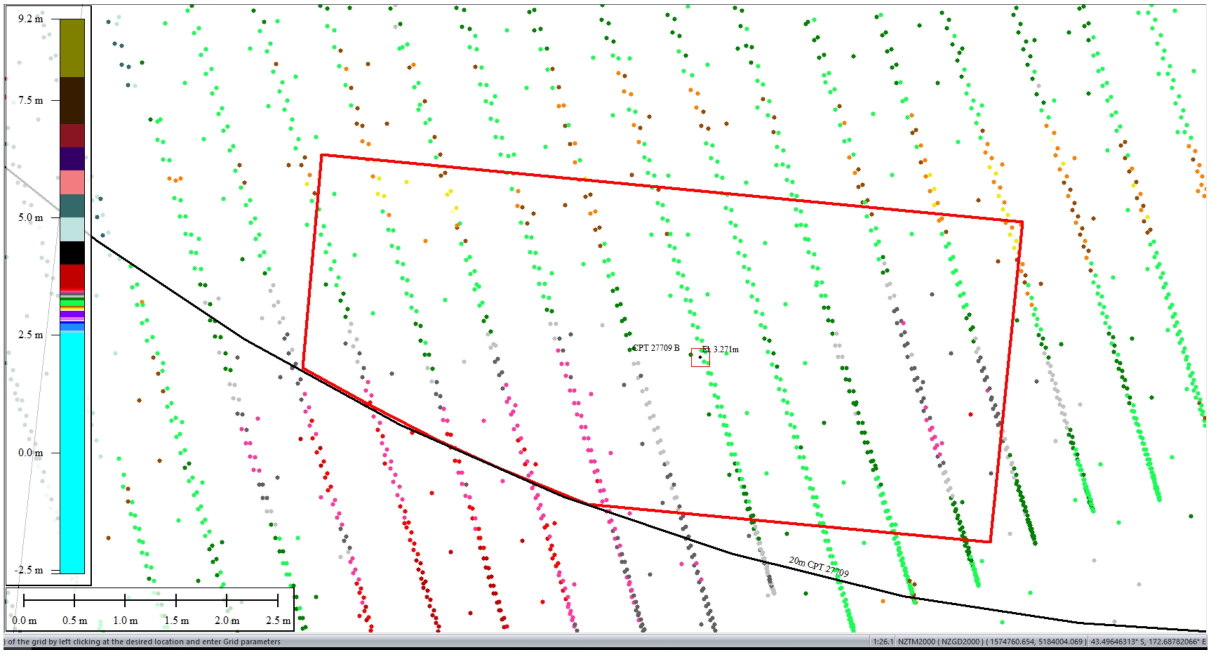

Figure 90: Ground surface elevation averaged over 20-m and 50-m buffers for Patch B for Oct 2015 LiDAR survey.

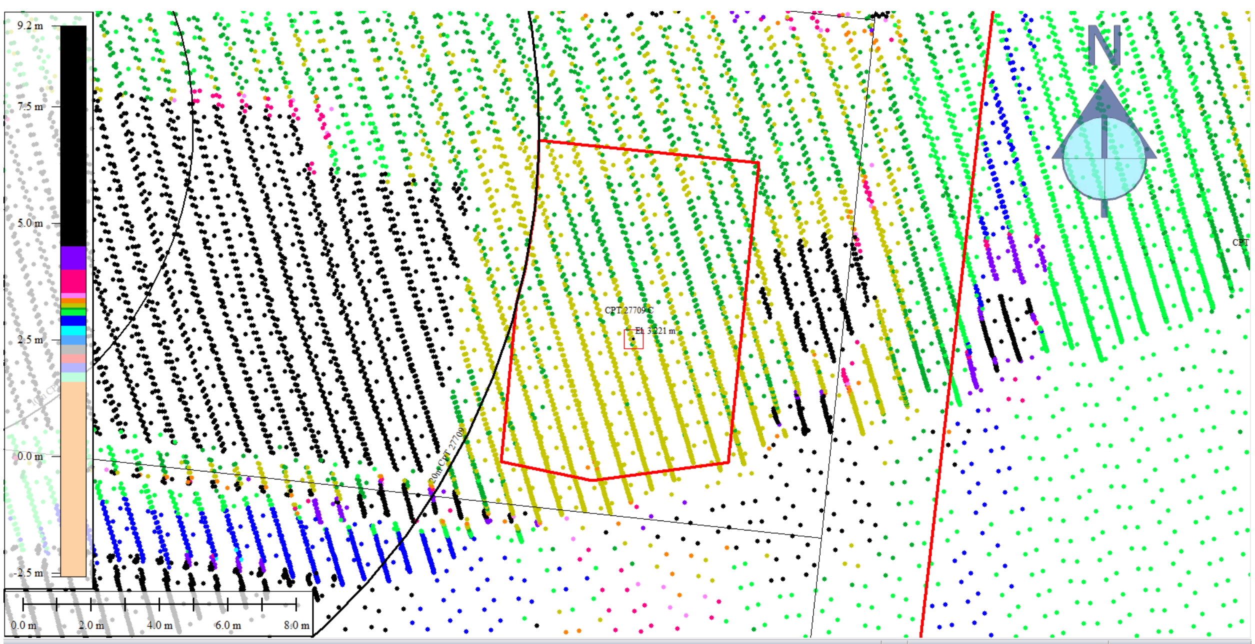

Figure 91: Ground surface elevation averaged over 50-m buffer for Patch C for Oct 2015 LiDAR survey.

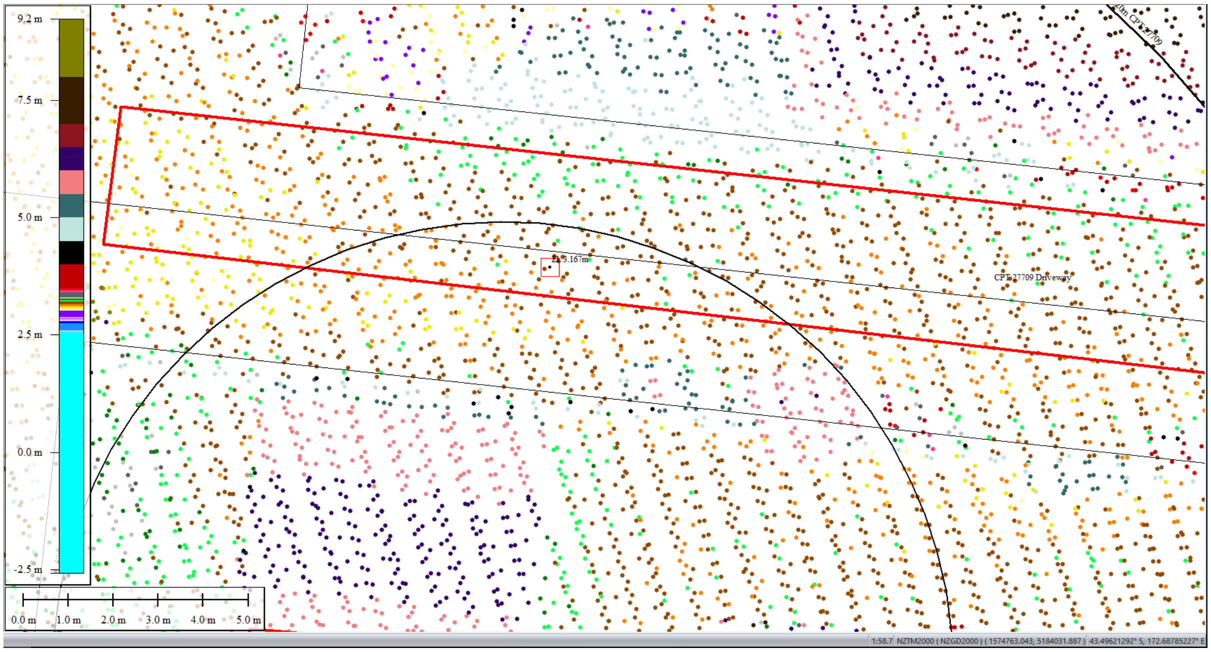

Figure 92: Ground surface elevation averaged over 10-m buffer for Driveway for Oct 2015 LiDAR survey.

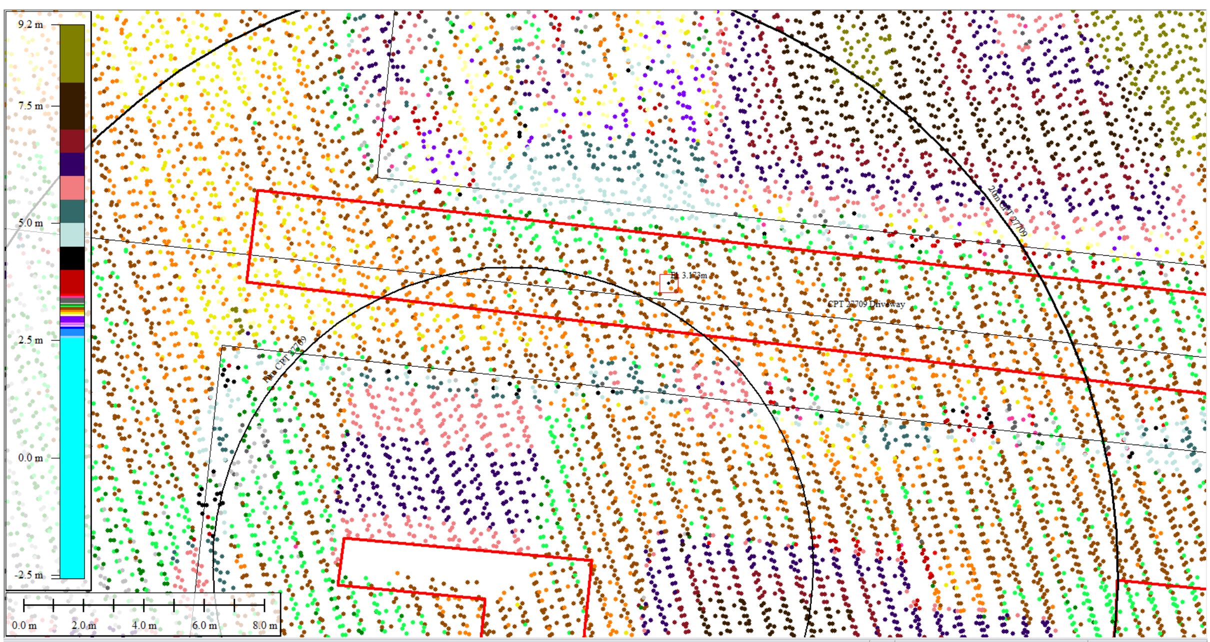

Figure 93: Ground surface elevation averaged over 20-m buffer for Driveway for Oct 2015 LiDAR survey.

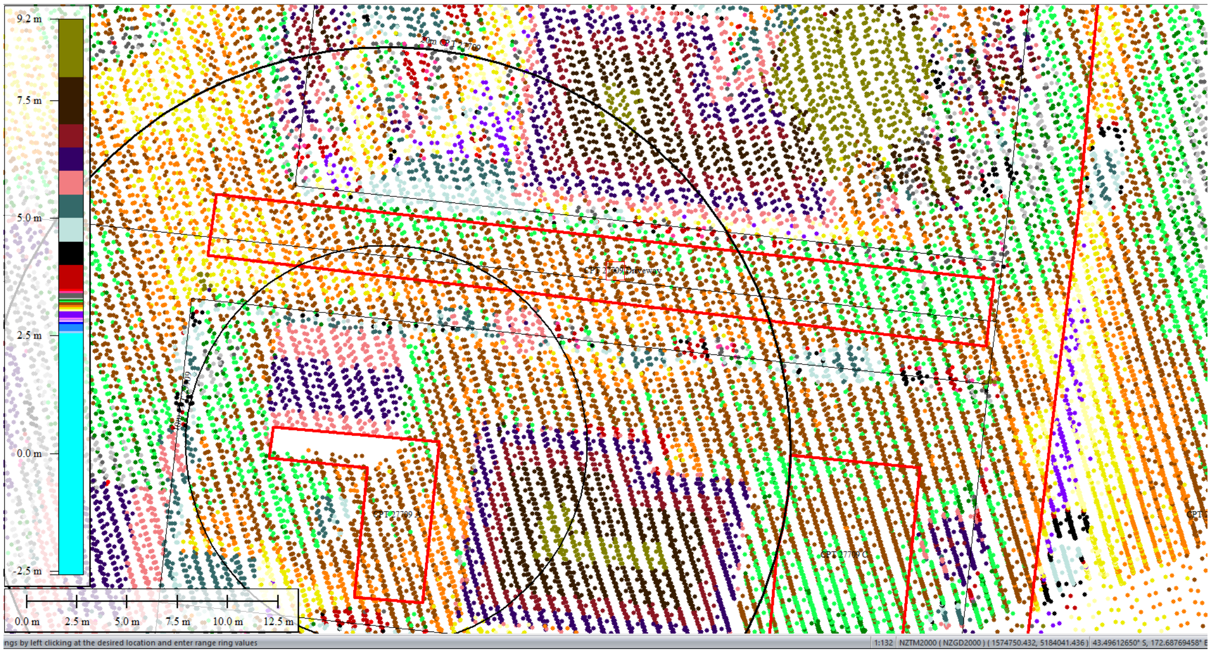

Figure 94: Ground surface elevation averaged over 50-m buffer for Driveway for Oct 2015 LiDAR survey.

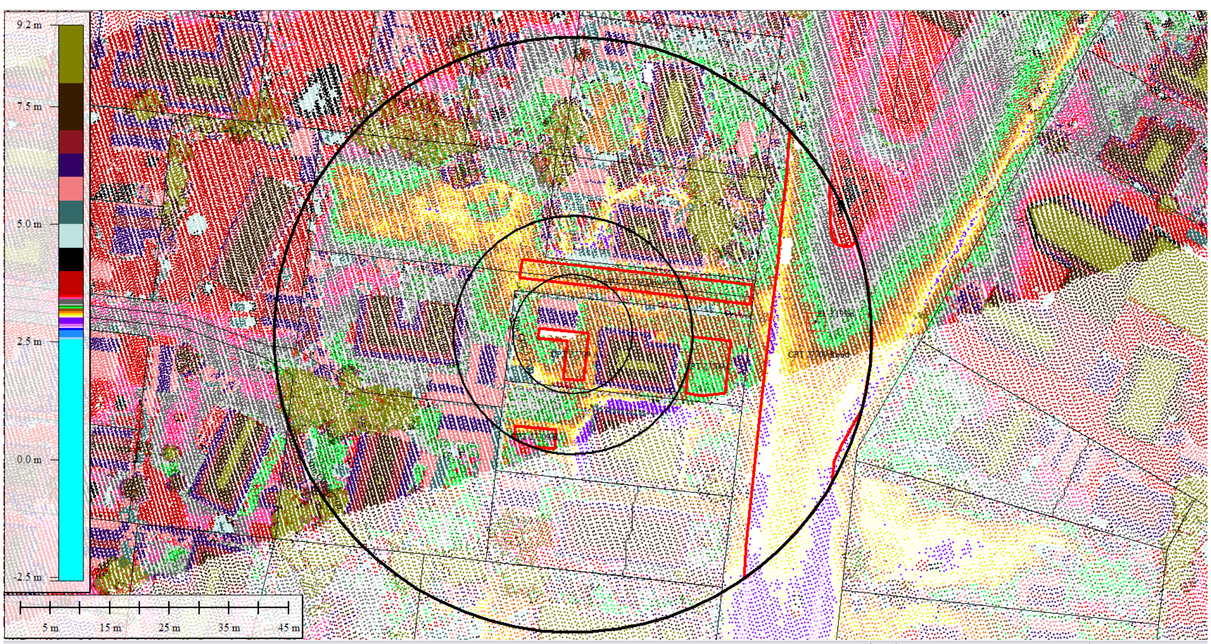

Figure 95: Ground surface elevation averaged over 50-m buffer for Road for Oct 2015 LiDAR survey.

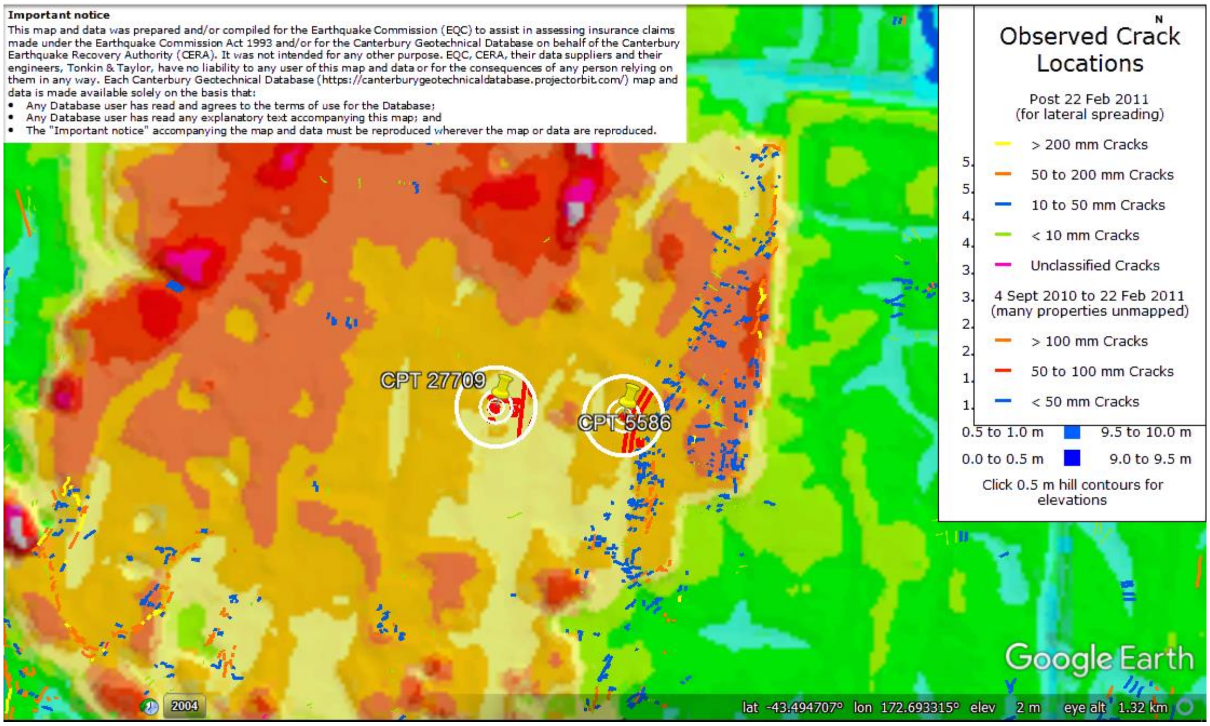

Figure 96: Ground surface elevation difference between the road and properties (Sep 2010 LiDAR DEM).

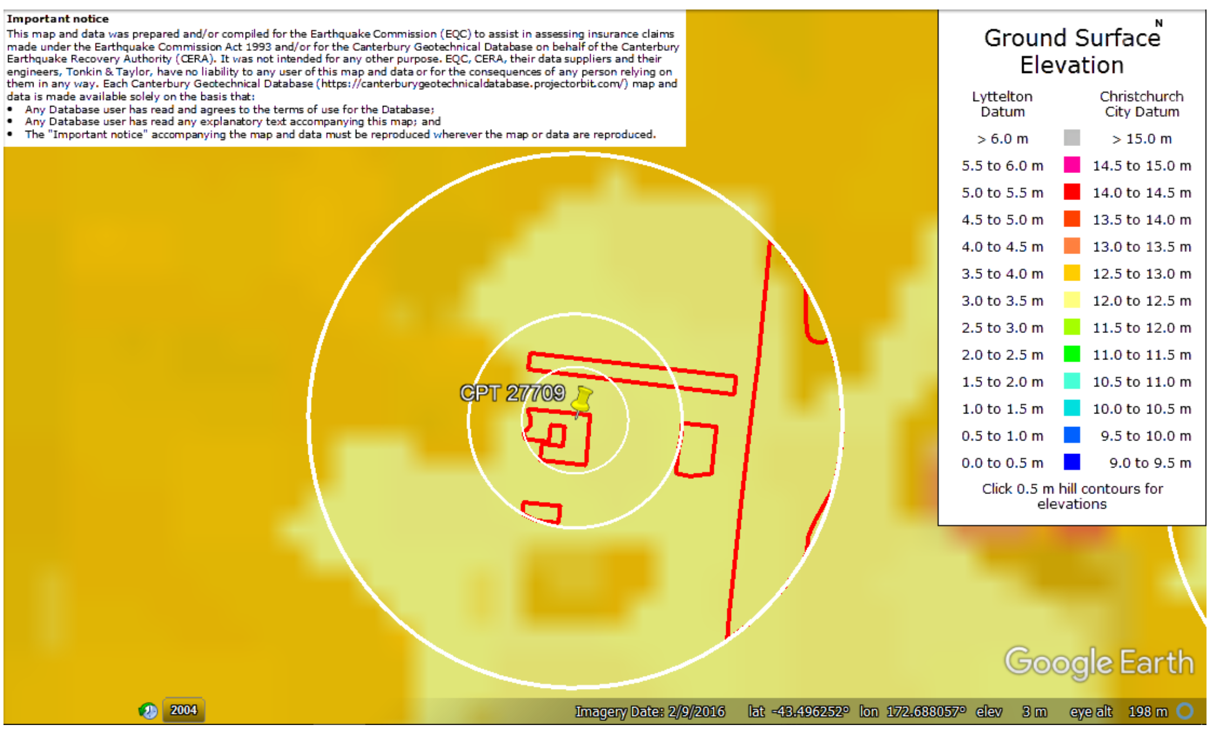

Figure 97: Enlarged view of ground surface elevation difference between the road and properties (Sep 2010 LiDAR DEM).

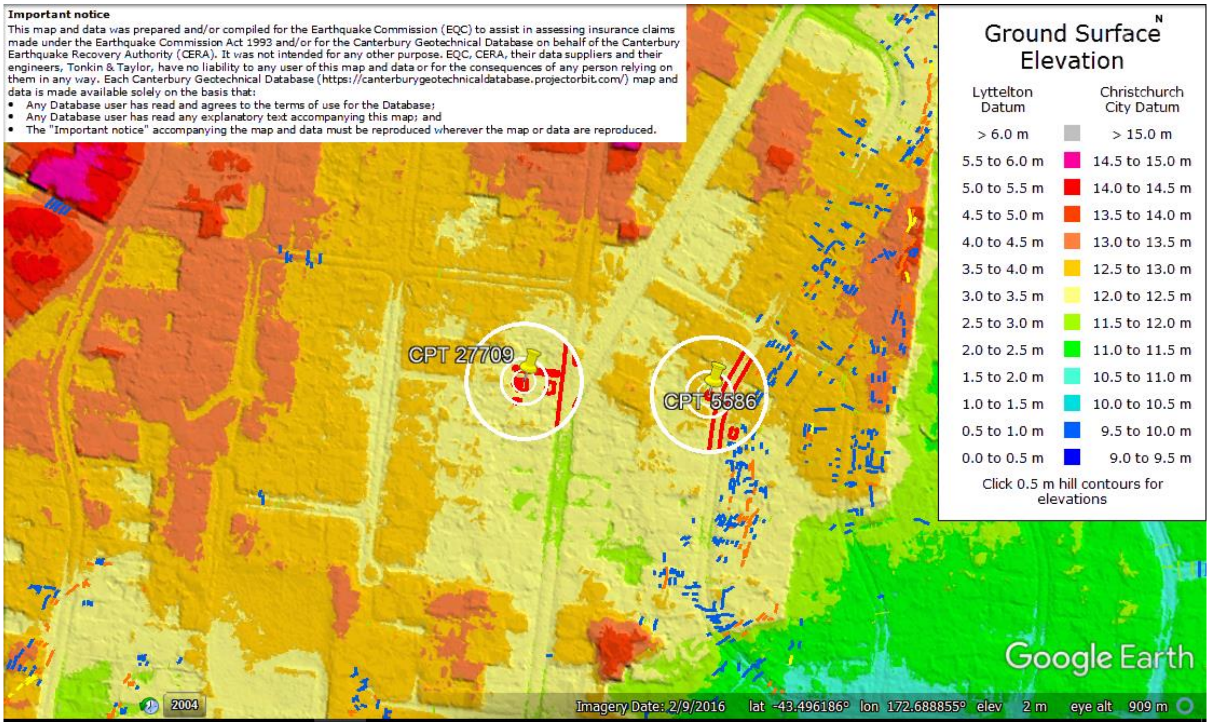

Figure 98: Enlarged view of ground surface elevation difference between the road and properties (Sep 2011 LiDAR DEM).

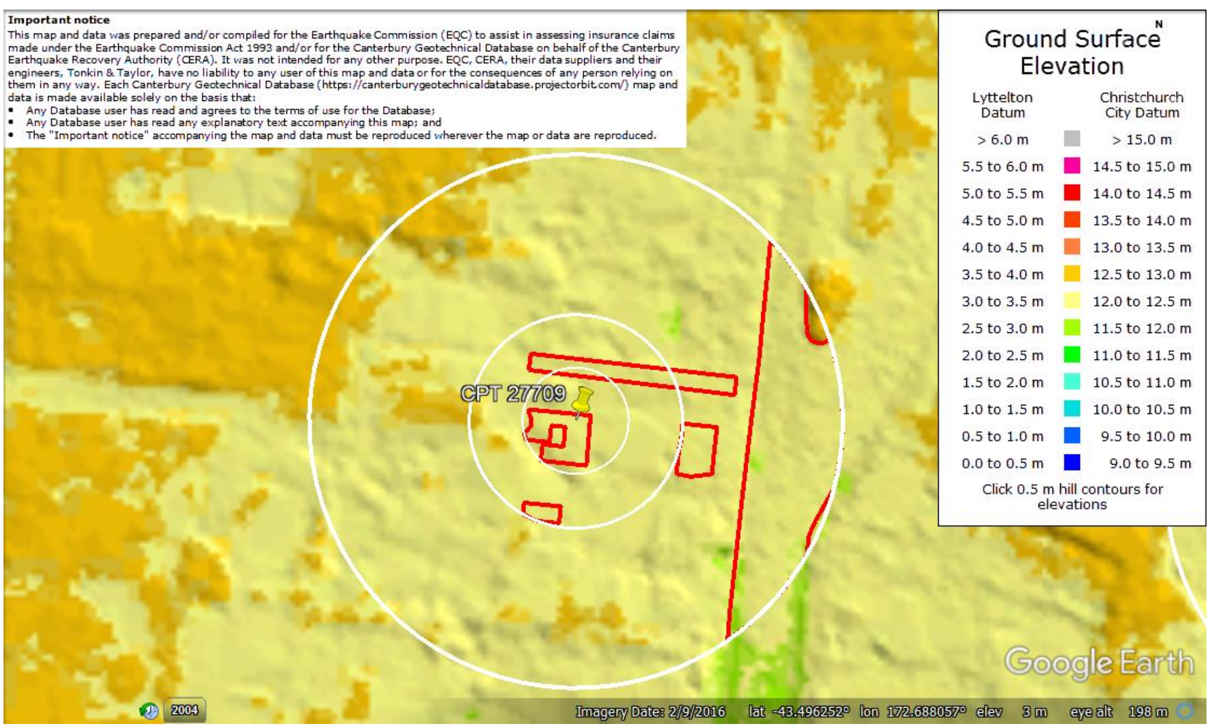

Figure 99: Ground surface elevation difference between the road and properties (Sep 2011 LiDAR DEM).

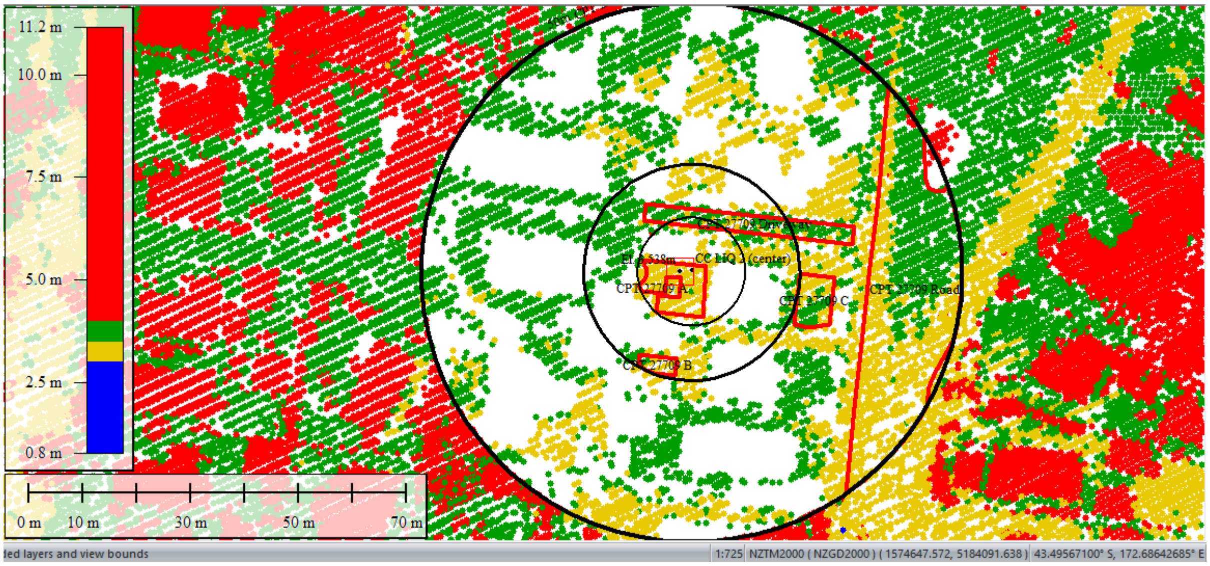

Figure 100: Ground surface elevation averaged over properties (Sep 2010 raw LiDAR).

Figure 101: No ejecta for Sep-10 EQ.

Figure 102: Ejecta outline for Feb-11 EQ.

Figure 103: Ejecta outline for Jun-11 EQ; photo acquired on 14-15 Jun 2011.

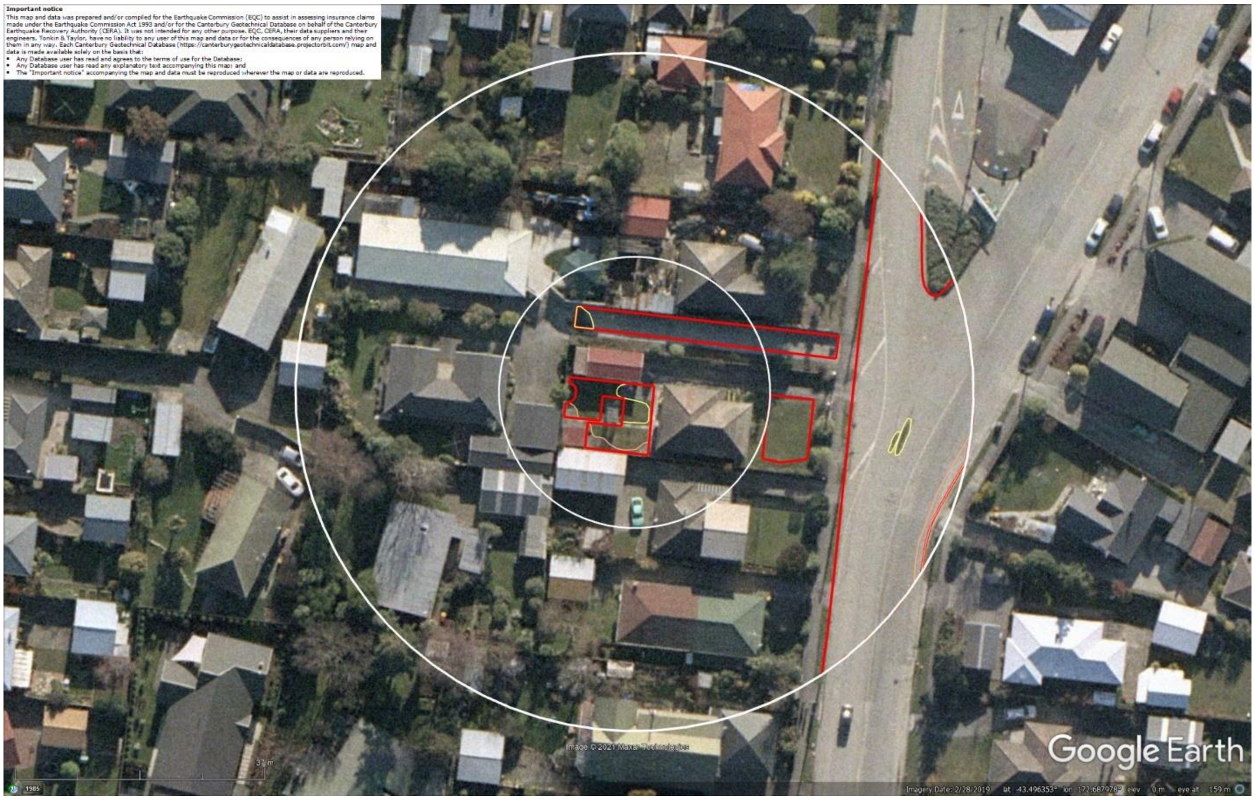

Figure 104: Ejecta outline for Jun-11 EQ; photo acquired on 16 Jun 2011.

Figure 105: Ejecta outline for Dec-11 EQ.

Figure 106: Presence of liquefaction ejecta sediments within Patch A during ground inspection in August 2011.

Figure 107: Presence of liquefaction ejecta sediments within Patch B during ground inspection in August 2011.

Figure 108: Patch C during ground inspection in August 2011.

Figure 109: Presence of liquefaction ejecta sediments near Driveway during ground inspection in August 2011.

Contents of this figure cannot be shared as doing so is restricted by a Non-Disclosure Agreement.

Figure 110: EQC LDAT property inspection report for Patch B.

Contents of this figure cannot be shared as doing so is restricted by a Non-Disclosure Agreement.

Figure 111: EQC LDAT property inspection report for Patches A and C.

Contents of this figure cannot be shared as doing so is restricted by a Non-Disclosure Agreement.

Figure 112: EQC LDAT property inspection report for Driveway.

Figure 113: PGA for Sep-10 EQ (st. dev. = 0.300-0.325 ln units).

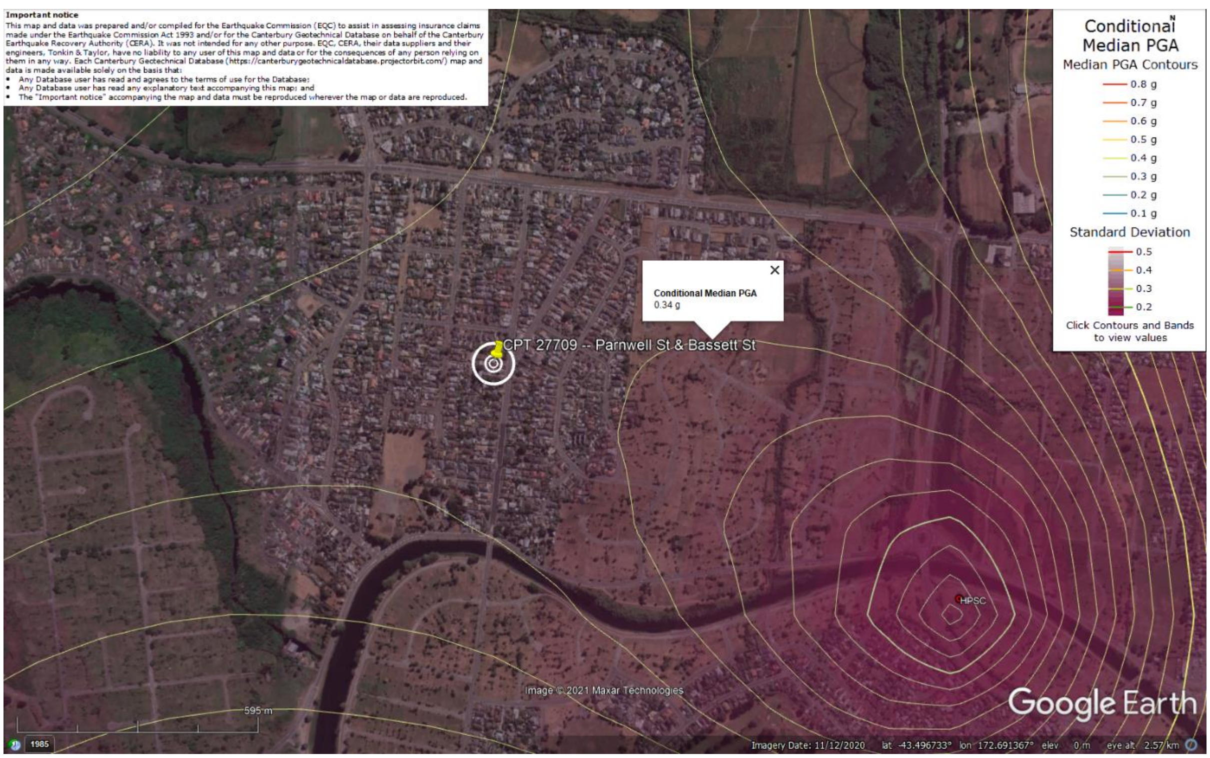

Figure 114: PGA for Feb-11 EQ (st. dev. = 0.325-0.350 ln units).

Figure 115: PGA for Jun-11 EQ (st. dev. = 0.350-0.375 ln units).

Figure 116: PGA for Dec-11 EQ (st. dev. = 0.350-0.375 ln units).

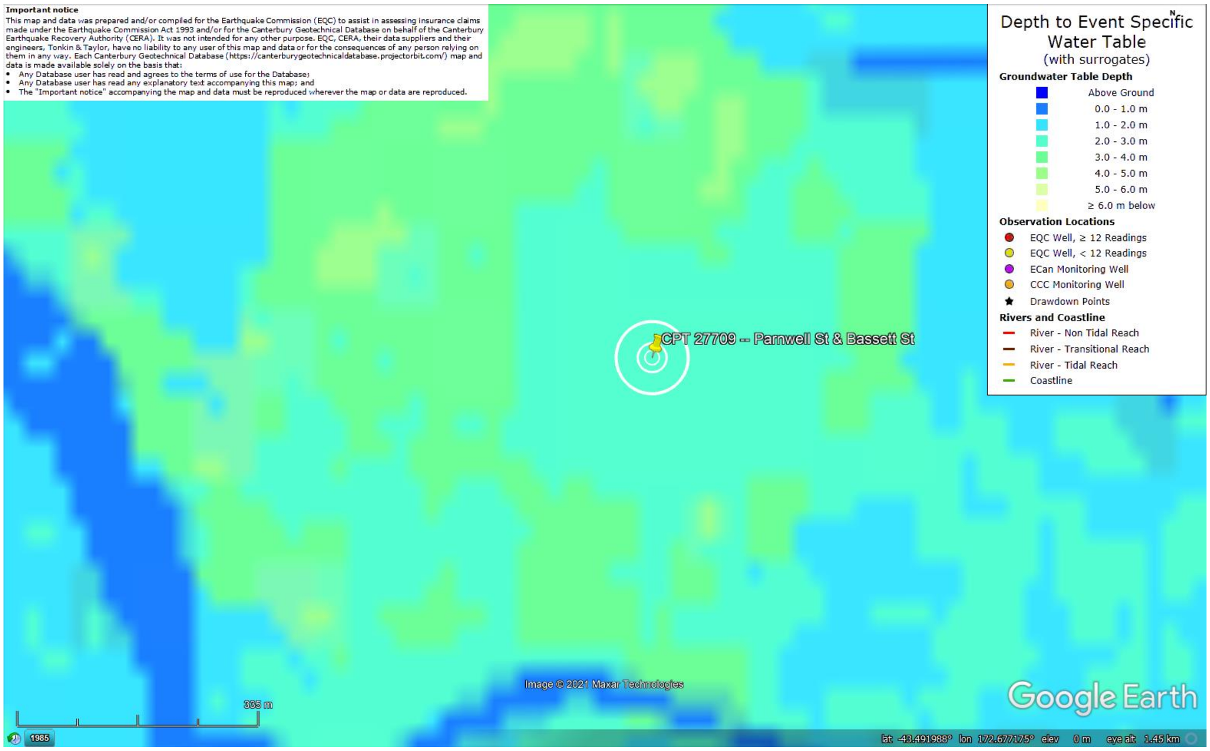

Figure 117: Depth to groundwater table for Sep-10 EQ.

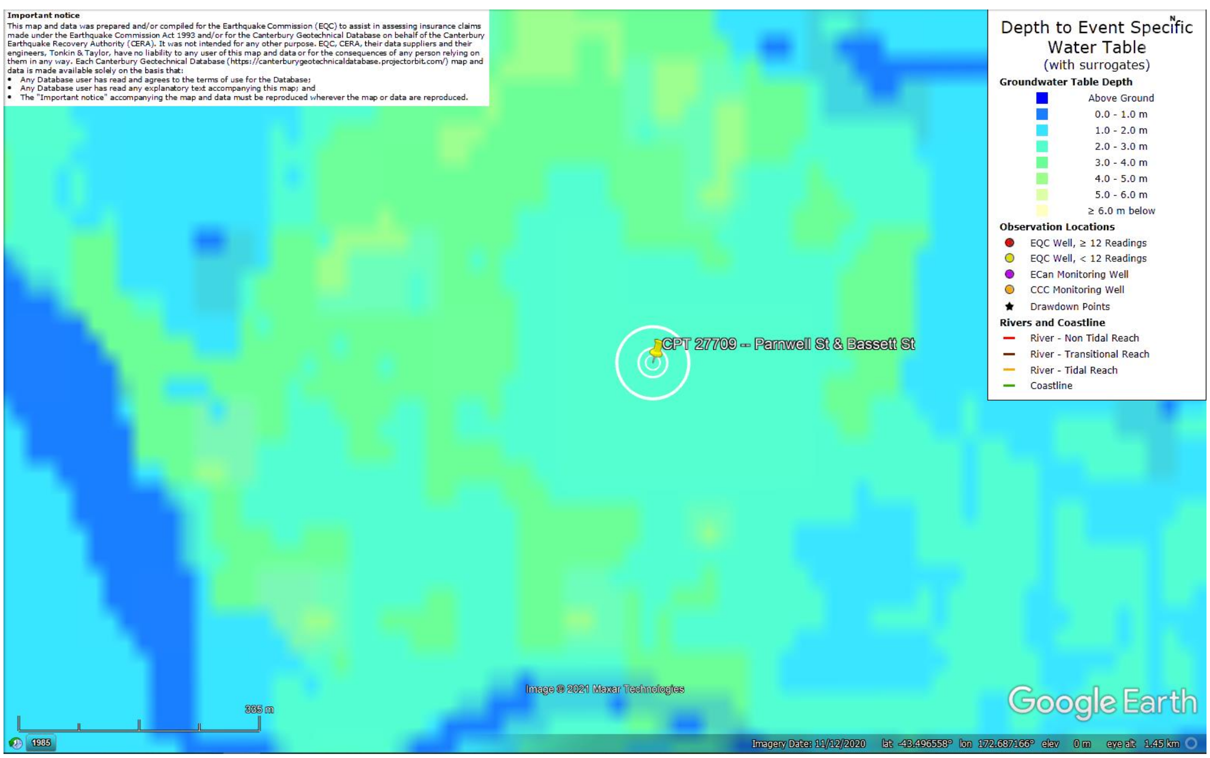

Figure 118: Depth to groundwater table for Feb-11 EQ.

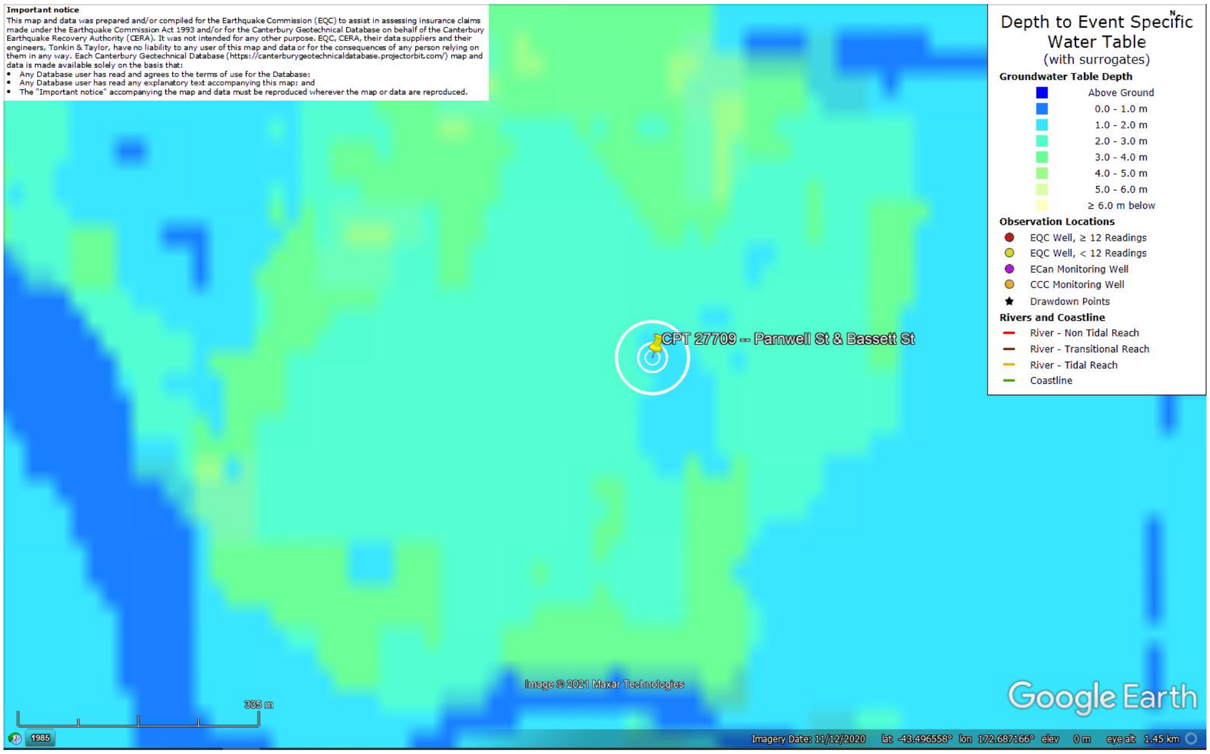

Figure 119: Depth to groundwater table for Jun-11 EQ.

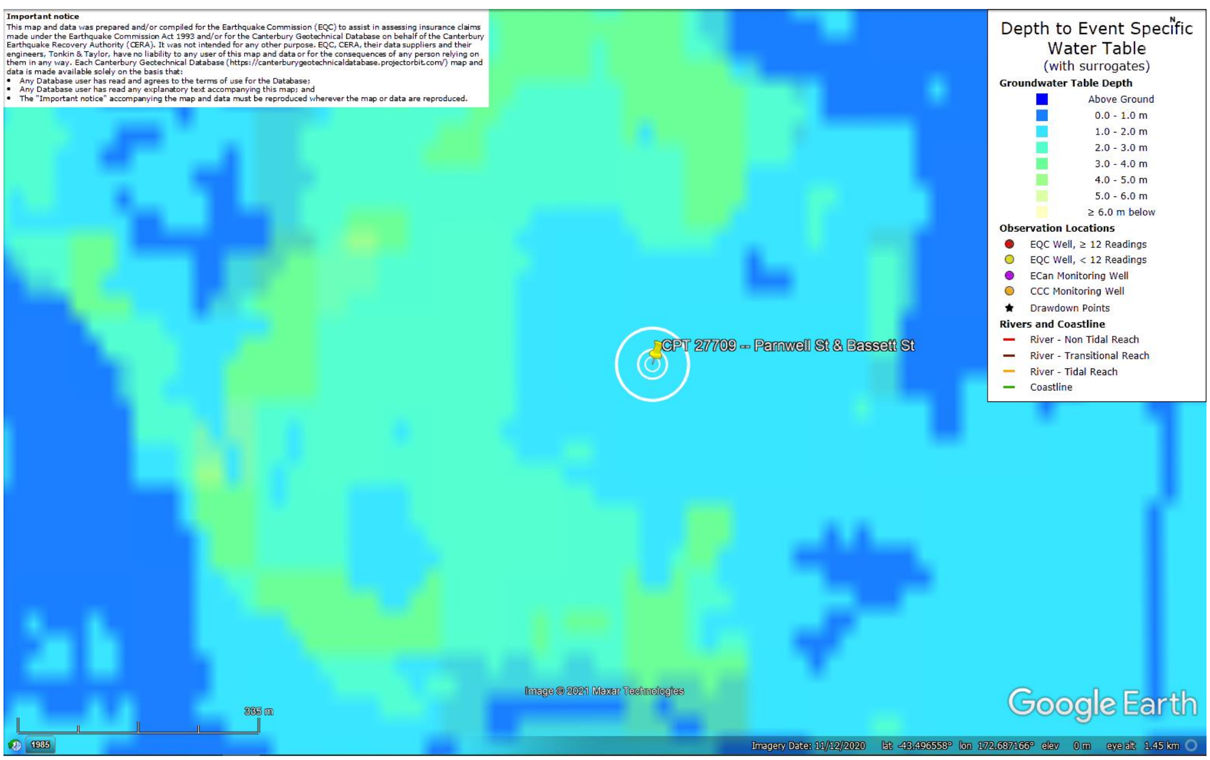

Figure 120: Depth to groundwater table for Dec-11 EQ.

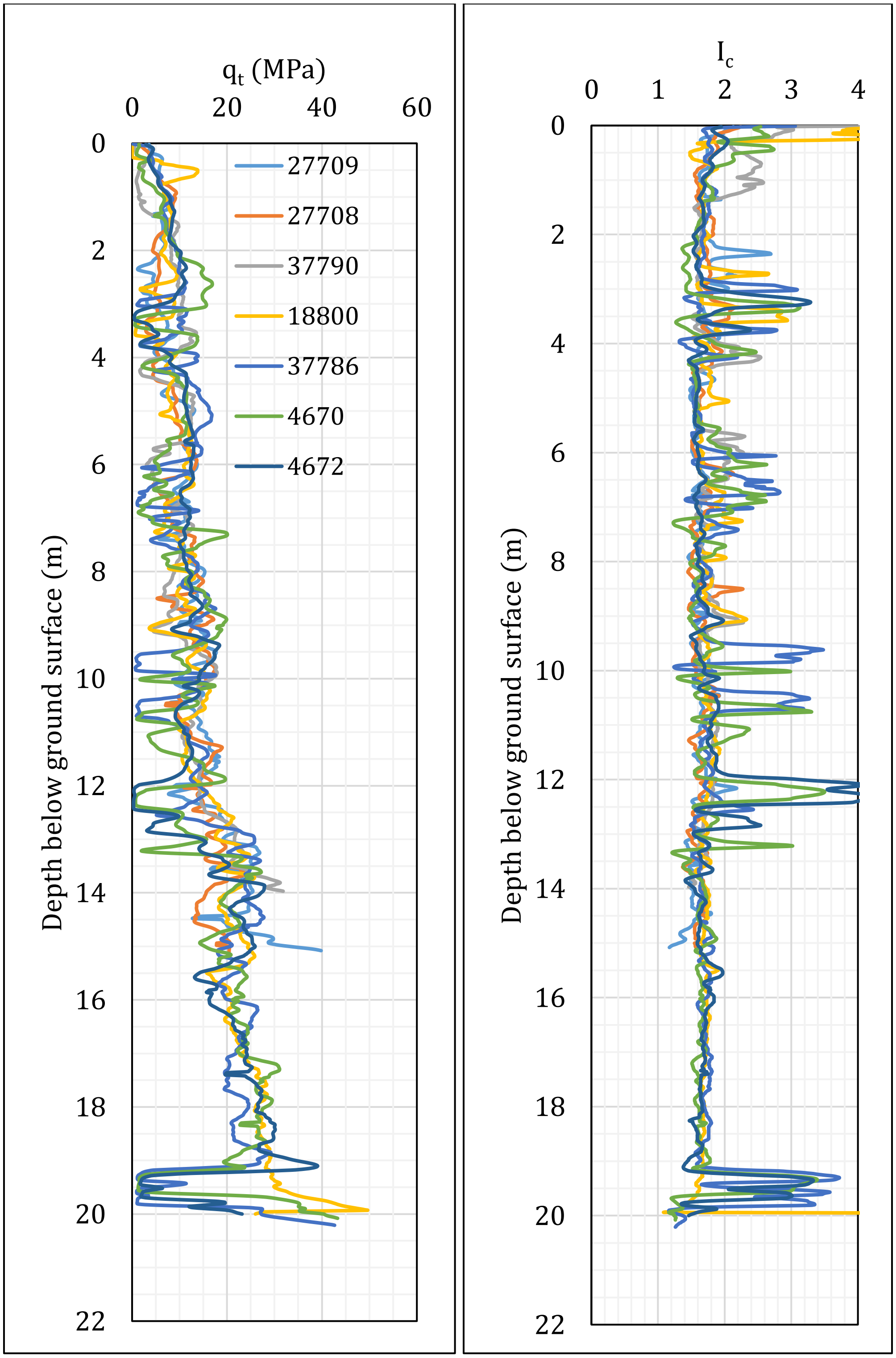

Figure 121: q_t and I_c profiles.

Note 7: The selection of CPTs for the area considered for settlement assessment (Figure 1) is based on the proximity of the CPTs to the considered areas. In accordance with that, the following table shows CPTs that were used for the volumetric settlement analysis in *Cliq v.3.0.3.2*, a CPT soil liquefaction software developed by GeoLogismiki. (The average volumetric settlements were reported in Table 8.)

Table 12: CPT profiles used in volumetric settlement analysis for areas selected for settlement assessment.

CPT ID No.	Patch A	Patch B	Patch C	Driveway	Road
27709	✓			✓	
37790		✓			
27708			✓	✓	✓
37786*					✓
4670					✓
4672					✓
18800					✓

Note: * denotes the CPT used to estimate the volumetric settlement within a depth range from 14/15m to 20m.

Table 13: CPT-based results.

		CPT ID							
EQ Event	Parameter	27709	27708	37790	18800	37786	4670	4672	$\Delta_{14/15m\text{-}20m}$*
Sep-10	S_{V1D} (mm)	14	13	13	3	15	29	16	3
	LSN	2	2	2	0	2	3	2	0
	LPI	0	0	0	0	0	0	0	0
	LPI_{ish}	0	0	0	0	0	0	0	--
	$D_{FS<1}$ (m)	undet.	undet.	undet.	undet.	undet.	10.9	undet.	--
Feb-11	S_{V1D} (mm)	75	102	73	54	55	93	72	5
	LSN	15	19	11	9	7	12	11	0
	LPI	4	6	6	2	3	6	4	0
	LPI_{ish}	1	1	1	1	0	0	3	--
	$D_{FS<1}$ (m)	2.64	2.58	4.03	6.84	6.19	4.06	3.32	--
Jun-11	S_{V1D} (mm)	26	35	29	9	23	44	28	3
	LSN	5	7	5	1	3	6	4	0
	LPI	1	0	0	0	0	1	1	0
	LPI_{ish}	0	0	0	0	0	0	0	--
	$D_{FS<1}$ (m)	undet.	undet.	4.10	undet.	undet.	10.8	12.7	--
Dec-11	S_{V1D} (mm)	82	108	71	52	52	88	67	5
	LSN	19	23	11	10	7	12	11	0
	LPI	5	7	5	2	3	6	4	0
	LPI_{ish}	1	2	1	1	0	0	3	--
	$D_{FS<1}$ (m)	2.46	2.02	4.03	4.24	6.19	4.06	3.32	--

Notes: $D_{FS<1}$ = Depth to the first liquefiable layer (FS_L<1) that is at least 200-mm thick, as determined by the Boulanger and Idriss (2016) liquefaction-triggering procedure (P_L=50%, C_{FC}=0.13, and $I_{c,cutoff}$ =2.6), and exported from *Cliq v.3.0.3.2*; undet. = the specified soil layer was not detected; * indicates the amount of S_{V1D} and LPI to be added to CPTs 27709, 27708, and 37790 due to their refusal depths being shallower than 20 m.

Note 8: Based on the borehole log (BH 8653, Figure 1), the groundwater table is at a depth of 1.5 m below the ground surface. The soil profile consists of (1) sandy, SP, fill to a depth of 0.5 m and (2) poorly graded sand, SP, of the Christchurch formation to a depth of 20 m. The fines content of the retrieved soil samples ranges from 5% to 17% with the median value of 9%.

Note 9: The ejecta-induced free-field settlement provided in Table 11 is an areal average settlement due to ejecta, which is based on the total settlement assessment area, A_T (provided in Table 9 and repeated in Table 14). However, the considered area was not always covered completely with ejecta; thus, it is important to provide the localized ejecta-induced settlement, too. The localized settlement due to ejecta is estimated using photographic evidence only as

$$S_{E,P\_localized} = \frac{V_E}{A_E}$$

where V_E is the total volume of ejecta within A_T and A_E is the total coverage area of ejecta within A_T. Please note that the areal ejecta-induced settlement provided in Table 14 as S_{E,P_areal} is the same as $S_{E,P}$ in Table 11, which was estimated as

$$S_{E,P\_areal} = S_{E,P} = \frac{V_E}{A_T}$$

where V_E is the total volume of ejecta within A_T and A_T is the total settlement assessment area.

Table 14a: Areal and localized ejecta-induced settlement estimates for Patch A (10-, 20-, and 50-m buffers) based on photographic evidence.

Earthquake Event	A_T (m^2)	A_E (m^2)	V_E (m^3)	S_{E,P_areal} (mm)	$S_{E,P\_localized}$ (mm)
Sep-10	98.0	0	0	0	0
Feb-11	98.0	70.6	6.2-11.1	90±25	120±35
Jun-11	98.0	56.4	1.2-2.8	20±10	35±15
Dec-11	98.0	13.4	0.4-0.6	5±5	40±10

Notes: S_{E,P_areal} = $S_{E,P}$ reported in Table 11 = areal ejecta-induced settlement; $S_{E,P\_localized}$ = localized ejecta-induced settlement; A_T = total settlement assessment area; V_E = total volume of ejecta within A_T; A_E = total area of ejecta within A_T; The estimates of both areal and localized ejecta-induced settlement are rounded to the nearest 5; Final plus/minus values are also rounded to the nearest 5.

Table 14b: Areal and localized ejecta-induced settlement estimates for Patch B (20-m and 50-m buffers) based on photographic evidence.

Earthquake Event	A_T (m^2)	A_E (m^2)	V_E (m^3)	S_{E,P_areal} (mm)	$S_{E,P\_localized}$ (mm)
Sep-10	20.0	0	0	0	0
Feb-11	20.0	20.0	0.2-0.6	20±10	20±10
Jun-11	20.0	0	0	0	0
Dec-11	20.0	0	0	0	0

Notes: S_{E,P_areal} = $S_{E,P}$ reported in Table 11 = areal ejecta-induced settlement; $S_{E,P\_localized}$ = localized ejecta-induced settlement; A_T = total settlement assessment area; V_E = total volume of ejecta within A_T; A_E = total area of ejecta within A_T; The estimates of both areal and localized ejecta-induced settlement are rounded to the nearest 5; Final plus/minus values are also rounded to the nearest 5.

Table 14c: Areal and localized ejecta-induced settlement estimates for Driveway (20-m buffer) based on photographic evidence.

Earthquake Event	A_T (m^2)	A_E (m^2)	V_E (m^3)	S_{E,P_areal} (mm)	$S_{E,P\_localized}$ (mm)
Sep-10	85.0	0	0	0	0
Feb-11	85.0	85.0	0.5-1.0	10±5	10±5
Jun-11	85.0	6.4	0.2-0.4	5±5	45±15
Dec-11	85.0	0	0	0	0

Notes: S_{E,P_areal} = $S_{E,P}$ reported in Table 11 = areal ejecta-induced settlement; $S_{E,P\_localized}$ = localized ejecta-induced settlement; A_T = total settlement assessment area; V_E = total volume of ejecta within A_T; A_E = total area of ejecta within A_T; The estimates of both areal and localized ejecta-induced settlement are rounded to the nearest 5; Final plus/minus values are also rounded to the nearest 5.

Table 14d: Areal and localized ejecta-induced settlement estimates for Driveway (50-m buffer) based on photographic evidence.

Earthquake Event	A_T (m^2)	A_E (m^2)	V_E (m^3)	S_{E,P_areal} (mm)	$S_{E,P\_localized}$ (mm)
Sep-10	124	0	0	0	0
Feb-11	124	124	0.6-1.2	10±5	10±5
Jun-11	124	6.4	0.2-0.4	5±5	45±15
Dec-11	124	0	0	0	0

Notes: S_{E,P_areal} = $S_{E,P}$ reported in Table 11 = areal ejecta-induced settlement; $S_{E,P\_localized}$ = localized ejecta-induced settlement; A_T = total settlement assessment area; V_E = total volume of ejecta within A_T; A_E = total area of ejecta within A_T; The estimates of both areal and localized ejecta-induced settlement are rounded to the nearest 5; Final plus/minus values are also rounded to the nearest 5.

Table 14e: Areal and localized ejecta-induced settlement estimates for Road (50-m buffer) based on photographic evidence.

Earthquake Event	A_T (m^2)	A_E (m^2)	V_E (m^3)	S_{E,P_areal} (mm)	$S_{E,P\_localized}$ (mm)
Sep-10	874	0	0	0	0
Feb-11	768	707	2.3-4.6	5±5	5±5
Jun-11	894	31.7	0.3-0.5	<5	10±5
Dec-11	880	21.4	0.3-0.6	<5	20±5

Notes: S_{E,P_areal} = $S_{E,P}$ reported in Table 11 = areal ejecta-induced settlement; $S_{E,P\_localized}$ = localized ejecta-induced settlement; A_T = total settlement assessment area; V_E = total volume of ejecta within A_T; A_E = total area of ejecta within A_T; The estimates of both areal and localized ejecta-induced settlement are rounded to the nearest 5; Final plus/minus values are also rounded to the nearest 5.

Summary 2:

- **The best estimate of the localized ejecta-induced free-field ground settlement at the Parnwell St and Bassett St site for the SEP 2010, FEB 2011, JUN 2011, and DEC 2011 earthquake is 0 mm, 120±35 mm, 35±15 mm, and 40±10 mm, respectively.**
- **The best estimate of the localized ejecta-induced settlement of the road at the Parnwell St and Bassett St site for the SEP 2010, FEB 2011, JUN 2011, and DEC 2011 earthquake is 0 mm, 5±5 mm, 10±5 mm, and 20±5 mm, respectively.**